Impacts of coal-fired power plants on aerosol particles in the Highveld

P van der Walt

orcid.org/0000-0001-9823-569X

Dissertation accepted in fulfilment of the requirements for the degree *Master of Science in Environmental Sciences* at the North-West University

Supervisor:	Prof RM Garland
Co-supervisor:	Prof RP Burger
Co-supervisor:	Mr M Naidoo

Graduation May 2023

22325239

DEDICATION

I dedicate this work to my parents, my wife, and my daughter.

To my parents, Lodewiekus and Daphné van der Walt, thank you for all your hard work, the sacrifices you made to afford my education and your unconditional love.

To my wife, Cara Terblanche, I would not have been able to finish this work without your patience and unwavering support.

To my daughter, Sophia Terblanche, you are my every reason, my light, my inspiration.

ACKNOWLEDGMENTS

I would like to express my deepest gratitude to my supervisors, Prof Rebecca Garland, Prof Roelof Burger and Mogesh Naidoo, for their patience, kindness, and invaluable feedback. I have learned so much from each one of you.

I would like to thank my friend and colleague, Lizette Kloppers, for proofreading my work.

Lastly, I would like to acknowledge the CSIR who developed the modelling platform for the Department of Forestry, Fisheries, and the Environment (DEFF) Highveld study and the Department for allowing me to use the modelling platform in my study. The model simulations were run at the Centre for High-Performance Computing (CHPC).

ABSTRACT

Industrialisation and urbanisation of the interior plateau of South Africa (i.e. the Highveld) have resulted in air quality that infringes on South Africans' right to an environment that is not damaging to human health or well-being. In March 2022, a judgement was handed down in the Pretoria High Court, ordering the government to execute the Highveld Priority Area Air Quality Management Plan. The judgement provided that failure to meet the National Ambient Air Quality Standards (NAAQS) in the area is sufficient evidence for a violation of the right to an environment that is protected and not detrimental to human health or well-being. The Highveld has meteorological conditions that are highly unfavourable air pollution dispersion. Combined with the industrialisation and urbanisation within the region, this has resulted in fine particulate air pollution (i.e., $PM_{2.5}$). $PM_{2.5}$ is an air pollutant that can remain in the atmosphere for days to weeks giving it the potential to reach remote regions of South Africa or neighbouring countries. When inhaled, it can penetrate deep into the respiratory system and cause many adverse health impacts. To effectively manage ambient air quality in the Highveld, we need to understand the relationship between these air pollutants and determine their significant sources in the region. This study looks at the impact of ambient $PM_{2.5}$, particularly secondary $PM_{2.5}$ (i.e., $PM_{2.5}$ formed in the atmosphere), attributed to coal-fired power plants in the Highveld. Coal-fired power plants are significant sources of sulphur dioxide (SO_2) and nitrogen oxides (NO_x), which are precursor gases of secondary $PM_{2.5}$, and most of the coal-fired power plants in South Africa are concentrated in the Highveld. This study was built upon an existing modelling platform developed for the Highveld Health Study (baseline simulation). A second concept simulation was run, where all large (≥1 000 MW) coal-fired power plant emissions were excluded. The annual average $PM_{2.5}$ attributable to the coal-fired power plants was determined by subtracting the concentrations in the concept simulation from those in the baseline simulation. The study found that the large coal-fired power plants were a significant source of ambient annual average $PM_{2.5}$, specifically secondary $PM_{2.5}$. The results show an opportunity to reduce the number of “All-cause” mortalities in the Highveld study area by up to ~1.32%. Reducing SO_2 and NO_x emissions from coal-fired power plants would have the greatest impact on lowering the ambient $PM_{2.5}$ attributed to these plants. A monetary value of R37.6 billion (SA2016R) was estimated for the relative reduction in the estimated mortality risk attributed to the large coal-fired power plants.

Keywords: aerosols, air pollution, coal-fired power, health impact, fine particulate, $PM_{2.5}$, secondary particulates, valuation

GLOSSARY

ACOM	Atmospheric Chemistry Observations and Modelling
AMA	Amajuba
APCV	Annual Precipitation Coefficient of Variation
AQG	Air quality guideline
AQMP	Air Quality Management Plans
BIC	Bushveld Igneous Complex
BOJ	Bojanala
CALPUFF	California Puff Model
CAMx	Comprehensive Air Quality Model with Extensions
CCRS	Coarse crustal
CDO	Climate Data Operators
CHPC	Centre for High Performance Computing
CO	Carbon monoxide
COPD	Chronic Obstructive Pulmonary Disease
CPRM	Coarse primary
CSIR	Council for Scientific and Industrial Research
CTM	Chemical Transport Model
DEA	Department of Environmental Affairs
DEAT	Department of Environmental Affairs and Tourism
DEFF	Department of Forestry, Fisheries, and the Environment
DM	District Municipality
EC	Elemental Carbon
ECLIPSE	Evaluating the Climate and Air Quality Impacts of Short-Lived Pollutants
EDGAR	Emissions Database for Global Atmospheric Research
EHL	Ehlanzeni
EKU	Ekurhuleni
FAC2	Fractions of Predictions within a Factor of Two of the observations
FB	Fractional Bias
FCRS	Fine crustal
FEZ	Fezile Dabi
FGD	Flue Gas Desulphurisation
FINN	Fire Inventory from NCAR
FPRM	Fine primary
GBD	Global Burden of Disease
GDP	Gross Domestic Product
GER	Gert Sibande
GEOS	Goddard Earth Observing System
GMAO	Global Modelling and Assimilation Office
GN	Government Notice
GG	Government Gazette
GRE	Greater Sekhukhune
HEI	Health Effects Institute
HNO_3	Nitric acid
HPA	Highveld Priority Area
HRAPIE	Health risks of air pollution in Europe
H2SO4	Sulphuric acid
IHD	Ischemic Heart Disease
JOH	City of Johannesburg
LNB	Low NO_x Burner
MAP	Mean Annual Precipitation
MAPE	Mean Annual Potential Evaporation
MASMS	Mean Annual Soil Moisture Stress
MAT	Mean Annual Temperature
MEGAN	Model of Emissions of Gases and Aerosols from Nature
MES	Minimum Emission Standards

MFD	Mean Frost Days
MG	Geometric Mean Bias
MM	Metropolitan Municipality
MOZART	Model for Ozone and Related Chemical Tracers
MW	Mega Watt
NA	Sodium
NAAQS	National Ambient Air Quality Standards
NAEIS	National Atmospheric Emissions Inventory System
NASA	National Aeronautics and Space Administration
NCAR	National Center for Atmospheric Research
NEMA	National Environmental Management Act (Act No. 107 of 1998)
NEM: AQA	National Environmental Management: Air Quality Act (Act No. 39 of 2004)
NetCDF	Network Common Data Form
NH_3	Ammonia
NH_4^+	Ammonium
NH_4NO_3	Ammonium nitrate
NKA	Nkangala
NMSE	Normalised Mean Square Error
NMVOC	Non-Methane Volatile Organic Compounds
NO	Nitrogen oxide
NO_2	Nitrogen dioxide
NO_3^-	Nitrate
NO_x	Nitrogen oxides
O_3	Ozone
OC	Organic Carbon
OECD	Organisations for Economic Co-operations and Development
PEC	Primary Elemental Carbon
PCL	Particulate Chloride
PH2O	Aerosol Water Content
PM	Particulate Matter
PNH4	Particulate Ammonium
PNO3	Particulate Nitrate
POA	Primary Organic Aerosol
PPP	Purchasing Power Parity
PSO4	Particulate Sulphate
SA	South Africa
SANRAL	South African National Roads Agency
SED	Sedibeng
SO_2	Sulphur dioxide
SO_4^{2-}	Sulphate
SOA	Secondary Organic Aerosols
Stats SA	Statistics South Africa
THA	Thabo Mofutsanyane
TROPOMI	TROPOspheric Monitoring Instrument
TSH	City of Tshwane
TUV	Tropospheric Ultraviolet and Visible
US EPA	United States Environmental Protection Agency
VG	Geometric Variance
VOC	Volatile Organic Compounds
VSL	Value of Statistical Life
VTAPA	Vaal Triangle Airshed Priority Area
WAT	Waterberg
WES	West Rand
WBPA	Waterberg Bojanala Priority Area
WHO	World Health Organisation
WRF	Weather Research and Forecasting
WTP	Willingness to pay
ZUL	Zululand

TABLE OF CONTENTS

LIST OF TABLES

LIST OF FIGURES

CHAPTER 1: INTRODUCTION

Chapter 1 provides a brief background on the relevance of atmospheric $PM_{2.5}$ and its risk to human health. It presents the motivation for the study in a problem statement, concluding with its primary aim and specific objectives.

1.1 Background

As a developing country, South Africa is confronted with the competing factors that come with growing an economy, i.e. ensuring social justice and protecting the environment. The battle is evident in, for example, the ongoing planned widespread electricity supply interruptions (i.e., load shedding) and the applications by the South African public power utility (Eskom) for relief[1] from the minimum emission standards (MES) specified for its combustion installations. Over the years, the power utility has been affected by many challenges including, but not limited to, a delay in the decision to start building new power generation capacity, delayed maintenance of its plants, returning to service of older power plants, supplying enough energy to meet demand, and complying with the MES for new plants (Pretorius *et al*., 2017; Eskom, 2019). Eskom appealed to the National Air Quality Officer that its existing coal-fired power plants cannot comply with the MES for new plants. Reasons for this include design-related limitations[2], its current financial constraints, the exorbitant cost of retrofitting abatement technologies, the age of the power plants, the quality of the coal used, the use and availability of water, and maintaining a reserve margin (Eskom, 2019). The plea by the power utility is real and severe, and most South Africans and the economy rely on Eskom to supply it with electricity. Competing with the electricity demand is the need for and the right to clean air for human health and well-being (Chen & Kan, 2008; Mabahwi *et al*., 2014; Murat, 2017). All South Africans have a right to a protected atmosphere that is not dangerous to their health or well-being, while supporting justified economic and social growth. A right enshrined in Section 24 of the Constitution of the Republic of South Africa (SA, 1996).

One region particularly affected by the competing factors of economic growth, social justice, and environmental protection is the Highveld. In March 2022, a judgement was handed down in the Pretoria High Court, ordering the government to implement and enforce the Highveld Priority Area (HPA) Air Quality Management Plan (AQMP). The judge stated: "*If air quality fails to meet the National Ambient Air Quality Standards, it is a prima facie violation of the right. When failure to meet air quality standards persists over an extended period of time, there is a greater likelihood that the health, well-being, and human rights of the people subjected to that air are being threatened and infringed upon*." (CER, 2022; Trustees for the time being of Groundwork Trust

[1] 2019 applications by Eskom for the suspension, alternative limits, or postponement of compliance to MES.
[2] The existing plants were designed before the promulgation of the MES and therefore were not designed to meet these standards.

and Another v Minister of Environmental Affairs and Others ZAGPPHC 208, 2022). In addition, the Highveld has meteorological conditions that are highly unfavourable for the dispersion of air pollution (Demircan & Sensoy, 2010; Garstang *et al*., 1996; Tyson *et al*.,1988; Tyson *et al*.,1996). The meteorological conditions combined with the industrialisation and urbanisation in the region have resulted in unsafe levels of fine particulate air pollution (e.g. $PM_{2.5}$) in many areas in the Highveld (Feig *et al*., 2019; Freiman & Piketh, 2002; Garland *et al.,* 2017*;* Govender & Sivakumar, 2019; Khumalo, 2020*;* Lourens, 2012; Muyemeki *et al*., 2020; Paton-Walsh *et al*., 2022; Scheifinger & Held, 1997; Venter *et al*., 2012).

1.2 Problem statement

$PM_{2.5}$ is an air pollutant that threatens human health and well-being. When inhaled, $PM_{2.5}$ can penetrate deep into the respiratory system and cause many adverse health impacts (US EPA, n.d.b; Falcon-Rodriquez *et al*., 2016; Nemmar, 2013; Nel, 2005; Bauer *et al.*, 2019). Long-term exposure to ambient $PM_{2.5}$ may even lead to premature death (Crouse *et al*., 2015; Dockery *et al*., 1993; Krewski *et al*., 2000; Lepeule *et al*., 2012). Exposure to ambient $PM_{2.5}$ dominates air pollution-related mortality over atmospheric gases (Bauer *et al.*, 2019) and is regarded as the most significant environmental risk factor in the world (HEI, 2020; GBD 2019 Demographics Collaborators, 2020). Liu *et al*. (2019) found that an increase of 10 $\mu g/m^3$ in $PM_{2.5}$ concentration was related to an increase of 0.68% (95% UI: 0.59 to 0.77) in a combined estimate of daily all-cause mortality globally and an increase of 0.8% (95% UI: 0.16 to 1.44) in South Africa.

The South African power generation sector, particularly coal-fired power plants, is a significant contributor to ambient $PM_{2.5}$ in the Highveld. Coal energy constitutes approximately 72% of the current installed power generation capacity in South Africa (SA. Department of Energy, 2019). Most of the coalfields in South Africa can be found in the Highveld (Jeffrey, 2005). The rich coal reserves and sufficient water resources at that time made this a prime area for coal-fired power plants (Scheifinger & Held, 1997), which resulted in most coal-fired power plants being located in the Highveld. Coal-fired power plants are known to generate air pollution, which could be harmful to human health (Barik, 2021; Koplitz *et al*., 2017; Langerman & Pauw, 2018; Zhao *et al*., 2021). These power plants are significant sources of sulphur dioxide (SO_2) and nitrogen oxides (NO_x), known precursor gases of secondary $PM_{2.5}$ air pollution (Bergin *et al*., 2005; Chow *et al*., 2004; Dodla *et al*., 2017; Kang *et al*., 2011; Watson *et al*., 2002; US EPA, 2019; Zhang, 2016). In South Africa, the power sector, particularly coal-fired power, is considered the highest contributor of $PM_{2.5}$ precursor gases (SO_2 and NO_x) (Pretorius *et al*., 2017; Ross, 2003; SA DEA, 2012a; Sivertsen *et al*., 1995; Scorgie *et al*., 2004; Scorgie & Thomas, 2006; SA DEA, 2012a).

Our understanding of the relationship between ambient $PM_{2.5}$, and the primary emissions of $PM_{2.5}$ and its precursor species from coal-fired power plants in the Highveld still needs improvement.

Several studies have examined the impact of criteria air pollutants from South African coal-fired power plants on human health. Of these studies, five (Gray, 2019; Marais *et al*., 2019; Myllyvirta, 2014; NEC & PAC, 2018; Steyn & Kornelius, 2018) considered the impact of $PM_{2.5}$. Myllyvirta (2014) used regression models taken from single-source chemical transport model runs (CAMx & CALPUFF). These model runs do not account for the complex atmospheric chemistry and circulation over South Africa, and the $PM_{2.5}$ emissions were estimated from the estimated PM_{10} emissions applying a ratio of 4/9. Marais *et al*. (2019) used a chemical transport model called GEOS-Chem. However, $PM_{2.5}$ was simulated over a large domain (Africa and South Africa) with a coarse grid (0.5° x 0.667°, ~50 km × 67 km). The study did not focus solely on coal-fired power plants but included emissions from natural gas- and bunker fuel-fired power stations and vehicle emissions. Gray (2019), Steyn & Kornelius (2018) and NEC (2018) used the CALPUFF dispersion modelling suite and simulated fine particulates over the Highveld. It is unclear if background conditions were considered, perhaps through the input of ambient values. However, none of the CALPUFF studies explicitly account for pollution transported across the boundary, nor do they explicitly account for all other major sources[3] in the Highveld in the formation of secondary $PM_{2.5}$. For instance, these studies do not explicitly account for particulates formed when ammonia emissions from agriculture neutralise sulphuric acid formed from SO_2 emissions from coal-fired power plants. Current studies, therefore, do not represent a complete estimate of the secondary $PM_{2.5}$ attributable solely to coal-fired power plants in the Highveld. Understanding the relationship between ambient $PM_{2.5}$, particularly secondary $PM_{2.5}$, and the contribution from significant sources, such as coal-fired power plants, in the Highveld, is essential in estimating the burden of disease associated with $PM_{2.5}$ air pollution in this region. The estimated health impact and its monetary value inform policymakers, supporting the development of strategies and plans to improve air quality. Source apportionment is valuable in understanding the relationships between pollutants and polluters. However, source apportionment of $PM_{2.5}$ is complex because most of the $PM_{2.5}$ is formed in the atmosphere (Langerman & Pauw, 2018; Maenhaut *et al*., 1996; Piketh *et al*., 1999a). This study simulated the Highveld atmospheric chemistry with and without emissions from the coal-fired power plants at a high spatial resolution with a chemical transport model (Parent domain: 0.06° x 0.06° & Nest domain: 0.02° x 0.02°) to investigate the impact of $PM_{2.5}$ attributable to coal-fired power plants. The chemical transport model, CAMx[4], used for this study is a photochemical grid model with a more complex chemical mechanism than the CALPUFF model ((Trozzi *et al*., 2009) used in the previous industrial Highveld studies. Most of the coal-fired power plants in the Highveld (i.e., 96% of the installed capacity, Figure 12) are operated by the public power utility Eskom. By subtracting a concept simulation, where all large (≥1 000 MW) coal-

[3] Examples include biomass burning, other industries, biogenic VOCs and ammonia from agriculture, domestic fuel combustion and on-road vehicles.
[4] Comprehensive Air Quality Model with Extensions.

fired power plant emissions are excluded, from the baseline simulation of the Highveld atmosphere, the study can attribute a more complete simulated impact of the large coal-fired power emissions on the annual average $PM_{2.5}$ over the Highveld.

1.3 Aims and objectives

The aim of this study is to evaluate the total contribution of coal-fired power plant emissions to ambient $PM_{2.5}$ and its impact on human health over the Highveld. The following objectives were formulated to achieve the aim of this study:

Objective 1: Examine the effect that coal-fired power plant emissions have on the secondary particulate chemistry of the atmosphere over the Highveld.

The emissions of primary particulates, precursor gases (SO_2, NO_x, ammonia (NH_3) and organic compounds) from coal-fired power plants and other sources, as well as the formation of secondary particulates in the Highveld atmosphere are simulated using the state-of-the-science chemical transport model, CAMx.

Objective 2: Evaluate the concentration of $PM_{2.5}$ attributable to the coal-fired power plants in the Highveld.

A contrast between two separate atmosphere simulations; a baseline simulation of the ambient $PM_{2.5}$ from all emitters within the Highveld compared to a concept simulation, where emissions from all large coal-fired power plants are excluded in CAMx. The comparison allows for the isolation of the $PM_{2.5}$.

Objective 3: Evaluate the impact of the $PM_{2.5}$, attributable to the coal-fired power plants in the Highveld, on human health.

The health impacts and economic value of $PM_{2.5}$ attributed to coal-fired power plants on the Highveld are evaluated by estimating the potential for avoidable premature mortality and the willingness to pay for marginal changes to reduce mortality risk.

CHAPTER 2: LITERATURE REVIEW

The literature review starts by briefly introducing air quality management in South Africa. Section 2.2 of Chapter 2 then discusses air quality in the Highveld region, first contextualising the Highveld region to better understand the circumstances that formed the setting for its industrialisation and urbanisation. This section then looks at the sources and their estimated contribution to air pollution, the meteorological conditions,and the movement of air masses over the Highveld. Section 2.2.5 considers air quality hotspot areas in the Highveld region and the criteria pollutants of concern in these areas, while Section 2.2.6 discusses the Highveld ambient $PM_{2.5}$ and the sources contributing to it. Section 2.3 focuses on one of the significant $PM_{2.5}$ source sectors identified in section 2.2.6, i.e. coal-fired power plants. Before concluding the literature review, Section 2.4 examines why long term exposure to $PM_{2.5}$ presents a risk to human health.

2.1 Air quality management in South Africa

Instrumental in controlling the competing factors that come with growing an economy, ensuring social justice, and protecting the air quality in South Africa is the Constitution of the Republic of South Africa (the Constitution). Section 24 of the Constitution (SA, 1996) enshrines the right to a natural environment (including the atmosphere) that is protected and not detrimental to the health or well-being of South Africans while supporting justified economic and social growth. To improve the law regulating air quality in line with Section 24 of the Constitution, South Africa promulgated the National Environmental Management Act (Act No. 107 of 1998) (NEMA) in 1998 and the National Environmental Management: Air Quality Act (Act No. 39 of 2004) (NEM: AQA) in 2004. In South Africa, acceptable levels of atmospheric pollutants that is not detrimental to human health or well-being was specified through the creation of the National Ambient Air Quality Standards (NAAQS) for criteria pollutants[5] in terms of Section 9(1) of NEM: AQA (SA DEA, 2009; SA DEA, 2012b; SA DEA, 2018). NEMA and NEM: AQA, in turn, are responsible for promulgating several lists, regulations, guidelines, and declarations aimed at achieving these standards and protecting the environment from air pollution. Of these, the declarations made in terms of Section 18 (1) of NEM: AQA and the list of activities published in terms of Section 21 of NEM: AQA require some contextualisation, as they are referred to in later sections and chapters.

Priority areas are declared in terms of Section 18 (1) of NEM: AQA when there is reason to believe that the NAAQS in an area is being or may be exceeded, or a situation exists that is causing or may cause a detrimental impact on the air quality in an area. To date, South Africa has declared three airshed priority areas at a national level. None have been declared at the provincial level.

[5] These criteria pollutants are sulphur dioxide (SO_2), nitrogen dioxide (NO_2), particulate matter 10 (PM_{10}), particulate matter 2.5 ($PM_{2.5}$), ozone (O_3), benzene (C_6H_6), lead (Pb) and carbon monoxide (CO).

The priority areas include the Highveld Priority Area (HPA), the Vaal Triangle Airshed Priority Area (VTAPA) and the Waterberg Bojanala Priority Area (WBPA) (SA, 2006; SA, 2007; SA, 2012). All three fall within the extensive interior plateau of South Africa. Air quality management plans (AQMPs) (SA DEA, 2012a; SA DFFE, 2021; SA DEA, 2015) have been developed for each priority area in terms of Section 19 of NEM: AQA.

Another important regulatory tool for achieving NAAQS is licensing atmospheric emissions from significant industries. The list of activities published in terms of Section 21 of NEM: AQA in Government Notice (GN) 893 in Government Gazette (GG) 37054 dated 22 November 2013 (as amended[6]) ("S21 listed activities") are activities believed to have or present significant detrimental effects on the environment. The S21 listed activities are divided into ten categories and cover a range of significant industries[7]. Minimum emission standards (MES) are specified for existing- and new plants for each S21 listed activity and compliance timeframes are provided for each type of plant. To ensure the regulation of the impact on air quality from these dangerous or potentially dangerous activities, Section 22 of NEM: AQA provides that no person may perform any S21 listed activity without an atmospheric emission license (AEL). Compliance with the maximum release rates (based on the MES) and other conditions within the AEL or provisional AEL are then tracked and enforced by Licensing Authorities and Environmental Management Inspectors.

2.2 Air quality in the Highveld region

2.2.1 Industry and urbanisation in the Highveld

The extensive interior plateau ("the greater Highveld") of South Africa (Scheifinger & Held, 1997) is marked by large industrial and urban areas (Freiman & Piketh, 2002; Lourens, 2012; Paton-Walsh *et al*., 2022; Scheifinger & Held, 1997; Venter *et al*., 2012). South Africa holds the largest share (91%) of the platinum group metals (PGM) reserves in the world (DMR, 2019; GCIS, 2012; Yager, 2022). Most of the PGM is produced in the Bushveld Igneous Complex (BIC) (Venter, 2012), a vast composite of plutonic and volcanic rocks (Cousins, 1959) stretching across the North-West, Gauteng, Mpumalanga, and Limpopo (Venter *et al*., 2012). The BIC also has significant reserves of chrome, vanadium, cobalt, nickel, tin, and copper (Venter, 2012). In addition, most of the coal reserves in South Africa (70%) can be found in the greater Highveld (Jeffrey, 2005). The Mpumalanga central basin, comprised of the Witbank-, Highveld- and Ermelo coalfields, yielded 82.5% of the coal in South Africa in 2016 (DMR, 2019). The significant deposits of many important minerals have given rise to the industrialised Highveld in Mpumalanga

[6] As amended by GN 551 of GG 38863 on 13 June 2015, GN 1207 in GG 42013 on 31 October 2018, GN 686 in GG 42472 on 22 May 2019.

[7] These include large combustion installations; petroleum production, handling, storage, and recycling; carbonisation and coal gasification; metallurgical activities; mineral processing, storage, and handling; activities in the inorganic chemicals industry; the thermal treatment of hazardous and general waste; pulp and paper manufacturing and animal matter processing.

(Freiman & Piketh, 2002; Paton-Walsh *et al*., 2022; Scheifinger & Held, 1997) and the large industrial areas over the western BIC (Venter *et al.,* 2012) along the northern side of the Magaliesberg mountains. The western limb of the BIC is the most exploited and developed (Venter *et al.,* 2012). The Gauteng province is centrally located between the Mpumalanga Highveld and the western BIC. In addition to having heavy industry, the urban areas, towns, and cities of Gauteng have integrated into a city region (GCRO, n.d). Gauteng is the smallest province in South Africa, however, most South Africans (26.6%) live in this province, making it the most densely populated province in South Africa and home to the Johannesburg-Pretoria megacity (Lourens, 2012; Stats SA, 2022).

2.2.2 Sources of air pollution in the Highveld

The air quality of the Highveld (mainly the industrial and urban areas) is impacted on by a wide range of air pollution sources that include but are not limited to, mining, industry, traffic, domestic fuel- and biomass burning (Altieri *et al*., 2022; Beukes *et al*., 2013; Feig *et al*., 2016; Lourens *et al*., 2011; Piketh *et al*., 1999a; Scorgie *et al.,* 2005; Venter *et al*., 2012). A concern that these sources may be causing a negative impact on the air quality of the Highveld has led to the declaration of three airshed priority areas in the region. These priority areas are the Highveld Priority Area (HPA), the Vaal Triangle Airshed Priority Area (VTAPA), and the Waterberg Bojanala Priority Area (WBPA) (SA, 2006; SA, 2007; SA, 2012). Within the HPA, primary sources include power generation, coal mining, primary metallurgy, secondary metallurgy, brick manufacturing, the petrochemical industry and other industries in Ekurhuleni and Mpumalanga (SA DEA, 2012a). Significant sources in the VTAPA include windblown dust from mine waste facilities, product stockpiles, ash storage facilities, domestic fuel burning, mobile sources, biomass burning, industrial sources, Biogenic volatile organic compound emissions and ammonia emissions from agriculture (SA DFFE, 2021). The WBPA comprises the Waterberg District Municipality (DM) and the Bojanala-Platinum DM. Power generation is considered the leading industrial source sector in the Waterberg DM within the WBPA (SA DEA, 2015). The Matimba coal-fired power plant and the Grootgeluk coal mine contributed to approximately 96% of emissions in the Waterberg DM. The AQMP notes that most of the mines did not provide their emission data, and it is, therefore, possible that the contribution of particulate matter 10 (PM_{10}) and sulphur dioxide (SO_2) emissions from coal-fired power plants are overestimated (SA DEA, 2015). Within the Bojanala-Platinum DM, mining and mineral processing is considered the primary source of emissions. The exploitation of the western BIC includes PGM mining, chromite mining, refineries, ferrochrome smelting, ferrovanadium production, vanadium pentoxide production and pyrometallurgical smelting (Venter *et al*., 2012). Other sources of concern include motor vehicle emissions, mining, domestic fuel burning in rural areas, waste disposal and burning of waste, biomass burning, agricultural activities and transboundary movement of air pollutants (SA DEA, 2015). The air

pollution sources within the Highveld range from mining, processing, refining, manufacturing, energy generation, agriculture, waste management, biomass burning, traffic, and domestic activities such as fuel burning and are more evident in the industrial and urban areas of the industrial Highveld, the western BIC, airshed priority areas and the Gauteng province.

2.2.3 Air pollution source contribution in the Highveld

The industrial sector is a significant contributor to air pollution in the HPA, the VTAPA and the WBPA (SA DEA, 2012a; SA DFFE, 2021; SA DEA, 2015). Approximately 90% of the estimated industrial emissions of particulate matter (PM), SO_2 and nitrogen oxides (NO_x) in South Africa originate from the industrial Highveld in Mpumalanga (Freiman & Piketh, 2002; Held *et al*., 1996; Wells *et al*., 1996). PM_{10} and $PM_{2.5}$ are particulate air pollutants with aerodynamic diameters less than 10 and 2.5 micrometres, respectively. Figure 1 shows that opencast mine haul roads account for approximately half of the estimated annual PM_{10} emissions in the HPA (SA DEA, 2012a). At the same time, coal-fired power generation emits 73% of the total estimated NO_x and 82% of the total estimated SO_2 (SA DEA, 2012a). The second generation AQMP for the VTAPA found the industrial sector to be the most significant contributor of SO_2 (99.8%), NO_x (93%) and PM_{10} (52%) emissions in the VTAPA. Figure 2 shows that windblown dust from mine waste facilities, product stockpiles and ash storage facilities are the main contributors to $PM_{2.5}$ (56%), followed by domestic fuel burning (29%). Carbon monoxide (CO) emissions were found to originate primarily from domestic fuel burning (28%), transport (27%), biomass burning (26%) and industrial sources (19%). 55% of non-methane volatile organic compounds (NMVOCs) were attributed to Biogenic volatile organic compound (VOC) emissions from plants, and agriculture was found to be the primary source of ammonia emissions (NH_3) (87%) (SA DFFE, 2021). Figure 3 shows that power generation is the leading industrial source sector in the Waterberg DM in the WBPA, contributing to 62% of PM_{10}, 99% of SO_2 and 99% of total NO_x emissions from industries in the municipality (SA DEA, 2015). Unlike the Waterberg DM, there is no significant outlier in the Bojanala-Platinum DM. Mining and mineral processing was found to be the primary source of PM_{10} (80%), SO_2 (78%) and NO_x (70%) emissions (SA DEA, 2015). The Waterberg DM is also home to two large coal-fired power plants, Matimba (3990 MW) and Medupi (4800 MW)[8][9]. The VTAPA AQMP attributes most of the SO_2 and NO_x in this area to the industrial sector. However, the large, Lethabo coal-fired power plant (3708 MW[10]) formed part of the industrial sources that contributed significantly to SO_2 and NO_x. It is, therefore, sensible that the power sector, particularly coal-fired power, is considered the highest contributor of SO_2 and NO_x in the Highveld (Pretorius *et al*., 2017; Ross, 2003; Sivertsen *et al*., 1995; Scorgie *et al*., 2004; Scorgie & Thomas, 2006).

[8] The total capacity (MW) for Matimba and Medupi was taken from Escience Associates, 2017.
[9] The Medupi coal-fired power plant only achieved commercial operation status in 2021.
[10] The total capacity (MW) for Lethabo was taken from NEC, 2018.

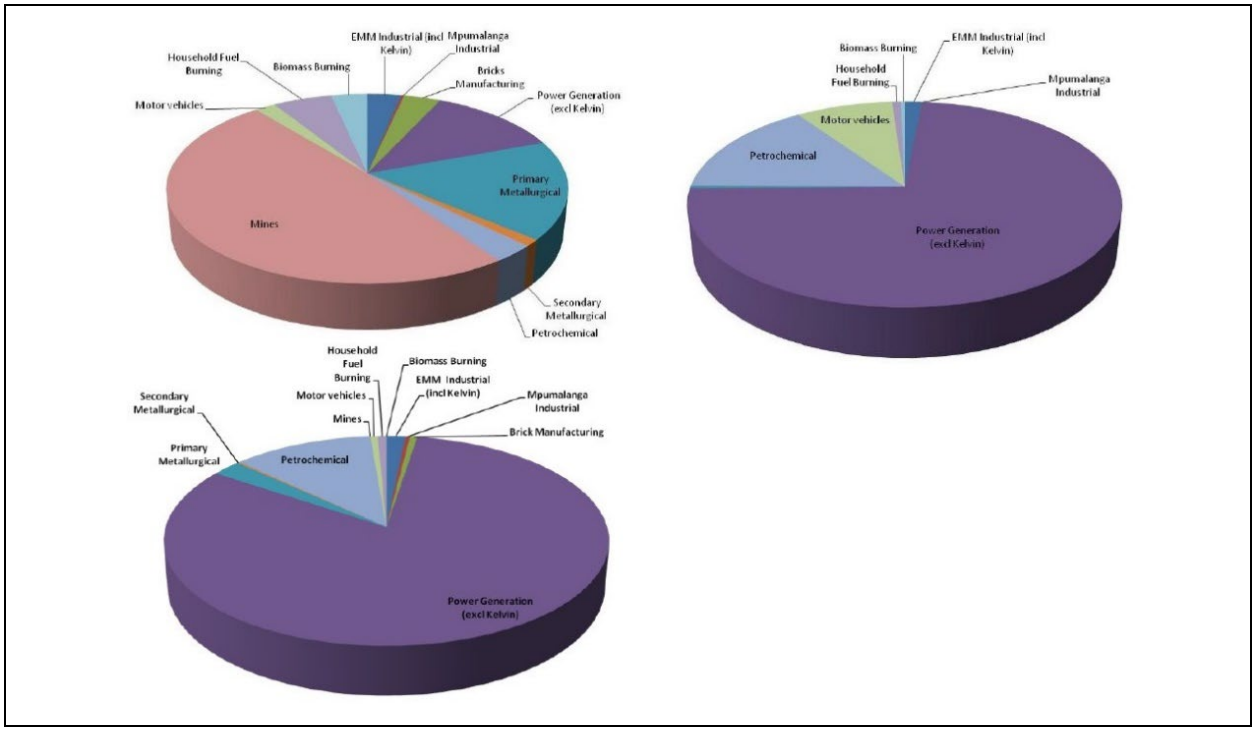

Figure 1: The relative contribution of significant polluters to total emissions of PM_{10} (top left), NO_x (top right) and SO_2 (bottom left) in the HPA (Adapted from SA DEA, 2012a).

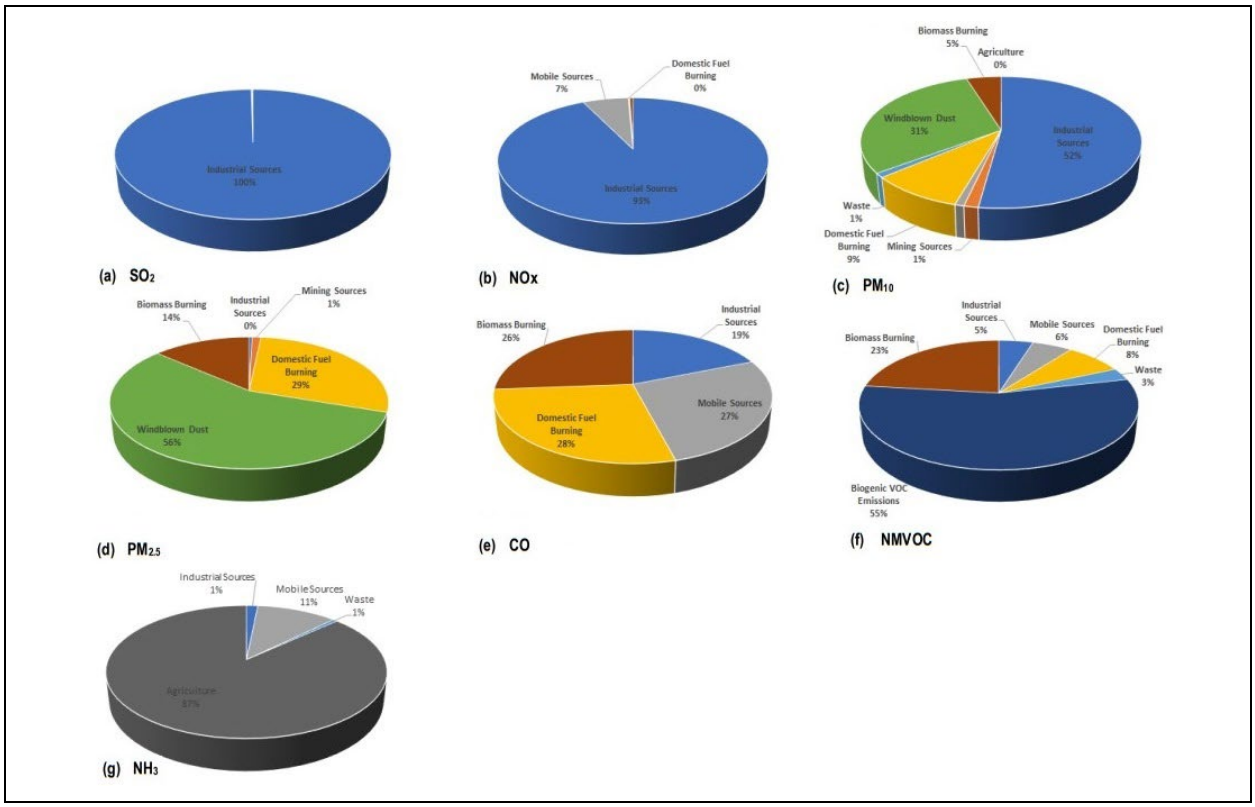

Figure 2: The relative contribution of significant polluters to total emissions of SO_2, NO_x, PM_{10}, $PM_{2.5}$, CO, NMVOC and NH_3 in the VTAPA (Adapted from SA DFFE, 2021).

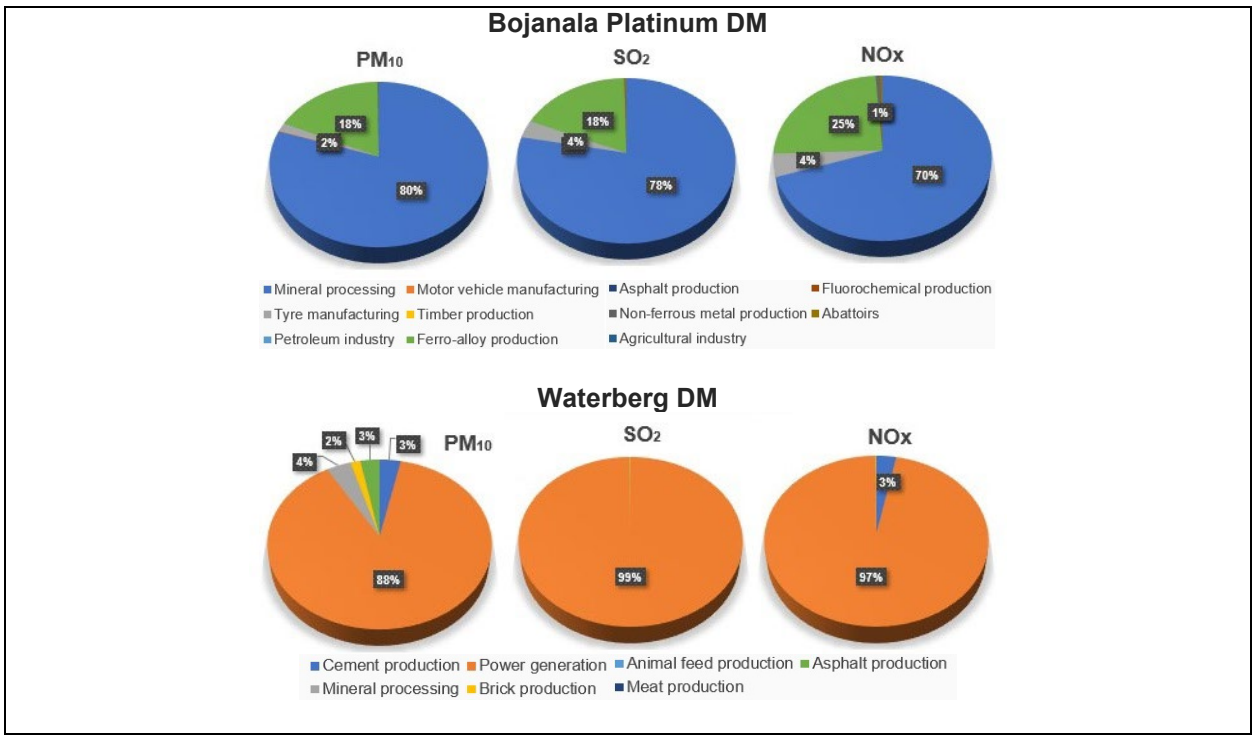

Figure 3: The relative contribution of significant industrial polluters to total emissions of SO_2, NO_x and PM_{10} in the WBPA (Adapted from SA DEA, 2015).

2.2.4 Atmospheric conditions and circulation in the Highveld

Meteorological conditions

The meteorology in the Highveld favours the accumulation of air pollution, especially in winter (Garstang *et al*., 1996; Tyson *et al*.,1988; Tyson *et al*.,1996). The Highveld climate is affected by four major circulation types: semi-permanent subtropical high-pressure, transient mid-latitude ridging high-pressure, westerly baroclinic disturbances, and barotropic quasi-stationary tropical easterly waves (Garstang *et al*., 1996; Tyson *et al*., 1996). Anticyclonic circulation prevails throughout the year, particularly in the winter (80%) (Garstang *et al*., 1996; Tyson *et al*.,1988; Tyson *et al*.,1996). South Africa falls south of 15 ºS in the subtropical high-pressure belt (Tyson *et al*., 1996). This region experiences large-scale subsidence (Garstang *et al*., 1996; Tyson *et al*., 1996). The air in the subtropics cools and descends, creating anticyclones (i.e., high-pressure areas) (Demircan & Sensoy, 2010). The descending air is warm and dry, and high-pressure areas are seen with clear atmospheres and low rainfall (Demircan & Sensoy, 2010). Elevated inversions are common in anticyclones (i.e., high-pressure areas) (Preston-Whyte & Tyson, 1993) and limit the height to which air pollutants can diffuse and disperse vertically (Igbafe, 2007). Elevated inversions promote the transport of air pollutants over long distances and the recirculation of air pollution (Diab, 1975; Harrison, 1993; Garstang *et al.*, 1996). Three main and frequently occurring stable layers control the vertical mixing and air transport at the dry season's end. The two lowest levels appear to be the most significant and occur with high regularity and spatial ambiguity. The lowest layer, approximately 1.5 km above the Highveld surface, is usually seen at the top of the

daytime mixing layer. This layer is broken by the regularly occurring westerly wave disturbances every 5 to 7 days (Garstang *et al.,* 1996). Above this layer, at approximately 3.5 km above the Highveld surface, is another stable layer that persists for up to 40 days (Garstang *et al.,* 1996). Transport to the upper troposphere can only occur when this layer is not present and strong, and deep lifting by convection occurs (Garstang *et al.,* 1996). A near-ground level (a few tens of meters) temperature inversion develops at night when the earth's surface cools. Surface inversions are stronger in drier atmospheres. A less intense inversion layer of a few hundred meters forms above this layer, and a third isothermal layer usually occurs above the second less intense inversion layer. These three layers form the stable night-time surface layer. In winter, the average inversion (280m deep, with a temperature difference of 7-8ºC between the near-ground and top of inversion levels) occurs every four out of five nights (Tyson *et al*.,1988). In summer, surface inversions may appear more than two out of three nights. Only clouds or fierce winds will prevent surface inversion from forming. Due to fierce winds, spring has the least frequent amount of inversions (Tyson *et al*.,1988). The Highveld falls within a summer rainfall region with frigid and dry winters. (Musina & Rutherford, 2010; Tyson *et al*., 1976). Figure 4 shows the average monthly precipitation and mean daily minimum and maximum temperatures for the grassland and savanna biomes in the Highveld. The semi-permanent anticyclonic circulations over the Highveld region result in meteorological conditions that are highly unfavourable for the dispersion of air pollution. These conditions include clear skies, a highly stable vertical atmosphere, low wind speeds, frequent surface- and elevated temperature inversions and low rainfall, particularly in the winter (Demircan & Sensoy, 2010; Garstang *et al*., 1996; Tyson *et al*.,1988; Tyson *et al*.,1996).

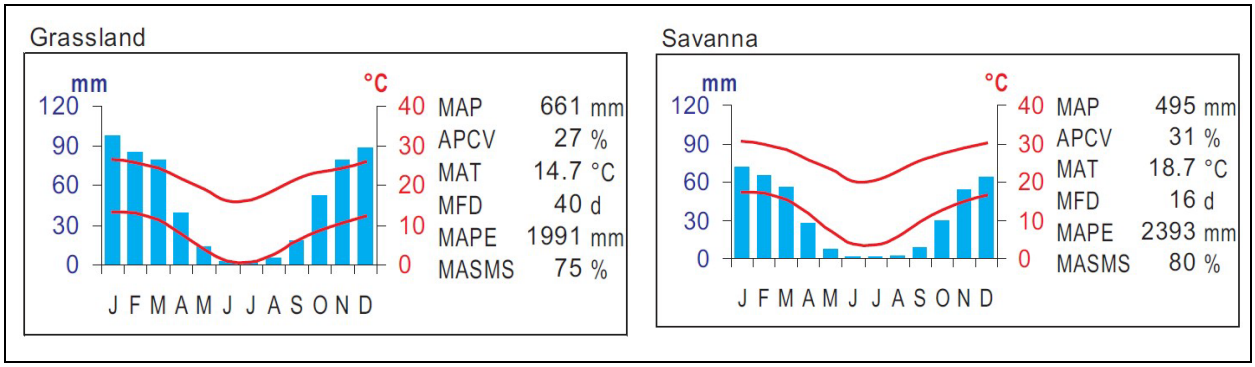

Figure 4: Climate diagrams of biomes extracted from Musina & Rutherford, 2010. The blue bars indicate the average monthly precipitation. The upper and lower red lines represent the mean daily maximum and minimum temperatures[11]*. The Grassland biome occurs over the greater part of the study area. Some areas fall within the Savanna biome, particularly the north-western corner of the study area. Climatically the Grassland and Savanna biomes are similar, with lower temperatures in the Grassland biome (Adapted from Musina & Rutherford, 2010).*

[11] MAP: Mean Annual Precipitation; APCV: Annual Precipitation Coefficient of Variation; MAT: Mean Annual Temperature; MFD: Mean Frost Days; MAPE: Mean Annual Potential Evaporation; MASMS: Mean Annual Soil Moisture Stress.

Air masses transported to the Highveld

Most of the air transported into the Highveld is clean marine air. However, the region can be impacted by emissions from subtropical Africa and South Africa (Freiman & Piketh, 2002). Figure 5 gives a rough illustration of the primary pathways of air transported into the Highveld and the percentage occurrence of the pathways. The four major transport pathways to the Highveld include airflow from the Atlantic Ocean, the Indian Ocean, subtropical Africa, and South Africa. Air is transported most frequently (43%) from the Atlantic Ocean, followed by the Indian Ocean flow (26%), the African flow (25%), and the subcontinental flow (7%). A sizeable portion of the air (at least 43%) impacting the Highveld is clean marine air (Freiman & Piketh, 2002). The African flow carries particulate emissions from substantial biomass burning and tall stacks north of South Africa into its centre (Andreae *et al*., 1996; Garstang *et al*., 1996; Piketh, 1996). The African flow may carry industrial emissions from as far as central-southern Africa, particularly from the Zambian “copper belt” over South Africa (Freiman & Piketh, 2002).

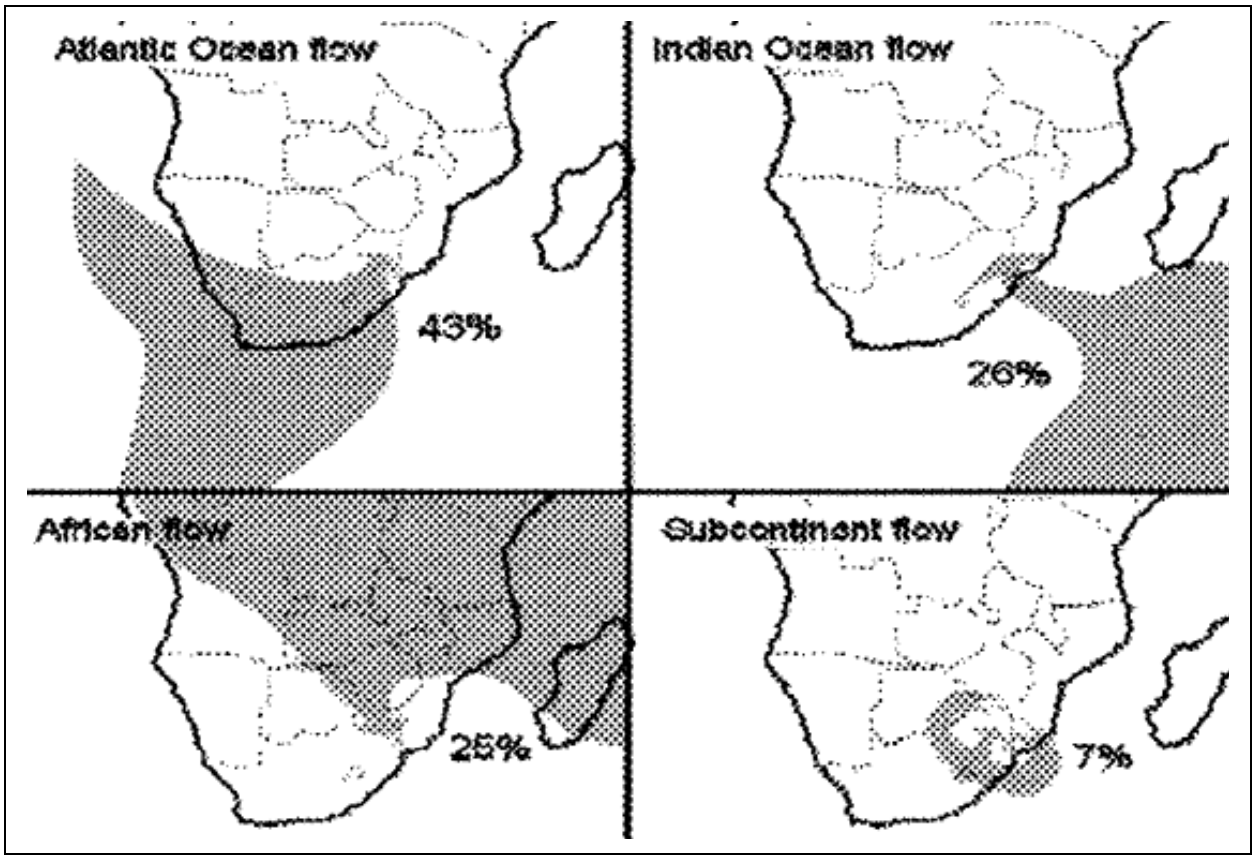

Figure 5: Air transport pathways (based on a group of trajectories between 850 and 700 hPa) and frequency (%) of occurrence of air moving to the Highveld (Taken from Freiman & Piketh, 2002).

Air masses transported from the Highveld

Air pollution transported out of the industrial Highveld in Mpumalanga can reach remote regions of South Africa and southern Africa (Piketh *et al*., 1999a; Piketh *et al*., 1999b). Air pollution is transported out of the Highveld through direct or recirculated low to mid-tropospheric flow. The

direct transport of material in a northerly (to the south Indian Ocean), easterly (the Atlantic Ocean), southernly (to equatorial Africa) and westerly (to the Indian Ocean) direction of the Highveld occurs with minor delay (Freiman & Piketh, 2002). The air passing over the industrial Highveld is transported mainly to the southwest and south Indian Ocean (45%), followed by regional and subcontinental scale recirculation (33%) and air transported to the Atlantic Ocean (14%) (Freiman & Piketh, 2002). Air masses over the central region of South Africa are expected, on average, to recirculate 40% of all days in a year, with the highest frequency (70%) in July. Up to 54% of the particulates transported across southern Africa complete one recirculation cycle before exiting to the Indian Ocean to the East. As much as 23% may be recirculated a second time (Tyson *et al.*,1996). Recirculation occurs over distances that range from tens to thousands of kilometres (Tyson *et al.*,1996). Depending on the scale of the circulation, local recirculation periods range from 2 to 9 days (Freiman & Piketh, 2002). The effects of recirculating particulates may be considerable (Tyson *et al.*,1996). Figure 6 gives a rough illustration of the primary pathways of air transported out of the Highveld and the percentage occurrence of the pathway. The recirculated air parcels can reach the remote regions of South Africa within hours to 2-7 days (Freiman & Piketh, 2002). A substantial portion (41%) of the direct and recirculated airflow originating over the industrial Highveld affects neighbouring countries, especially Botswana, Mozambique, and Zimbabwe (Freiman & Piketh, 2002). In stable atmospheric conditions, the air from the industrial Highveld may reach as far as Kenya and Zaire (Freiman & Piketh, 2002; Gatebe *et al.*, 1999).

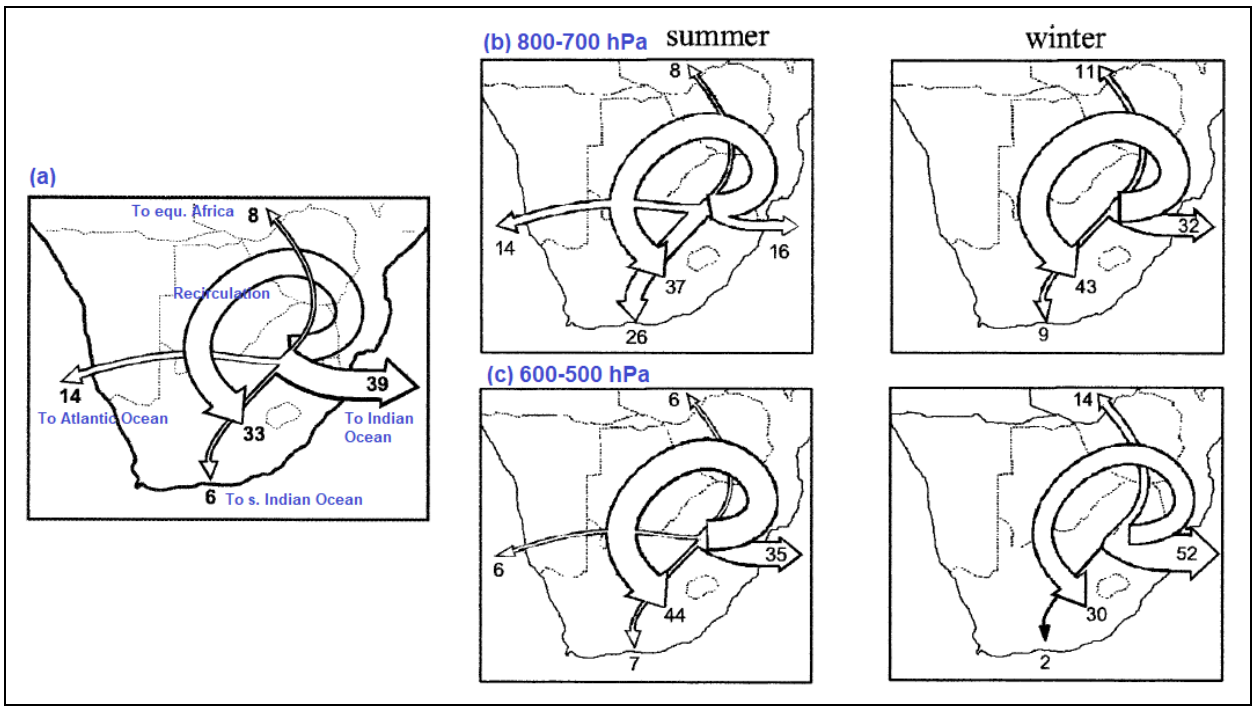

Figure 6: (a) The primary pathways of air transported out of the Highveld at 800-700 hPa and the occurrence (%) the pathway. (b) Seasonal air transport at 800-700 hPa. (c) Seasonal air transport at 600-500 hPa (Adapted from Freiman & Piketh, 2002).

2.2.5 Air quality hotspot areas in the Highveld

Air pollution contributes significantly to premature mortality. A large body of evidence suggests that exposure to air pollution can have severe health impacts (Brook *et al*., 2004; Brook *et al*., 2010; Dockery *et al*., 1993; Hystad *et al*., 2020; Lim *et al*., 2020; Mannucci & Franchini, 2017; McGranahan & Murray, 2003; Pope *et al*., 2002; Rao, 2015; Schraufnagel, 2018a; Schraufnagel, 2018b). Lelieveld *et al*. (2015), following the 2010 global burden of disease, calculated 3.3 million (95% UI: 1.16 to 4.81 million) premature mortality globally per year (predominantly in Asia) and projected that, based on a business-as-usual scenario, the impact of outdoor air pollution could double by 2050. However, the 2020 Global Burden of Disease study found that in 2019, air pollution already contributed to an estimated 6.67 million premature loss of life (95% UI:5.9 to 7.49 million) globally. Air pollution has become the fourth overall and the leading environmental risk factor for premature mortality (GBD 2019 Demographics Collaborators, 2020, HEI, 2020; WHO, 2021b). Bauer et al. (2019) estimated that 89% of premature deaths in South Africa are due to air pollution from anthropogenic emissions.

The presence of significant emitters in the Highveld (Altieri *et al*., 2022; Beukes *et al*., 2013; Feig *et al*., 2016; Lourens *et al*., 2011; Piketh *et al*., 1999a; SA, 2006; SA, 2007; SA, 2012; Scorgie *et al*., 2005; Venter *et al*., 2012), the air pollution from the African flow (Andreae *et al*., 1996; Freiman & Piketh, 2002; Garstang *et al*., 1996; Piketh, 1996) and the meteorological conditions unfavourable for atmospheric dispersion (Garstang *et al*., 1996; Tyson *et al*.,1988; Tyson *et al*.,1996) have created areas in the Highveld region where levels of criteria air pollutants are in exceedance or likely to exceed the NAAQS for these pollutants (Feig *et al*., 2019; Garland *et al*., 2017; Govender & Sivakumar, 2019; Khumalo, 2020; Lourens *et al.*, 2012; Venter *et al*., 2012; SA, 2006; SA, 2007; SA, 2012). Nine hotspot areas where ambient concentrations of PM_{10}, SO_2 and NO_2 exceed or are likely to exceed national ambient air quality standards have been identified in the HPA. These hotspot areas include Emalahleni, Kriel, Steve Tshwete, Ermelo, Secunda, Ekurhuleni, Lekwa, Balfour and Delmas (SA DEA, 2012a). PM_{10} exceeds or is predicted to exceed its ambient standards in all hotspot areas except Kriel and Delmas. NO_2 exceeds or is predicted to exceed its ambient standards in Steve Tshwete and Secunda. SO_2 exceeds or is predicted to exceed its ambient standards in all hotspot areas except Balfour (SA DEA, 2012a). Global maps from satellite retrievals show the Highveld as a prominent NO_2 hotspot (Lourens *et al.*, 2012). Lourens *et al*. (2012) found a second NO_2 hotspot, the Johannesburg-Pretoria megacity, where peak morning and afternoon NO_2 levels exceeded the maximum daily levels found over the Highveld. Six hotspot areas have been identified in the VTAPA. These hotspot areas include the residential areas of Sasolburg, Zamdela and Coalbrook (Zone 1), an area just south of the residential area of Vereeniging (Zone 2), developments of Vanderbijl Park and Sebokeng (Zone 3), residential developments of Vereeniging and Meyerton (Zone 4), residential developments of

Orange Farm, Evaton and Ennerdale (Zone 5) and the residential area of Soweto. PM_{10}, SO_2 and NO_x, are of concern for all zones. VOCs are of concern for all zones except Zone 2, and H_2S is of concern in Zone 1. Odour is of concern in Zone 3, and ozone (O_3) is a concern in Zone 3 and 4 (SA DFFE, 2021). Areas of concern in the WBPA include high concentrations of SO_2 affecting towns in the Phalaborwa region and predicted exceedances of the PM_{10} National NAAQS near human settlements around Lephalale (SA DEA, 2015). It is anticipated that the WBPA will be impacted by the extended transport of emissions from the Morupule Power Plant near Palapye in eastern Botswana (SA DEA, 2015).

2.2.6 Ambient $PM_{2.5}$ in the Highveld

Ambient $PM_{2.5}$ exceeding NAAQS in the Highveld

Among all the criteria air pollutants, $PM_{2.5}$ may present the most significant risk to human health in the Highveld. Annual average levels of SO_2 at several sites, except for eMalahleni, within the HPA, the VTAPA and the WBPA, were considerably lower than its NAAQS (Feig *et al*., 2019; Khumalo, 2020). In contrast, the annual average levels of PM_{10} and $PM_{2.5}$ were found in non-compliance with historical and current NAAQSs (Feig *et al*., 2019; Garland *et al*., 2017; Govender & Sivakumar, 2019; Khumalo, 2020). Sampling from 2008 to 2010 at Marikana found ambient concentrations of PM_{10} and O_3 to frequently exceed their respective NAAQS (Venter *et al*., 2012). The 2019 global burden of disease study found air pollution to be the leading environmental risk factor for premature mortality and considers long-term exposure to $PM_{2.5}$ as its dominant contributor (GBD 2019 Demographics Collaborators, 2020, HEI,2020). The relationship between exposure to $PM_{2.5}$ air pollution and the increased risk of health effects is well-documented (Chung *et al*., 2015; Krewski *et al*., 2009; Lepeule *et al*., 2012; Lin *et al*., 2017; Liu *et al*., 2019; Ostro *et al*., 2015; Pope *et al*., 2002; Valavanidis *et al*., 2008; Yang *et al*., 2019). In South Africa, and therefore over the Highveld, the current NAAQS for annual $PM_{2.5}$ is 20 µg/m^3 and 15 µg/m^3 from 1 January 2030 (SA. DEA. 2012b). The NAAQS in South Africa are much higher than those recommended by the WHO (2005 AQG: 10 µg/m^3 & 2021 AQG: 5 µg/m^3, WHO, 2006), and adverse health effects have been found to persist at concentrations far below those recommended by the WHO (Brauer *et al*., 2019; Shah *et al.,* 2013; Wellenius *et al.,* 2012). The increased risk of health effects from exposure to $PM_{2.5}$ air pollution is well documented. However, ambient $PM_{2.5}$ in South Africa is regulated at levels well above those recommended by the WHO and those found to present adverse impacts on human health. This means that even if $PM_{2.5}$ levels in South Africa fell below the NAAQS, there is still a risk that it may impact human health.

Regardless of the higher standard for annual average $PM_{2.5}$ (compared to WHO guidelines), several areas within the Highveld region experience $PM_{2.5}$ at levels exceeding the current NAAQS for annual average $PM_{2.5}$, signifying the severity of the problem in South Africa (Garland *et al.*, 2017; Govender & Sivakumar, 2019; Khumalo, 2020). Figure 7 shows the annual average

concentrations of $PM_{2.5}$ at Ermelo, Hendrina, Middelburg, Secunda and eMalahleni within the HPA with frequent exceedances of the NAAQSs for annual average $PM_{2.5}$ from 2009 to 2019 evident. Exceedances of the NAAQSs for annual average $PM_{2.5}$ are even more prevalent at Diepkloof, Kliprivier, Sebokeng, Sharpeville, Three Rivers and Zamdela in the VTAPA. Govender & Sivakumar (2019), in a decadal analysis of $PM_{2.5}$ ground-level concentrations in the VTAPA, found Kliprivier to have the highest frequency exceedances of the daily NAAQS for $PM_{2.5}$ over ten years (2017 to 2017). $PM_{2.5}$ monitoring results from 2013 to 2019 for sites in the WBPA show that ground-level concentrations of $PM_{2.5}$ at Lephalale did not exceed the the current and previous NAAQS annual average $PM_{2.5}$ standard limit. At Mokopane, the annual average concentrations of $PM_{2.5}$ exceeded the 2012-2015 NAAQS for annual average $PM_{2.5}$ in 2013; however, it fell below it in 2014. The graph for the WBPA in Figure 7 gives no results for 2015 and 2016. In 2017, it reached the current NAAQS for annual average $PM_{2.5}$; however, it fell below it again in 2018 and 2019. For Thabazimbi, there are only $PM_{2.5}$ results for 2013, 2018 and 2019 in the WBPA graph in Figure 7. The annual average concentrations of $PM_{2.5}$ for 2013 fell below the 2012-2015 NAAQS, and in 2018 and 2019, it reached the current NAAQS. The annual average $PM_{2.5}$ at all the sites mentioned above within the HPA, the VTAPA and the WBPA persist above the planned 2030 NAAQS for annual average $PM_{2.5}$. Secunda (2018), eMalahleni (2017), Kliprivier (2018), Sebokeng (2016 & 2018), Three rivers (2016), Zamdela (2016 to 2018) and Xanadu (2018 & 2019) continue to have annual average concentrations of $PM_{2.5}$ above the previous NAAQS annual average $PM_{2.5}$ standard limit. Some areas in the Highveld region have ambient $PM_{2.5}$ exceeding the current and future NAAQS for annual average $PM_{2.5}$, which are well above those recommended by the WHO and those found to present adverse impacts on human health.

Although the general trend for ambient $PM_{2.5}$ shows a decrease (Feig *et al*., 2019; Garland *et al*., 2017; Govender & Sivakumar, 2019), many of the areas in the HPA and VTAPA show persistent trends of non-compliance with the current and future annual average NAAQS for $PM_{2.5}$ for several years to come (Feig *et al*., 2019). Based on historical trends of observed data, it is anticipated that the ambient PM2.5 at Kliprivier and Three Rivers will only comply with the current annual NAAQS in 2035 and 2039, respectively and the 2030 annual NAAQS in 2042 and 2053, respectively (Feig *et al*., 2019). Figure 8, taken from a study evaluating the potential use of remote $PM_{2.5}$ data retrieved from satellites in mapping ground-level $PM_{2.5}$ for the VTAPA, shows the spatial variations of satellite-derived annual $PM_{2.5}$ concentrations with an increase in annual $PM_{2.5}$ from 2009 (33 $\mu g/m^3$) to 2016 (41 $\mu g/m^3$) over the VTAPA evident, most significantly in 2015 and 2016. A possible explanation for the high $PM_{2.5}$ concentrations in 2015 and 2016 is an increase in the aerosol optical depth due to the changes in aerosol mass movement during El Niño episodes in South Africa (Muyemeki *et al*., 2020). It should be noted that studies have found weak agreement between the satellite-retrieved data and ground-level measurements, with the satellite

retrievals tending to overestimate $PM_{2.5}$ (Muyemeki *et al*., 2020; Garland *et al.,* 2017). The exceedance of the current and future NAAQS for annual average $PM_{2.5}$, which are well above those recommended by the WHO and those found to present adverse impacts to human health, may persist for several years.

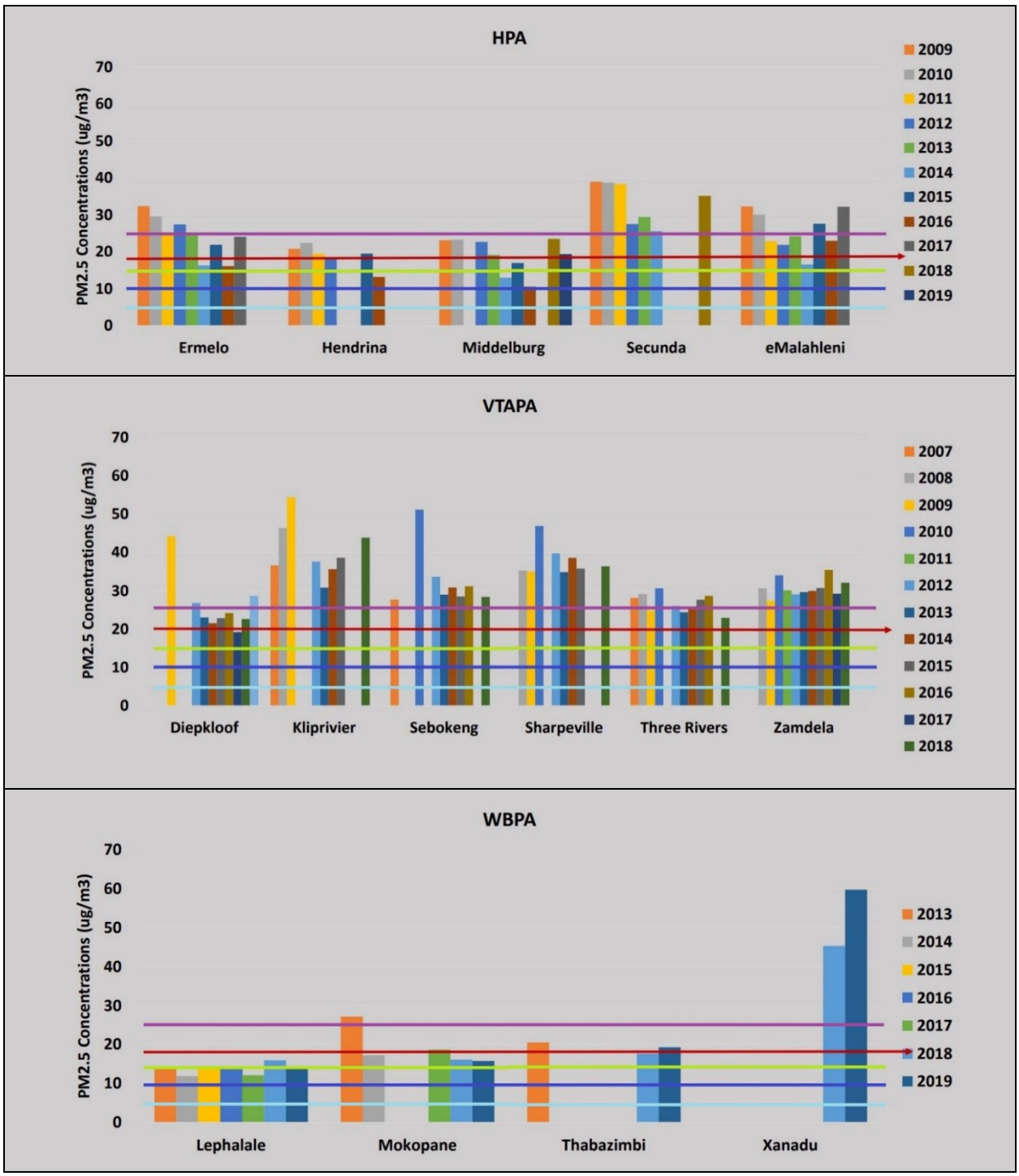

Figure 7: Annual average $PM_{2.5}$ concentrations (µg/m^3) for sites within the HPA, VTAPA and WBPA. The red line approaches the current NAAQS (2016-2029). The purple line represents the past NAAQS (2012-2015). The green line represents the future NAAQS (from 2030). The dark blue and light blue represents 2005 and 2021 WHO air quality guidelines, respectively (Adapted from Khumalo, 2020 by adding the purple, green and blue lines).

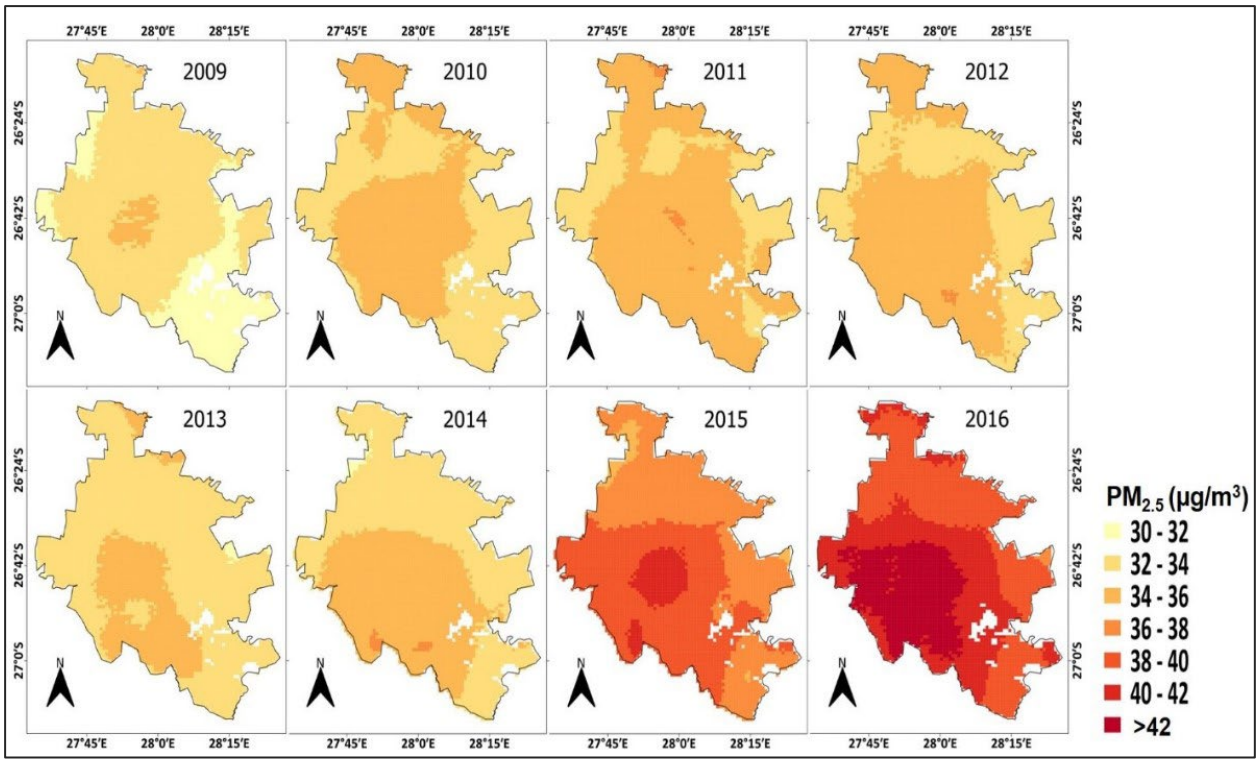

Figure 8: Spatial variations of satellite derived annual $PM_{2.5}$ concentrations from 2009 to 2016 over the VTAPA (Taken from Muyemeki et al., 2020).

Sources of ambient $PM_{2.5}$ in the Highveld

Anthropogenic sources contributing to $PM_{2.5}$ air pollution are vast (Charlson *et al*., 1992; Karagulian *et al*., 2016; Tomasi & Lupi, 2017; US EPA, 2019); therefore, identifying the major source contributors in the Highveld is critical to developing a targeted approach to air quality management. Temporal variations and the chemical composition of ambient $PM_{2.5}$ can give valuable insights into the major sources of $PM_{2.5}$ in the Highveld region.

Temporal variations of $PM_{2.5}$ ground-level concentrations can infer local sources of $PM_{2.5}$ in the Highveld region. Figure 9 and Figure 10 show strong seasonal and diurnal trends of $PM_{2.5}$ in Johannesburg (Buccleuch) and the VTAPA (Hersey *et al.,* 2015; Govender & Sivakumar, 2019). The highest levels of $PM_{2.5}$ were found in the early morning, early in the evening and generally during winter (Govender & Sivakumar, 2019; Hersey *et al.,* 2015). Hersey *et al.* (2015) found that the highest concentrations of particulates occurred in the winter for all study sites (i.e., township/domestic burning, urban/suburban residential and traffic) except industrial areas. For industrial areas, the maximum particle concentrations were found in summer and were attributed to secondary particle formation from industrial precursor gases (Hersey *et al.,* 2015). Hersey *et al.* (2015) explain that in winter, stack emissions are generally emitted above the less stable boundary layer into a stable atmosphere and in summer, the deeper boundary layers increase to above stacks resulting in the industrial emissions staying in the less stable boundary layer. The obvious diurnal patterns of particulates throughout all the seasons highlight domestic burning as

an important source contributor in the Highveld throughout the year (Hersey *et al.,* 2015). Although domestic burning can have regional impacts on air quality (Kok *et al.,* 2021; Venter *et al.*, 2012; Tiitta *et al*., 2014), it impacts air quality most dramatically close to the emission source (Hersey *et al.,* 2015). Govender & Sivakumar (2019) found that the $PM_{2.5}$ peaks during early morning and late afternoon corresponded with domestic fuel use and high traffic volumes. Natural and domestic biomass burning are likely source contributors to the higher $PM_{2.5}$ concentrations in winter (Govender & Sivakumar, 2019; Laban *et al.,*2015; Tshehla & Wright, 2019).

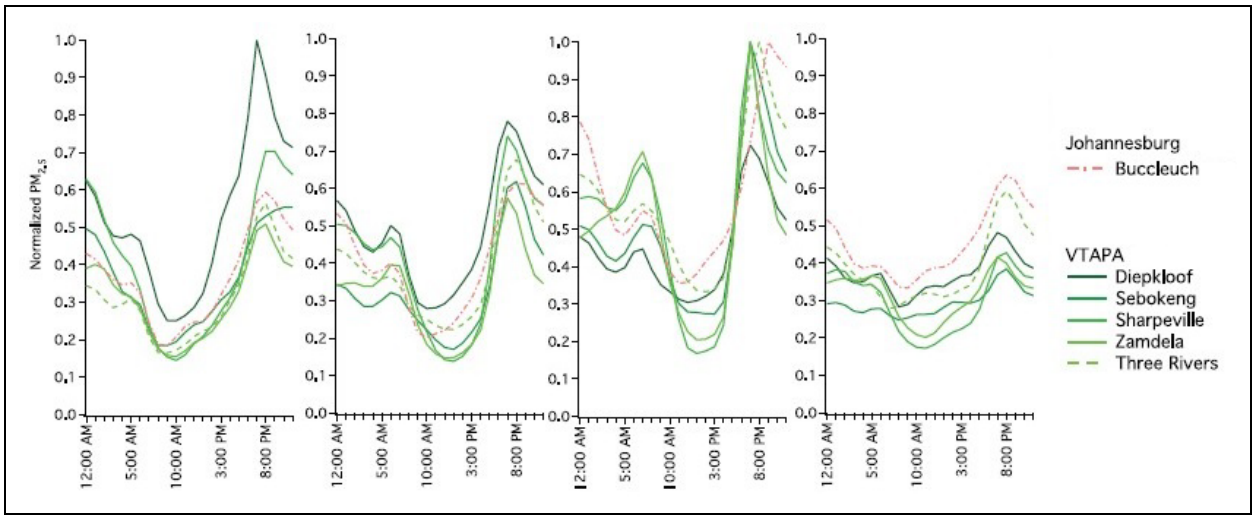

Figure 9: Seasoned-averaged diurnal $PM_{2.5}$ for sites within Johannesburg (2004 to 2011) and the VTAPA (2007 to 2012). Sites influenced by domestic fuel burning are represented with solid lines. Coarse dashed lines represent industrial sires and dashed dot dash lines represent sites influenced by traffic (Adapted from Hersey, 2015).

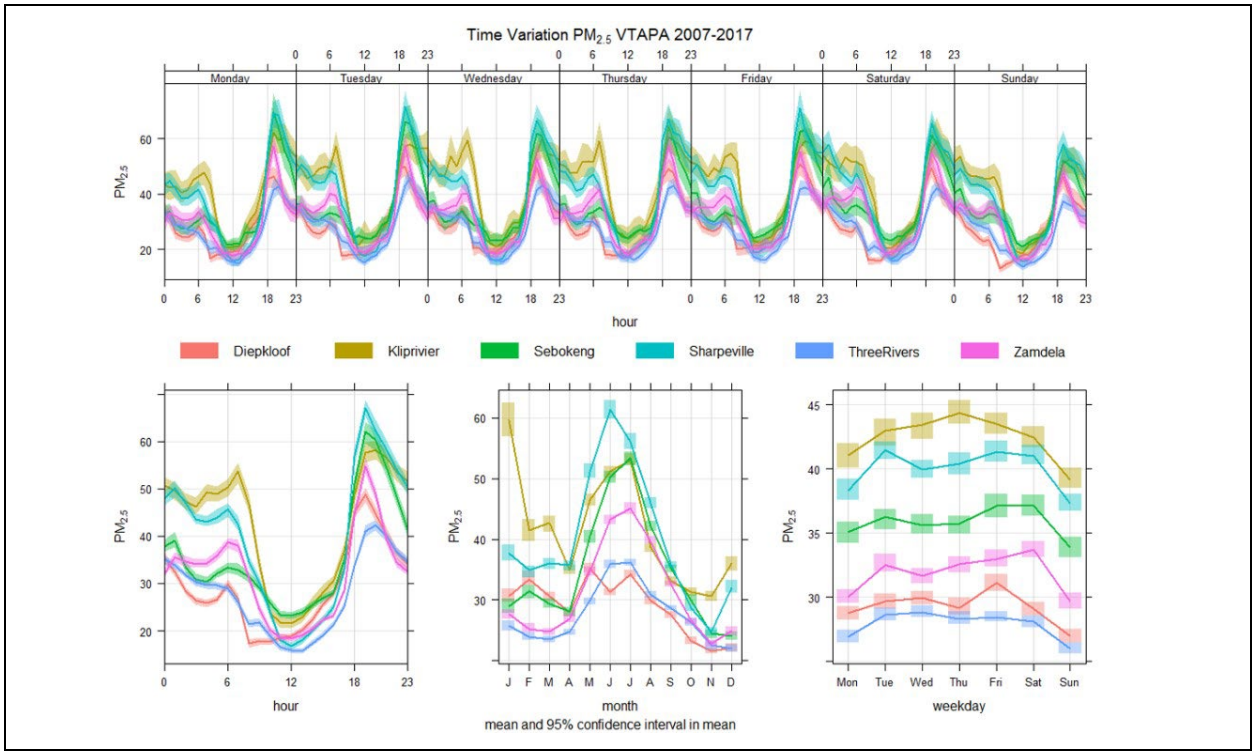

Figure 10: Daily average $PM_{2.5}$ concentrations (µg/m^3) for 2007 to 2017 for sites within the VTAPA (Taken from Govender & Sivakumar, 2019).

The chemical composition of $PM_{2.5}$ can be used to identify major local and regional source contributors. The size distribution and composition of $PM_{2.5}$ are greatly influenced by its source (Pope & Dockery, 2006; Lindeque, 2018; Warneck, 1988; WHO, 2006). Table 1 shows the effect of boiler technology and control equipment on the characteristics of particulates from coal-fired power plants (Chow *et al.,* 2004; Watson *et al*., 2001). Table 2 shows that sulphates and organic carbon can form significant (each >20%) components of ambient $PM_{2.5}$, and that sulphates may be higher in the immediate area of coal-fired power plants. Conradie *et al.* (2016) found SO_4^{2-} to be the most abundant species in the wet deposition samples taken at at Amersfoort, Vaal Triangle, Louis Trichardt and Skukuza, followed by NO_3^- and NH_4^+. SO_4^{2-} concentrations were four times higher at Amersfoort and the Vaal Triangle than in Louis Trichardt and Skukuza. NO_3^- and NH_4^+ concentrations were two to three times higher at Amersfoort and the Vaal Triangle than in Louis Trichardt and Skukuza. Conradie *et al.* (2016) point out that fossil fuel combustion is a significant source group in Amersfoort (situated close to the industrialised Highveld) and the Vaal Triangle. Muyemeki *et al*. (2021) found coal burning, secondary particulates, industry, and wood- and biomass burning to be significant sources of $PM_{2.5}$ in the VTAPA. Coal and biomass combustion-related elements were dominant in the fine fraction ($PM_{2.5}$) of the samples. The secondary particulates consisted mainly of SO_4^{2-}, NO_3^- and NH_4^+ formed through the chemical transformation of precursor emissions from local- or possibly regional sources outside the boundary of the VTAPA. Secondary particulates at Kliprivier were found to be likely from coal-fired power plants (Muyemeki *et al*., 2021). Walton *et al*. (2021) assessed the chemical composition of fine ($PM_{2.5}$) and coarse particulates ($PM_{2.5-10}$) at two residential areas, Embalenhle and Kinross, in the HPA. The average $PM_{2.5}$ concentrations at both sites were higher in winter than in the summer. $PM_{2.5}$ at both sites were primarily comprised of Si, Al, S, SO_4^{2-} and NH_4^+ during both winter and summer. Of these species, SO_4^{2-} and NH_4^+ were the most abundant. Na was abundant at both sites during winter, and Ca was abundant during summer. The elements, Si, Al, Ca, and Na suggest a crustal origin or coal combustion (Maenhaut *et al*., 1996; Walton *et al*., 2021). All these species can originate from coal combustion, and the ratios of NO_3^- / SO_4^2 point to Industry as a dominant source. The study identified dust, secondary aerosols (primarily due to coal combustion), residential combustion, wood and biomass burning, and industry (including a neighbouring petrochemical plant and coal-fired power plants) as significant source contributors of fine and coarse particulates (Walton *et al*., 2021). Altieri *et al*. (2022) considered the isotopic composition of nitrates to identify significant sources of NO_x in the VTAPA in the winter. The coarse mode samples were taken at two densely populated settlements (Sebokeng and Zamdela) and one low-density area (Kliprivier) in the VTAPA in July 2018. The study found coal-fired power plants, biomass burning and vehicles to be major contributors of nitrates in the VTAPA, with coal-fired power plants contributing to more than two-thirds of the nitrates (Altieri *et al*., 2022). In no order, the chemical composition of $PM_{2.5}$ identifies dust, coal burning, secondary

particulates, industry, vehicles, residential combustion of waste (i.e., domestic and garden waste) and wood- and biomass burning as significant sources of ambient $PM_{2.5}$ in the Highveld (Altieri *et al*., 2022; Conradie *et al*., 2016; Muyemeki *et al*., 2021; Walton *et al*., 2021).

Table 1: Percentage constituents of $PM_{2.5}$ emissions from coal-fired power plants in the United States (Chow et al., 2004; Watson et al., 2001)[12] [13].

Size	Control	SO_4^{2-}	NO_3^-	NH_4^+	OC	EC
*550 MW	Wet limestone scrubber & baghouse	~11.4	~2.5	~0.7	~62.9	~2.7
*600 MW	Baghouse Low sulphur coal	~5.7	~1	~0.5	~55.7	~2.4
600 MW	Baghouse Low sulphur coal	~9.5	~0.1	~0.3	~22.8	~0.6
*545 MW (Aluminium plant)	Dry limestone scrubber & potliner material	~45.6	~0.1	~0.7	~4.2	~1.6
*550 MW	Electrostatic precipitator & Baghouse	~46.2	~0.1	~5.1	~10.3	~0.1
*550 MW	Electrostatic precipitator & Baghouse	~62.2	~0.0	~5.3	~0.9	~0.1
**428 MW Unit 1 & 428 MW Unit 2	SO_2 wet scrubber & Electrostatic precipitator	~22.8	~0.2	~2.8	~2.2	~8.1
**408 MW	Dry lime SO_2 scrubber Fabric baghouse	~12.7	~0.8	~0.1	~2.6	~1.2
***184 MW	Ammonia injection Electrostatic precipitator	~3	~0.3	~1.5	~34.1	~4.3
***262 MW	Ammonia injection Electrostatic precipitator	~10.0	~0.1	~9.2	~0.5	~0.4
Average		~22.9	~0.5	~2.6	~19.6	~2.1

The chemical composition of $PM_{2.5}$ air pollution can also give insight into the contributions of the highly industrialised and urbanised areas in the Highveld region on the ambient $PM_{2.5}$ in more remote areas in the greater Highveld. As mentioned, $PM_{2.5}$ can be transported over long distances in the atmosphere. It is, therefore, possible for $PM_{2.5}$ from sources in, for instance, the industrialised Highveld in Mpumalanga to impact areas further away. The Welgegund monitoring station is located approximately 25 km northwest of Potchefstroom. The location of the station is characterised as a regional background site. There are no major air pollution sources close to the site. The nearest coal-fired power station, Lethabo, is located approximately 104 km east of the Welgegund station. The site, however, frequently experiences air pollution from the Johannesburg and Pretoria metropolitan areas (~120km to the northeast), the western and eastern BIC, the Vaal Triangle, and the industrialised Mpumalanga Highveld, often balanced by clean air from the west (Beukes *et al*., 2013; Tiitta *et al*., 2014; Welgegund.org). Based on measurements taken from September 2010 to August 2011, Tiitta *et al.* (2014) found PM1 at Welgegund comprised primarily of OA (48%) and SO_4^{2-} (33%), while NH_4^+ and NO_3^- contributed to 13% and 6%, respectively. The highest OA concentrations were observed during the dry season and were attributed to local and regional savannah fires. The highest concentrations of SO_4^{2-} were attributed to air masses that had moved over the industrial Highveld (where most of

[12] Elements were excluded from the table.
[13] *Pulverised coal dry bottom boiler with tangential injection. ** Bituminous coal (S = 0.4%). *** Bituminous coal (S = 0.46%).

the coal-fired power plants are located). Venter *et al*. (2018) focused on inorganic species and, based on measurements taken from November 2010 to December 2011, found SO_4^{2-} and NH_4^+ comprised most of the PM_1 size fraction and SO_4^{2-} and NO_3^- comprised most of the $PM_{1-2.5}$ and $PM_{2.5-10}$ at Welgegund. NO_3^- contributed most in the $PM_{2.5-10}$ size fraction, and SO_4^{2-} was more predominant in the PM_1 and $PM_{1-2.5}$ fractions. The SO_4^{2-} and NO_3^- levels measured at Welgegund were attributed to old air masses that had moved over regions with major anthropogenic sources. When the inorganic ion concentrations collected at Welgegund were compared to levels measured in the western BIC (Marikana; November 2008-October 2009), the comparative ratio of SO_4^{2-} at Marikana to Welgegund ($SO_4^{2-}{}_{Marikana}$/ $SO_4^{2-}{}_{Welgegund}$) was significantly lower than the ratios of nearly all of the other inorganic ions. The lower ratio of SO_4^{2-} shows that Welgegund is receiving a disproportionate amount of SO_4^{2-}, sugesting that Welgegund it is not only impacted by SO_4^{2-} from Marikana but by SO_4^{2-} from sources further away. The lower ratio is attributed to SO_4^{2-} formed from distant sources of SO_2 and submicron particulates of SO_4^{2-} that can be transported over long distances in the atmosphere. Tiitta *et al.* (2014) and Venter *et al*. (2018) found that aged air masses over major anthropogenic sources in the Highveld contribute to secondary $PM_{2.5}$ in the atmosphere over Welgegund.

Table 2: Percentage constituents of ambient $PM_{2.5}$ in cities in China and Korea[14].

Source	Site	SO_4^{2-}	NO_3^-	NH_4^+	EC	OC
Song *et al.* (2007)	Five urban sites and one rural site	14.5	7.5	6	8	36
Ye *et al.* (2003)	Two urban sites	23.4	8.7	9.6	11.1	30.3
Son *et al.* (2012)	Urban (Commercial & residential)	15.5	16.3	8.6	8.3	23.4
Zhao *et al.* (2021)	Four coal-fired power plant sites	32.5	-	2.3	3.1	7.1
Average		21.5	10.8	6.6	7.6	24.2

Once the significant source sectors have been identified, apportioning ambient $PM_{2.5}$ to the significant sources in the Highveld region is challenging (Langerman & Pauw, 2018; Maenhaut *et al*., 1996; Piketh *et al*., 1999a). As previously mentioned, ambient $PM_{2.5}$ constitutes primary $PM_{2.5}$ emitted to the atmosphere, and secondary $PM_{2.5}$ formed in the atmosphere. Secondary $PM_{2.5}$ is formed from the photochemical oxidation reaction of both inorganic and organic precursors gases of natural and anthropogenic origin, which accounts for a large fraction of the $PM_{2.5}$ mass (Bergin *et al*., 2005; Malfroy *et al*., 2005; Srivastava *et al*., 2022; Tomasi & Lupi, 2017; US EPA, 2019; Wang-Li, 2015). These precursor gases include SO_2, NO_x, NH_3 and VOCs. NH_3 plays a role in neutralising sulphuric (H_2SO_4) and nitric acid (HNO_3), leading to the formation of more stable particulates with lower volatility (e.g., ammonium nitrate [NH_4NO_3]). The oxidation of VOCs also contributes to the formation of secondary organic aerosols (SOA) (Alfarra, 2004; Seinfeld & Pandis, 1998; Srivastava *et al*., 2022; Tomasi & Lupi, 2017; US EPA, 2019; Wang-Li, 2015). Since

[14] Elements were excluded from the table.

$PM_{2.5}$ is emitted and formed in the atmosphere (secondary $PM_{2.5}$), it is not easy to apportion ambient $PM_{2.5}$ among the vast sources in the Highveld. Figure 11 illustrates the interaction of emissions from various sources in the formation of $PM_{2.5}$ and its transport and removal from the atmosphere.

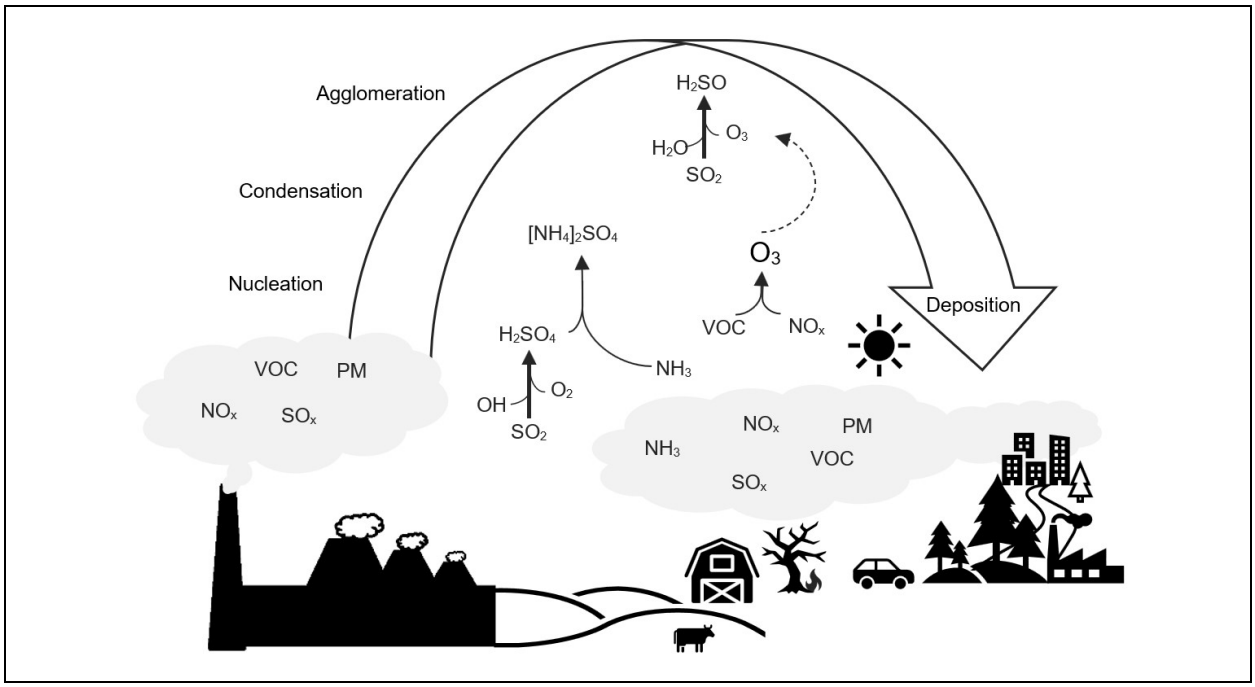

Figure 11: An illustration of the diversity of anthropogenic sources of $PM_{2.5}$ and its formation in, transport and removal from the atmosphere (Adapted from Bergin et al., 2005).

2.3 Ambient $PM_{2.5}$ attributable to coal-fired power plants in the Highveld

The South African power generation sector, particularly coal-fired power, is a significant contributor to ambient $PM_{2.5}$ in the Highveld. Figure 12 gives the current and planned energy mix for South Africa. Figure 12 shows coal energy dominates the current and planned energy mix in South Africa (SA. Department of Energy, 2019). The emerging long-term resource plan endeavours to diversify the energy mix in South Africa and decrease the installed coal energy capacity by approximately 10% (SA. Department of Energy, 2019). Coal will, however, continue to play a significant role in electricity generation for time to come, with an estimated 58.8% contribution to the annual energy by 2030 (SA Department of Energy, 2019). Most (~90%) of South Africa's electricity is generated by its public power utility, Eskom (Department of Energy, 2019; Eskom, 2022). Figure 13 gives the installed capacity of Eskom's generation mix and shows 85% of its installed capacity comprises of coal fired power plants (Eskom, 2022). Figure 14 gives the percentage installed capacity of major coal-fired power plants in the Highveld and shows Eskom held approximately 96% of the coal-fired power capacity in the Highveld in 2016. The majority of these plants are located in the Highveld (Scheifinger & Held, 1997; Shikwambana *et al*., 2020) and are considered significant emitters of secondary $PM_{2.5}$ precursor species SO_2 and NO_x in the Highveld (Altieri *et al*., 2022; Pretorius *et al*., 2017; Ross, 2003; SA DEA, 2012a;

Scorgie *et al*., 2004; Scorgie & Thomas, 2006; Sivertsen *et al*., 1995). Collett *et al*. (2010) found that diurnal variations of SO_2 and NO_x concentrations in Elandsfontein point to coal-fired power plants, while Igbafe (2007) also found diurnal variations of SO_2 concentrations in Elandsfontein related to coal-fired power plants. Morosele *et al*. (2020) found a strong positive relationship between ambient SO_2 and emissions from one coal-fired power station (Grootvlei). Muyemeki *et al*. (2021) found that secondary particulates at Kliprivier were likely from coal-fired power plants. Altieri *et al*. (2022) found that during winter, coal-fired power plants can contribute to more than two-thirds of the nitrates in the VTAPA. Conradie *et al.* (2016) consider fossil fuel combustion as a significant source of the SO_4^{2-} in the wet deposition samples taken at Amersfoort (situated close to the industrialised Highveld) and the Vaal Triangle. Walton *et al*. (2021) found coal combustion, most likely from industry, to be the source of the secondary $PM_{2.5}$ at two residential sites in the HPA.

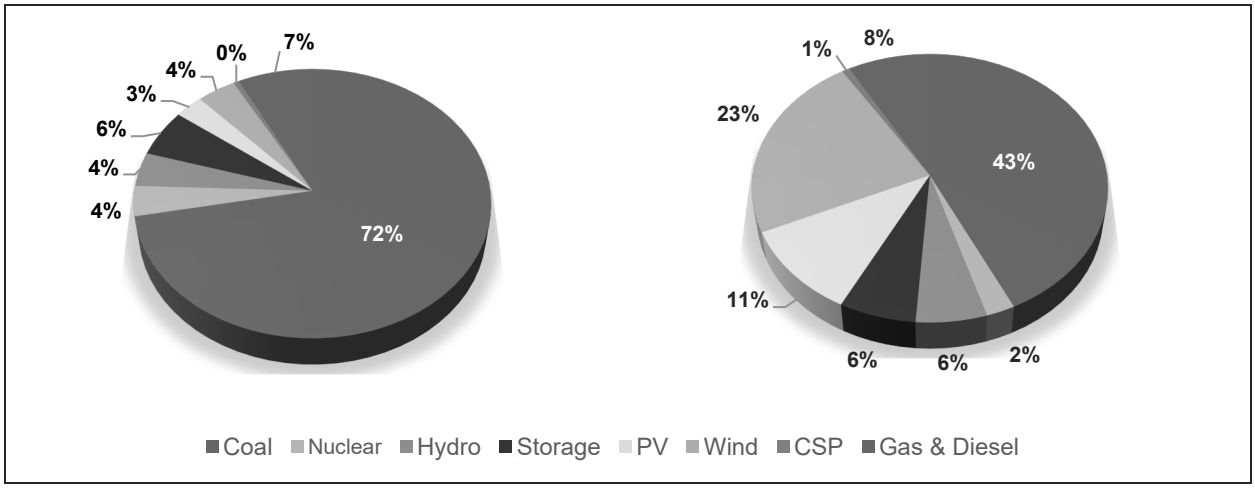

Figure 12: The current and planned energy mix in South Africa. The chart on the left illustrates the current installed MW capacity, and the chart on the right illustrates the capacities planned for 2030. These charts are based on figures from Table 5 in the 2019 Integrated Resources Plan.

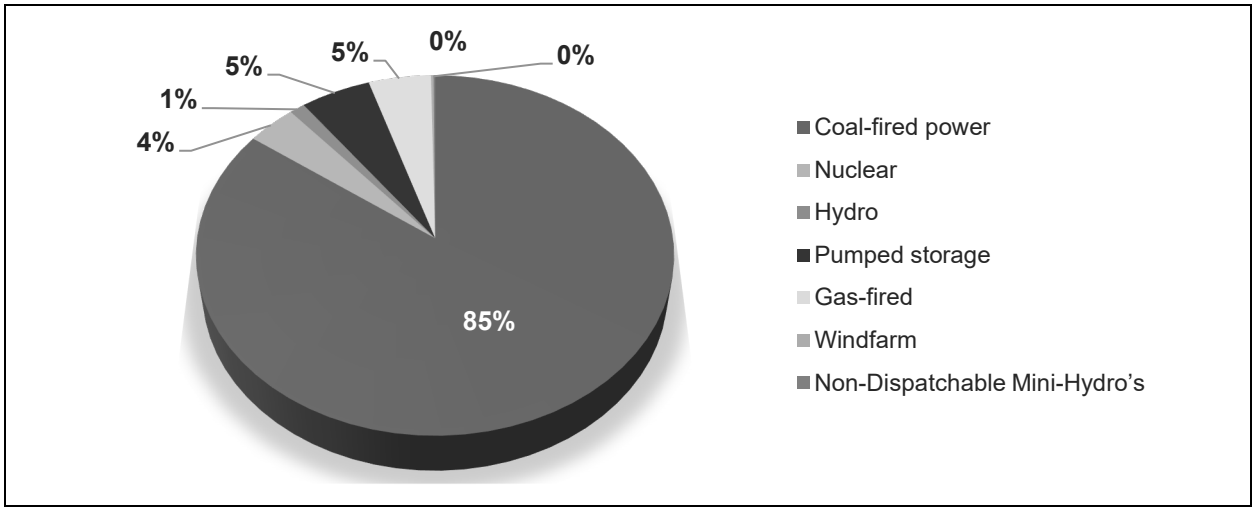

Figure 13: The current (2022) installed capacity (MW) of the generation mix of South Africa's public power utility, Eskom. This chart is based on figures from an Eskom Fact Sheet (Eskom, 2022).

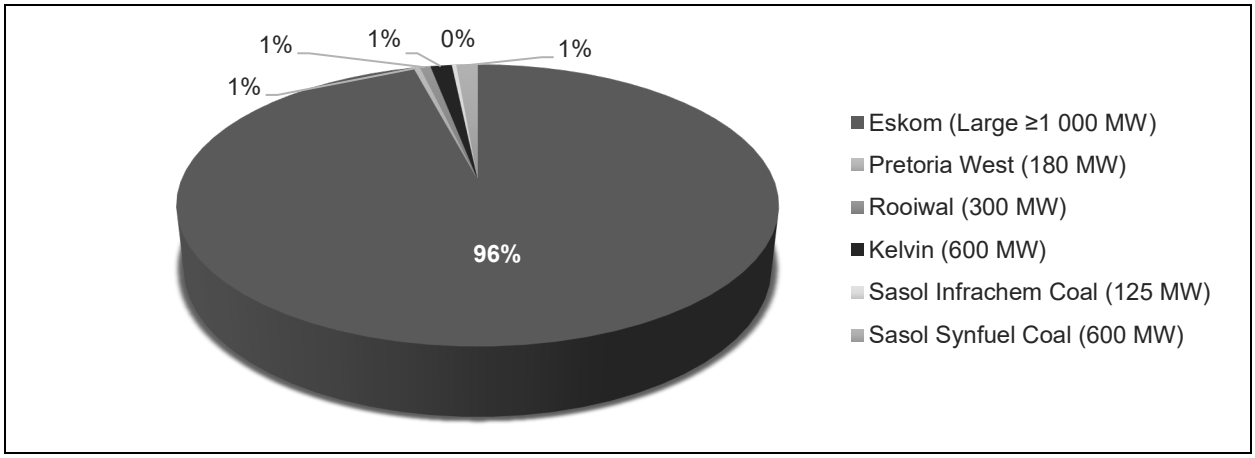

Figure 14: Capacity of the major coal-fired power installations in the Highveld in 2016. This chart is based on MW capacities taken from Africon (2005), Escience Associates (2017), Eskom (n.d.a), Eskom (n.d.c), GEM Wiki (2022), and the SA. Department of Energy (2019).

Most Eskom coal-fired plants do not comply with the new plant MES[15], particularly SO_2 and NO_x. Historically air pollution controls for the Eskom coal-fired power plants were focused on particulates (Eskom, 2019; Table 3). In 2016, none of the power plants in the existing fleet had been fitted with NO_x or SO_2 control (Eskom, 2016). Kendal and Matimba have boilers with Low NO_x designs. A Low NO_x Burner (LNB) was installed at Camden in 2016/2018. The new Medupi coal-fired power plant was commissioned with control technology to meet the MES for particulate matter (PM) and NO_x. Eskom plans to retrofit Medupi with Flue Gas Desulphurisation (FGD) for SO_2 abatement in 2023/2024. The new Kusile coal-fired power plant will be commissioned with control technology to meet new plant MES for PM, NO_x and SO_2 (Eskom, 2019). In its application for relief of compliance with new plant MES for its coal and liquid fuel-fired power plants, Eskom prioritised the reduction of PM emissions and proposes to reduce NO_x emissions at the three greatest emitting power plants: Tutuka, Matla and Majuba (Eskom, 2019).

Table 3: Overview of Eskom's current (2019) and future compliance with MES (Adapted from Eskom, 2019). Green represents compliance with MES. Orange reflects plants where some units comply with MES. Red represents non-compliance with MES.

Plant	Existing plant MES (2015-2020)			New plant MES (2020-2025)			New plant MES (2025-2030)		
	PM	SO_2	NO_x	PM	SO_2	NO_x	PM	SO_2	NO_x
Kusile									
Medupi									
Majuba									
Kendal									
Matimba									
Lethabo									
Tutuka									
Duvha									
Matla									

[15] The MES are prescribed in the "List of activities which result in atmospheric emissions which have or may have a significant detrimental effect on the environment, including health, social conditions, economic conditions, ecological conditions, or cultural heritage" published in Government Notice (GN) 893 in Government Gazette (GG) 37054 dated 22 November 2013 (as amended).

Kriel									
Hendrina							Decommissioning[16]		
Arnot									
Camden							Decommissioning		
Grootvlei							Decommissioning		
Komati							Decommissioning		

The contribution of the Eskom coal-fired power plants to air pollution is exacerbated by the decline in thermal efficiency due to increased energy demands, delayed maintenance, and the return to service of older, less efficient power plants (Pretorius *et al*., 2015a; Pretorius *et al*., 2015b). A Free Basic Electricity Policy was implemented in 2001 (Pretorius *et al*., 2017). This policy resulted in an increase in demand for electricity due to economic growth. This increase in demand and a delay in building new power generation capacity placed the country in an ongoing energy crisis since 2007 (Pretorius *et al*., 2017). The increase in energy demand was met by delaying maintenance of the power plants (IRP, 2013) and the return to service of three older power plants, mothballed during the 1980s and early 1990s (Pretorius *et al*., 2017). The delay in the maintenance of the power plants resulted in a decline in their performance (IRP, 2013). The older, previously mothballed, coal-fired power plants have lower thermal efficiencies and less effective pollution control technologies (Pretorius *et al*., 2017). This thermal efficiency decline means more coal must be combusted to deliver the same amount of electricity (Pretorius *et al*., 2017).

Our understanding of the relationship between ambient $PM_{2.5}$ and the emissions of $PM_{2.5}$ and its precursor gases from coal-fired power plants in the Highveld remains limited. Although several studies have identified coal-fired power plants as significant contributors to ambient $PM_{2.5}$, fewer studies have attributed ambient $PM_{2.5}$ solely to coal-fired power plants in the Highveld (Gray, 2019; Steyn & Kornelius, 2018; NEC & PAC, 2018; Myllyvirta, 2014). Several studies (Gray, 2019; Marais *et al.*, 2019; Myllyvirta, 2014; NEC & PAC, 2018; Pretorius *et al.*, 2017; Scorgie & Thomas, 2006; Steyn & Kornelius, 2018; Van Horen, 1996) have used modelling to look at the impact of air pollution from coal-fired power plants on human health in South Africa. Five of these studies (Gray, 2019; Marais *et al.*, 2019; Myllyvirta, 2014; NEC & PAC, 2018; Steyn & Kornelius, 2018) considered the impact of $PM_{2.5}$ air pollution from coal-fired power plants on human health in South Africa. Four studies attribute annual average $PM_{2.5}$ solely to coal-fired power plants in the Highveld (Gray, 2019; Steyn & Kornelius, 2018; NEC & PAC, 2018; Myllyvirta, 2014). Gray (2019) simulated the cumulative impact of three major source sectors (Eskom coal-fired power plants, Sasol Synfuels and Natref refinery) on $PM_{2.5}$. Steyn & Kornelius (2018) simulated the cumulative impact of two major source sectors, coal-fired power plants and Sasol Synfuels in Secunda, on SO_2 and sulphates. NEC (2018) simulated the cumulative impact of Eskom coal-fired power

[16] Decommissioned by 2030, as per the Integrated Resource Plan (IRP) and Eskom Consistent Data Set using a 50-year life expectancy (Eskom, 2019).

plants on $PM_{2.5}$. All three studies considered secondary $PM_{2.5}$. It is unclear if background conditions were considered, perhaps through the input of ambient values. However, none of these studies explicitly account for pollution transported across the boundary or all other major sources in the Highveld (e.g., biomass burning, other industries, biogenic VOCs and ammonia from agriculture, domestic fuel combustion and on-road vehicles) in the formation of secondary $PM_{2.5.}$ Myllyvirta (2014) used regression models derived from single-source CTM (CAMx & CALPUFF) model runs and estimated $PM_{2.5}$ emissions based on a ratio with PM10 of 4/9. The other three studies used the CALPUFF chemical transport model (Gray, 2019; Steyn & Kornelius, 2018; NEC & PAC, 2018). Each of the four studies has limitations and does not represent a complete estimate of the secondary $PM_{2.5}$ attributable solely to coal-fired power plants in the Highveld. The impact of these coal-fired power plants on human health and well-being in the Highveld region may be underestimated. These studies and how they compare to this study are discussed in more detail in section 4.5 and Table 16.

2.4 The dangers of $PM_{2.5}$ air pollution

The small size of $PM_{2.5}$ is one of the main reasons contributing to its threat to human health. $PM_{2.5}$ is particles less than 2.5 micrometres in aerodynamic diameter (HEI, 2020; Malfroy *et al*., 2005; Seinfeld & Pandis, 2006; Tomasi & Lupi, 2017; US EPA, n.d.a; WHO, 2006; WHO, 2021a; Xing *et al*., 2016). Figure 15 shows a range of sizes of typical particulate air pollution. Its size allows it to bypass the natural defences such as coughing and sneezing out larger particulates. This bypass allows $PM_{2.5}$ to penetrate deep into the respiratory system, reaching the lower respiratory tract, particularly the small peripheral airways and the alveoli (US EPA, n.d.b; Falcon-Rodriquez *et al*., 2016; Nemmar, 2013; Nel, 2005; Bauer *et al.*, 2019). Inhaled $PM_{2.5}$, deposited in the airways and alveoli, may dissolve partially or totally, or stay intact (Alfarra, 2004; Seinfeld & Pandis, 1998; Seinfeld & Pandis, 2006; US EPA, n.d.b; Xing, 2016). Clearance of particulates accumulated on the respiratory epithelium of the alveoli occurs through absorptive and non-absorptive processes. The mechanism of respiratory absorption is poorly understood. However, evidence exists for both passive and active movement (Lippmann *et al*., 1980; Morrow, 1973). The primary non-absorptive process is phagocytosis. Macrophages ingest the particulates and move them to the tracheobronchial airways. Here the particulates are swallowed or expectorated (Lippmann *et al*., 1980; US EPA, n.d.b). The clearance half-times of insoluble particulates have been measured as days, months, or years (Lippmann *et al*., 1980). Figure 16 illustrates the compartmental deposition of particulate air pollution. $PM_{2.5}$ also has atmospheric lifetimes of days to weeks, which allows them to be transported on a regional scale (Andreae *et al.*, 1996; Bergin *et al*., 2005; Finlayson-Pitts & Pitts, 2000; Garstang *et al.*, 1996; Karagulian *et al*., 2016; Piketh, 1996; Pope & Dockery, 2006; Tiitta *et al.*, 2014; Tomasi & Lupi, 2017; Venter *et al*., 2018; WHO, 2006).

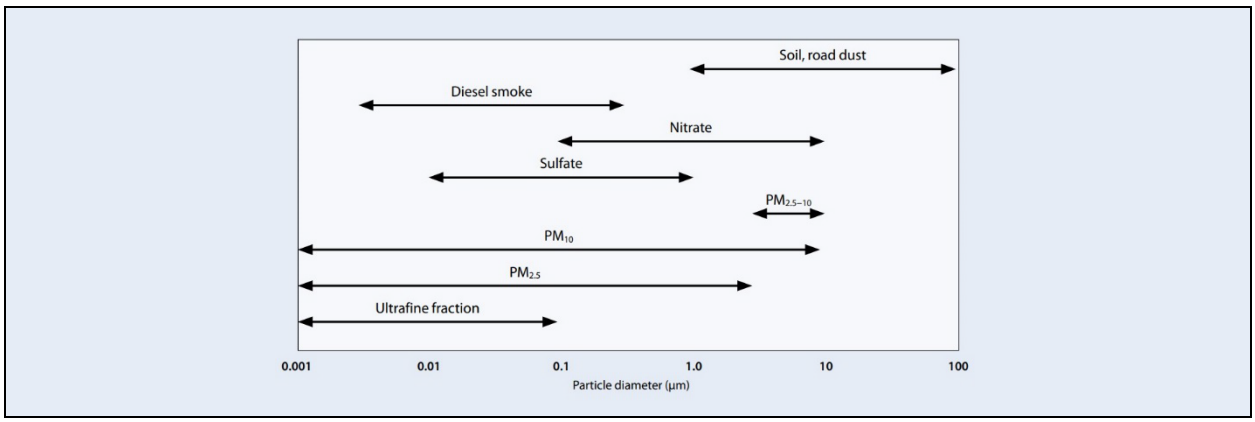

Figure 15: The range of sizes (on a logarithmic scale) of particulate air pollution, showing the size range of the $PM_{2.5}$ fraction and some of its major components (i.e., sulphates and nitrates) (Taken from WHO, 2006).

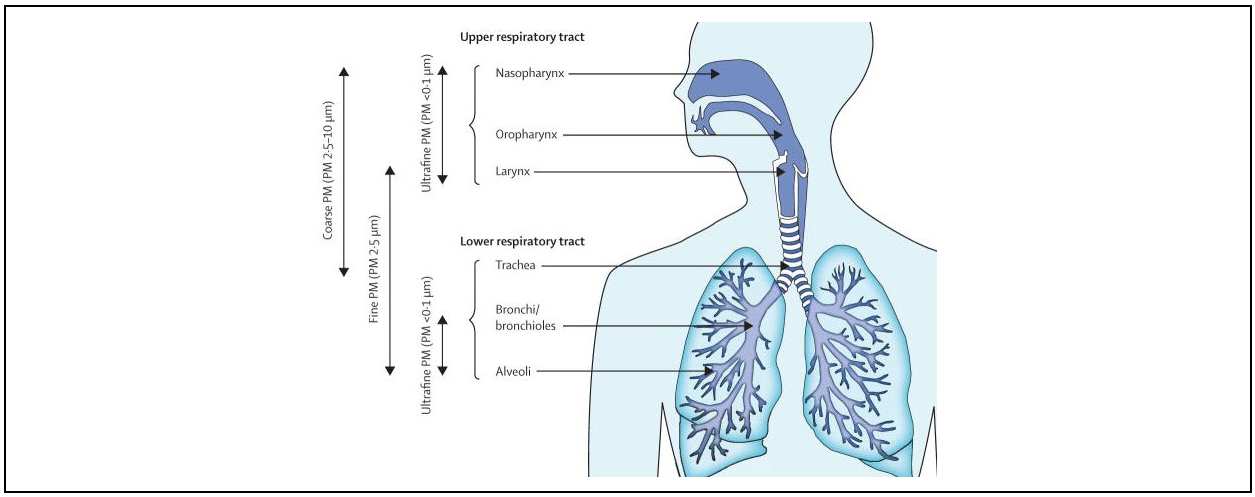

Figure 16: An illustration of the compartmental deposition of particulate air pollution (Taken from Guarnieri & Balmes, 2014).

The composition of $PM_{2.5}$ is also significant to its impact on health (Lindeque, 2018; Li *et al.,* 2021; Kelly & Fussell, 2012; Reiss *et al*., 2007; Son *et al.*, 2012; Stanek *et al.*, 2011). $PM_{2.5}$ can be made up of a mixture of inorganic and organic particulates, it can be in a solid or liquid state, it can vary in quantity, size, structure, surface area, chemical composition, and solubility (Pope & Dockery, 2006; Lindeque, 2018; Warneck, 1988; WHO, 2006). $PM_{2.5}$ can consist of fungal spores, pollen, polycyclic aromatic hydrocarbons, environmentally persistent free radicals, metals, sulphates, nitrates, ammonium, carbon, silicon, sodium ion, and other harmful particulates (Dominici *et al.*, 2015; Guarnieri & Balmes, 2014; Pope & Dockery, 2006; Raes *et al.*, 2000; Warneck, 1988). The alveolar epithelium is very thin, and soluble particulates that reach this deep in the respiratory system are believed to enter the blood in the lungs within minutes (Lippmann *et al*., 1980). Although very slowly, particulates that penetrate the alveoli can also transfer through the lymphatic drainage system to the lymph nodes and subsequently to the systemic circulation and organs (Falcon-Rodriquez *et al*., 2016; Lippmann *et al*., 1980; Nemmar, 2013; US EPA, n.d.b). Li *et al.* (2021) found a positive association between the $PM_{2.5}$ constituents: EC, OC and NO_3 and all-cause mortality. All three species were significantly linked with cardiovascular disease. EC was

also significantly linked with respiratory mortality, and NO_3^- was linked with endocrine disease and neoplasm. Son *et al.* (2012) found a significant link between an increase in Mg and total mortality. A moderate association was found between NO_3, SO_4 and NH_4 and cardiovascular mortality and Mg, Cl, and respiratory mortality.

Evidence suggests that long-term exposure to $PM_{2.5}$ can lead to premature death. The US EPA conducted a broad review of epidemiology literature on the links between short- and long-term exposure to $PM_{2.5}$ and respiratory-, cardiovascular-, metabolic-, nervous system-, reproductive- and developmental effects, cancer, and mortality (Table 4). The latest Integrated Science Assessment (ISA) for particulate matter by the US EPA determined that there is a causal relationship between short-term and long-term exposure to $PM_{2.5}$ and cardiovascular effects and mortality (US EPA, 2019) (Table 4). The ISA recently received criticism for lack of transparency on data evaluation and the conclusions that resulted in causal associations (Prueitt *et al.*, 2021). Notwithstanding the evidence for a correlation between long-term exposure to fine particulate matter and mortality (Chen *et al*., 2016; Crouse *et al*., 2015; Dockery *et al*., 1993; Enstrom, 2017; Garcia *et al*., 2015; Hart *et al*., 2011; Hart *et al*., 2015; Kloog *et al*., 2013; Krewski *et al*., 2000; Lepeule *et al*., 2012; Lipfert *et al*., 2006; Ostro *et al*., 2015; Pinault *et al*., 2016; Puett *et al*., 2011; Thurston *et al*., 2016; Turner *et al*., 2016; Wang *et al*., 2016; Wang *et al*., 2017; Weichenthal *et al*., 2014; Zeger *et al*., 2008) is substantial and growing.

Table 4: Causality determinations for $PM_{2.5}$ exposure and health impacts (US EPA, 2019).

Health effects	**Exposure**	
	Short-term	**Long-term**
Respiratory effects	Likely to be causal	Likely to be causal
Cardiovascular effects	Causal	Causal
Metabolic effects	Suggestive of, but not sufficient to infer	Suggestive of, but not sufficient to infer
Nervous system effects	Suggestive of, but not sufficient to infer	Likely to be causal
Reproductive and developmental effects	Suggestive of, but not sufficient to infer	Suggestive of, but not sufficient to infer
Cancer	Suggestive of, but not sufficient to infer	Likely to be causal
Mortality	Causal	Causal

The premature mortality attributed to long-term exposure to unsafe levels of ambient $PM_{2.5}$ may be reduced by reducing emissions of precursor gases (such as SO_2, NO_x, NH_3 and VOCs) from significant sources within the industrial centres and urban areas in the Highveld. The estimated willingness to pay in South Africa for a relative reduction in mortality risk could justify some of the policies necessary to effect these changes. Norman *et al.* (2007) estimated that exposure to PM_{10} and $PM_{2.5}$ in urban areas caused an estimated 0.9% of all mortality in 2000 (4 637 premature mortalities). Altieri & Keen (2019) estimated 14 000 premature mortalities could have been avoided in 2012 if South Africa met its current NAAQS (20 µg/m^3) for an annual average $PM_{2.5}$.

The relative reduction in the estimated mortality risk has an estimated economic value of 14.0 billion US dollars (US2011$) which is comparable to 2.2% of the country's 2012 GDP (World Bank PPP US2011$).

Emissions of secondary $PM_{2.5}$ precursor species (e.g. SO_2 and NO_x) from the energy sector, specifically coal-fired power plants, present a significant risk to human health and well-being in South Africa and the Highveld. Lacey *et al.* (2017) estimated that 10 868 premature mortalities could be avoided by 2030 by switching half of the energy production in South Africa to renewable technologies. Coal-fired power plants generate air pollution harmful to human health (Barik, 2021; Koplitz *et al*., 2017; Langerman & Pauw, 2018; Zhao *et al*., 2021). Marais *et al.* (2019) found that exposure to annual average ground-level concentrations of $PM_{2.5}$ from 2030 fossil-fuel use in South Africa could result in an estimated mortality number of 10 400 (2 000-18 300). Myllyvirta (2014) found that the annual average ground-level concentrations of $PM_{2.5}$, attributable to coal-fired power plants, contributed to an estimated mortality number of 2 238 (729-4 237) (Baker & Foley model) and 2 731 (890-5 171) (Zhou *et al.* model) within South Africa. This impact on health translates to an estimated value of thirty billion Rand (Baker & Foley 2011 model). In a more refined study focused on the Highveld, Gray (2019) estimated that the annual average ground-level concentrations of $PM_{2.5}$, attributable to coal-fired power plants, contributed to an estimated mortality number of 471.2 (315.3-673.6) in the industrial Highveld.

2.5 Conclusion to literature review

The concentration of coal-fired power plants within the industrial Highveld, exacerbated by its meteorological conditions, may be contributing to the exceedance of the annual average $PM_{2.5}$ NAAQS limits and the continued existence of airshed priority areas in the region. There are nineteen major coal-fired power plants in the Highveld region. Seventeen of these are concentrated in the industrial Highveld. The clear skies, highly stable vertical atmosphere, low wind speeds, frequent surface- and elevated temperature inversions and low rainfall in the Highveld region, particularly during winter, are highly unfavourable for the dispersion of air pollution (Demircan & Sensoy, 2010; Garstang *et al*., 1996; Tyson *et al*.,1988; Tyson *et al*.,1996). Unstable conditions, increased rainfall, ambient temperatures, and solar radiation in the summertime are favourable for forming secondary particulates (Igbafe, 2007). Ambient $PM_{2.5}$ has been found to exceed the NAAQS for annual average $PM_{2.5}$ in several areas in the Highveld, and exceedances may persist for several years. Through emission inventories, analysis of diurnal variations, chemical composition and modelling, several studies have been able to identify coal-fired power plants as significant contributors to ambient $PM_{2.5}$, particularly secondary $PM_{2.5}$, in the Highveld (Altieri *et al*., 2022; Collett *et al*., 2010; Igbafe, 2007; Morosele *et al*., 2020; Muyemeki *et al*., 2021; Pretorius *et al*., 2017; Ross, 2003; SA DEA, 2012a; Scorgie *et al*., 2004; Scorgie & Thomas, 2006; Sivertsen *et al*., 1995).

Although coal-fired power plants have been identified as a significant source contributor to ambient $PM_{2.5}$ in the Highveld, our understanding of the relationship between levels of ambient $PM_{2.5}$, and the emissions of primary $PM_{2.5}$ and precursor species from these coal-fired power plants remains limited. The impact of these coal-fired power plants on human health and well-being in the Highveld region may be underestimated. Several studies have identified coal-fired power plants as significant contributors to ambient $PM_{2.5}$, particularly secondary $PM_{2.5}$, in the Highveld. Fewer studies have attributed ambient $PM_{2.5}$ solely to coal-fired power plants in the Highveld (Gray, 2019; Steyn & Kornelius, 2018; NEC & PAC, 2018; Myllyvirta, 2014). It is unclear if background conditions were considered, perhaps through the input of ambient values. However, neither of these studies explicitly account for pollution transported across the boundary or all other major sources in the Highveld in the formation of secondary $PM_{2.5}$. Ambient $PM_{2.5}$ in the Highveld is regulated at levels (SA. DEA. 2012b) well above those recommended by the WHO and those found to present adverse impacts on human health (Brauer *et al*., 2019; Shah *et al.,* 2013; Wellenius *et al.,* 2012). Even small contributions by source sectors to long-term $PM_{2.5}$ exposure can have significant impact on human health (Gray, 2019; WHO, 2006).

CHAPTER 3: METHODOLOGY

Chapter 3 presents the methodology applied to achieve the objectives in Chapter 1. It describes the model setup, data used, the model performance evaluation, the health impact function, and the valuation method.

3.1 Simulating atmospheric chemistry in the Highveld

This study is the first to use a Eulerian chemical transport model to simulate the emissions from coal-fired power plants in the Highveld with other major sources at a comparatively fine horizontal grid resolutions to estimate the $PM_{2.5}$ attributable to the coal-fired power plants. There are two types of chemical transport air quality models, Eulerian- and Lagrangian. The main distinction between these two models is how they treat flow. Eulerian models have a coordinate system fixed in space, whereas the coordinate system in the Lagrangian models follows the air parcels (Ramboll, 2020). Due to their inherent computational efficiency, Eulerian models may be more complex. They can be built to give a more comprehensive (non-linear chemistry) simulation of the atmosphere within a region of interest (Ramboll, 2020). Eulerian models, therefore, require ample resources, skill, and time (Ramboll, 2020). Of the previous studies using chemical transport models focussing on fine particulates, three used a Lagrangian model called CALPUFF (Gray, 2019; NEC, 2018; Steyn & Kornelius, 2018), while Marais *et al.* (2019) used a Eulerian model called GEOS-Chem. However, as mentioned in Chapter 2, Marais *et al.* (2019) looked at the impact of fossil-fuel use (coal, natural gas- and bunker fuel-fired power plants) and transport on human health in Africa and used a coarse grid (0.5° x 0.667°, ~50 km × 67 km). This study used simulations by a Eulerian chemical transport model, the Comprehensive Air Quality Model with Extensions (CAMx, version 6.30), to assess the annual average $PM_{2.5}$ attributed solely to coal-fired power plants in the industrial Highveld at a comparatively fine horizontal grid resolution.

This study improves on previous CALPUFF studies (Gray, 2019; NEC, 2018; Steyn & Kornelius, 2018) that assessed fine particulate air pollution from coal-fired power plants in the Highveld, particularly concerning secondary $PM_{2.5}$. CALPUFF and CAMx can treat secondary $PM_{2.5}$ formation and transport. However, MESOPUFF II, the internal chemical mechanism in CALPUFF, is less complex than the Carbon Bond 05 mechanism in CAMx. The chemistry in CALPUFF can only produce aggregates of sulphates and nitrates, while CAMx can also treat organic aerosols and elemental carbon (Trozzi *et al*., 2009). A model comparison of CALPUFF and CAMx based on case studies in Italy for regional air quality planning found CALPUFF a better choice for total particulate evaluation. However, CAMx performs better in secondary particulate formation, particularly with sulphates (Trozzi *et al*., 2009). This study simulated all operational coal-fired power plants in the Highveld and accounted for the effects of boundary conditions and

background emissions from biomass burning, industry, biogenic VOCs and ammonia from agriculture, domestic fuel combustion and on-road vehicles.

This study was built upon an existing modelling platform developed by the Council for Scientific and Industrial Research (CSIR) for the Department of Environmental Affairs (now the Department of Forestry, Fisheries, and the Environment) funded by the Highveld Health Study. The model simulations were run at the Centre for High-Performance Computing (CHPC). The model platform was set up by the CSIR over the Highveld using comparatively fine horizontal grid resolutions. CAMx is a photochemical grid model. The model comprises a “one-atmosphere” treatment of tropospheric air pollution and can cover spatial ranges from neighbourhoods to continents (Ramboll Environ, 2016). Photochemical grid models can account for chemical interactions between emissions from various sources within a domain (Koo *et al*., 2009), making them valuable tools in assessing the relationship between air pollution and secondary particulates in the atmosphere.

3.1.1 Model setup

Domain

Figure 17 shows the study area is focused over the industrial Highveld and includes most of the Gauteng province, the entire HPA, most of the VTAPA and a portion of the WBPA and western BIC. The model platform was setup with two domains, a parent domain with a horizontal grid resolution of 0.06° x 0.06° (~ 6 km x 6 km) and a fine nest domain over the Highveld area with a horizontal grid resolution of 0.02° x 0.02° (~ 2 km x 2 km). There are twenty levels in the vertical, with the first 7 levels below 1000 m; and the highest at approximately 11 km. Although the study focused on the Highveld area (“CAMx Nest”), the larger parent domain is necessary to account for the transboundary transport of pollutants into and out of the Highveld area, and those recirculated.

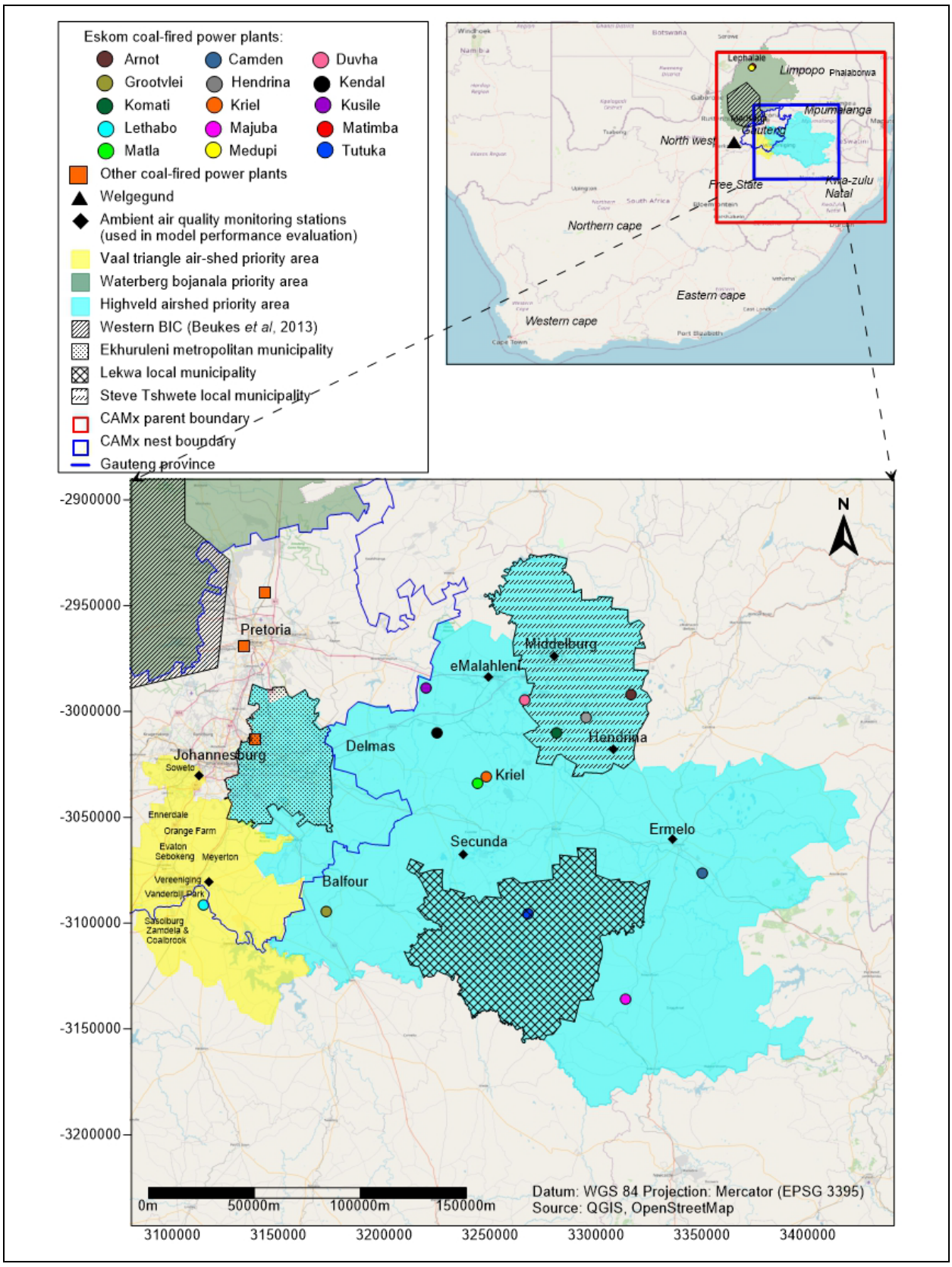

Figure 17: Map of the study area and model domains. The smaller map in the top corner illustrates the boundaries of the CAMx model domains. The red boundary illustrates the parent grid covering the greater Highveld area. The blue boundary illustrates the nested grid over the Highveld Priority Area (HPA) and most of the Vaal Triangle Air-Shed Priority Area. The larger map shows the distribution of the coal-fired power plants within the nested grid and the locations of the ambient air quality monitoring stations used in the model performance evaluation.

Scenarios

For this study, two scenarios were simulated. A baseline scenario simulating all significant sources within the Highveld and a “concept scenario” where the emissions of all Eskom (i.e., large, ≥1 000 MW) coal-fired power plants in the HPA and VTAPA were excluded (“turned off”). Eskom coal-fired power plant capacities range from 1 000 MW (Komati) to 4 800 MW (Medupi). Other coal fired power plants in the Highveld have capacies below 1000 MW (Figure 14).

Initial and boundary conditions

CAMx is a limited area air quality model, which requires initial- and boundary conditions. Ideally, these conditions should be based on ambient air quality observations for the modelling period and representative of the individual boundaries. However, such high-resolution observations are not always available (Jiménez, P. *et al*., 2006). Observational data representative of each side (including model top) of the 6 km parent domain was unavailable. Therefore, the initial and boundary conditions were taken from the MOZART-4[17] (Emmons *et al*., 2010) global chemical transport model. The MOZART-4 output was obtained through the WRF-Chem community via the NCAR ACOM[18] MOZART.

The emission inventory for the boundary conditions used MEGAN biogenic emissions, FINN biomass burning, and worldwide anthropogenic emissions based on Streets *et al.* (2003). It is assumed that the coarsely resolved global chemical transport model will not capture emissions from smaller emitters near the 6 km boundary. However, the emissions from regional sources in worldwide inventories are represented. The regional sources of primary concern to the parent domain, such as biomass burning in the north and east, as well as windblown dust from the west, feed into the Highveld nest domain (CSIR, 2018). Boundary conditions were not required for the smaller 2 km domain because it is a nest. Using two-way nesting, CAMx allows the domains to interact (CSIR, 2018).

As model studies are affected by assumed conditions, it is crucial to minimise the influence of initial and boundary conditions on a study (Jiménez, P. *et al*., 2006). Initial conditions usually influence a brief period after initialisation, the effects of input emissions and chemistry dominate. The CAMx simulations for this study were initialised five days before the start of each month. The impact of the initial conditions was minimised by the five-day spin-up period. Impacts from the boundary on the Highveld domain are minimised by using the parent/nest configuration.

[17] Model for Ozone and Related Chemical Tracers (MOZART).
[18] National Center for Atmospheric Research (NCAR) Atmospheric Chemistry Observations and Modeling (ACOM).

Meteorology

The ACOM MOZART simulation, used in the parent domain, used meteorological fields from NASA GMAO GEOS[19]-5 to drive MOZART-4. CAMx used meteorological input data simulated through the WRF[20] model version 3.8.1 (Skamarock *et al*., 2008; CSIR, 2018). WRF was configured for three domains, i.e., 18 km, 6 km and 2 km horizontal resolution domains centred over the HPA.

Model chemistry

The Highveld has many different air pollution sources, and each emits particulates with different constituents. The model was setup using the Carbon Bond 05 chemical mechanism (Yarwood *et al*., 2005; CSIR, 2018) for gas-phase chemistry. Aerosol chemistry is described using the CF (Coarse-Fine) scheme, which divides the size distribution into fine or coarse. All secondary aerosols formed are in fine mode. Inorganic aerosol chemistry is processed through the ISORROPIA scheme (Nenes *et al.,* 1998; 1999), while organic aerosol chemistry is processed through the SOAP scheme (Strader *et al.,* 1999). Each source within the model setup is associated with a speciation profile for non-methane volatile organic compounds (NMVOC) and particulate matter (PM). The speciation profiles were taken from the US EPA SPECIATE database (Simon *et al*., 2010; CSIR, 2018). The Speciation Tool, developed by ENVIRON, was used to map the SPECIATE database profiles to what is required for CAMx (CSIR, 2018). NMVOC and PM emissions from the coal-fired power plants were speciated with the closest profile description in the SPECIATE database (S32-1178; Coal-Fired Boiler - Electric Generation for NMVOC and 92095; Draft Bituminous Coal Combustion - Simplified for PM).

Photolysis rates

The chemical process, where molecules are broken down into smaller molecules through light absorption, is called photolysis (Britannica, 2018). Photolysis rate inputs are crucial for the CAMx photochemical mechanisms (Ramboll Environ, 2016). The photolysis rates were estimated by the NCAR TUV[21] radiation model and various reference tables developed by the CAMx model developer Ramboll Environ (CSIR, 2018).

Emission inventory

As mentioned earlier, an emission inventory was developed for input into the MOZART-4 for the purpose of determining the model boundary conditions. However, a separate emission inventory was developed for the study domain in the CAMx model. The CAMx emission inventory accounted for biomass burning, industry, biogenic VOCs and ammonia from agriculture, domestic fuel

[19] National Aeronautics and Space Administration (NASA) Global Modeling and Assimilation Office (GMAO) Goddard Earth Observing System (GEOS)
[20] Weather Research and Forecasting (WRF).
[21] Tropospheric Ultraviolet and Visible (TUV).

combustion and on-road vehicles (CSIR, 2018). The emission inventory used in the CAMx model was based on that of the Highveld Health Study but crossed check with coal-fired power emissions data in Eskom annual reports and where necessary updated (Table 5).

The emission inventory was developed for the target year of 2016 for both the parent and nest domains. Data for previous years were applied where data for 2016 was not available. Emissions were gridded at the domain resolution and vary temporally by the hour. Only industry (including power plants) and biomass burning were treated as point sources to account for plume rise and other tall stack (high source) characteristics.

In 2016, Eskom owned fifteen coal-fired power plants: Arnot, Camden, Duvha, Grootvlei, Hendrina, Kendal, Komati, Kusile, Kriel, Lethabo, Majuba, Matimba, Matla, Medupi, and Tutuka (Eskom, n.d.c). The City of Tshwane Metropolitan Municipality owns the Rooiwal coal-fired power plant and the Pretoria West coal-fired power plant. The Rooiwal coal-fired power plant did not operate in 2016. Emissions were reported on NAEIS for the Pretoria West coal-fired power plant. However, comparing these emissions to those of the Eskom coal-fired power plants, it is possible that the plant only operated for testing purposes. Kelvin, a privately owned coal-fired power plant, operated in 2016 and was included in the baseline scenario. Thirteen of the Eskom coal-fired power plants operated in 2016. These included Arnot, Camden, Duvha, Grootvlei, Hendrina, Kendal, Komati, Kriel, Lethabo, Majuba, Matimba, Medupi, and Tutuka. The Kusile coal-fired power plant was under construction in 2016. Its first unit was brought into full commercial operation in August 2017, and Unit 2 and Unit 3 attained commercial operation status in October 2020 and March 2021, respectively (Power Technology, n.d.). Construction of Medupi commenced in 2007 (Eskom, 2020), and it attained commercial operation status in August 2021 (Planting, 2021). Although Medupi only attained its commercial operation status in August 2021, the NAEIS shows it did operate in 2016. Comparing its 2016 emissions to those of other Eskom coal-fired power plants, it is possible that Medupi only operated for testing purposes. These thirteen coal-fired power plants were included in the baseline scenario and “switched off” in the concept scenario.

The emissions from biomass burning were extracted from the FINN[22] dataset (Wiedinmyer *et al*., 2011; CSIR, 2018). Emissions from industrial facilities, including the coal-fired power plants, were taken from the South African NAEIS[23] (CSIR, 2018). Biogenic emissions were simulated using the MEGAN[24] (Guenther *et al*., 2006; CSIR, 2018). Ammonia from agricultural activities was based on the ECLIPSE[25] version 5 worldwide emissions dataset (Klimont *et al*., 2013, CSIR,

[22] Fire Inventory from NCAR (FINN).
[23] National Atmospheric Emissions Inventory System (NAEIS).
[24] Model of Emissions of Gases and Aerosols from Nature (MEGAN).
[25] Evaluating the Climate and Air Quality Impacts of Short-Lived Pollutants (ECLIPSE).

2018). Only emissions from wood, LPG, coal, and paraffin use were estimated for domestic fuel combustion. The emissions from coal, LPG and paraffin use were based on national residential fuel consumption data taken from the commodity flows and energy balances for 2014 developed by the Department of Energy. The emissions from wood use were based on surveyed average per household fuel consumption data and the number of households in each small area level taken from the Stats SA 2016 Community Survey. The emission factors used were taken from several sources (Ballard-Tremeer, 1997; Makonese *et al*., 2015; Scorgie *et al*., 2004; Scorgie, 2012; US EPA AP-42); only a few South African specific studies were available. Emissions from on-road vehicles were estimated based on vehicle kilometres travelled and emission factors derived from the COPERT 5 (version 5.0.1145) model developed by EMISIA SA. The estimates of vehicle kilometres travelled were based on provincial fuel sales, fuel efficiency data, travel activity, road count data, typical average annual daily traffic data and official national road delineations. The activity data were obtained from the: National Geospatial information services; National Household Travel Survey 2013 (Stats SA, 2014a); SANRAL yearbook traffic summaries for 2016; GAUTRANS Gauteng manual counts for 2015; Mpumalanga Provincial Road Asset Management system; South African Road Classification and Access Management Manual (Committee of Transport Officials, 2012) and the 2011 Census (Stats SA, 2014b) (CSIR, 2018).

Highveld Health Study model performance evaluation

This section summarises the WRF model performance as assessed within the Highveld Health Project. This provides important background information on the performance of the WRF model as this was not reassessed in this study. The performance of CAMx in simulating ambient concentrations was performed in this study as described in Section 3.1.3

The WRF model output was compared with meteorological measurements for 2016 from ten ambient air quality stations (Ermelo, Hendrina, Middelburg, Secunda, Witbank (Emalahleni), Camden, Grootdraaidam, Grootvlei, Komati and Phola). Rainfall data from these stations were erroneous (provided an average of its readings for hourly rainfall instead of the total rainfall for each hour). They could not be used in the assessment of the model performance.

On average, the WRF model underestimated temperature by -1.27°C. The U-Wind (east-west direction) wind speed was overestimated by approximately 1.65 m/s. The model correlated well with the observed diurnal and seasonal temperature and U-Wind profiles. The performance of V-Wind was less consistent than U-Wind (CSIR, 2018).

The emission inventory used in this study was based on that of the Highveld Health Study but updated with improved coal-fired power emissions data. The CAMx model output for this study focused on $PM_{2.5}$. The simulated $PM_{2.5}$ concentrations for this study were compared with ambient air quality measurements of $PM_{2.5}$ in Section 4.1.

Table 5: Eskom coal-fired power plant stack parameters and annual emissions in 2016 (tonnes).

Plant	Coordinates (lat, lon in degrees)	Stack Height (m)	Stack Diameter (m)	Gas Exit Temp. (°C)	Gas Exit Vel. (m/s)	NO_X	SO_2	CO	VOC	PM_{10}	$PM_{10\ c}$	PM_{25}
Arnot	-25.95, 29.80	193	11	418.2	34.4	43 455.9	98 015.0	3 903.0	5 010.6	1 348.0	1 348.0	0.0
Camden	-26.62, 30.08	154	8.7	423.2	13.9	28 625.0	66 184.0	483.2	1 617.4	1 021.4	1 018.5	2.9
	-26.62, 30.09	154	8.7	423.2	13.9	17 351.5	48 703.0	362.4	1 213.1	245.0	244.3	0.7
Duvha	-25.96, 29.34	300	7.2	423.2	28.6	67 335.0	139 031.0	1 636.3	3 819.3	4 849.3	4 797.2	51.9
Grootvlei	-26.76, 28.49	152	9	418.2	14.1	15 567.3	31 114.4	575.0	1 523.6	424.4	423.9	0.5
Hendrina	-26.03, 29.60	156	11.1	401.2	20.7	39 034.3	103 500.9	1 217.3	4 829.0	1 024.9	1 019.5	5.5
Kendal	-26.08, 28.96	275	7.8	413.2	27.6	44 041.0	120 722.0	1 936.1	3 673.8	3 092.6	3 086.5	6.1
	-26.09, 28.97	210	7.8	413.2	27.6	41 729.0	127 986.0	1 936.1	3 673.8	3 878.9	3 871.7	7.2
Komati	-26.08, 29.47	220	8	423.2	23.8	19 403.5	11 180.4	192.5	1 124.9	350.9	349.0	1.9
	-26.10, 29.49	220	8	418.2	23.8	10 987.2	18 951.8	192.5	899.9	442.0	439.6	2.4
Kriel	-26.28, 29.15	213	14.3	403.2	18.7	82 937.0	117 779.0	1 699.8	4 371.6	5 847.6	5 816.5	31.1
Kusile	The Kusile coal-fired power plant was under construction in 2016.											
Lethabo	-26.74, 27.97	275	7.7	418.2	24.7	80 001.6	186 902.0	3 517.2	8 419.6	6 830.6	6 815.0	15.6
Majuba	-27.09, 29.77	250	8	398.2	35.3	135 595.0	222 921.0	3 353.4	6 305.2	2 173.2	2 171.0	2.3
Matimba	-23.66, 27.61	250	7.2	408.2	22.3	58 710.0	309 649.6	1 531.4	7 142.8	1 743.6	1 743.6	0.0
Matla	-26.28, 29.14	213	13.8	441.2	14.4	0.0	0.0	0.0	0.0	0.0	0.0	0.0
		275	6.8	441.2	19.9	0.0	0.0	0.0	0.0	0.0	0.0	0.0
Medupi	-23.70, 27.56	220	8.9	413.2	17.9	10 406.0	54 129.7	0.0	205.1	473.9	0.0	473.9
Tutuka	-26.77, 29.34	275	6.5	408.2	34.6	39 410.0	106 731.0	1 154.0	2 505.3	9 176.5	9 069.0	107.5
	-26.77, 29.35	275	6.5	408.2	34.6	29 990.0	89 396.0	1 154.0	2 505.3	5 992.8	5 922.6	70.2

3.1.2 Model output

All CAMx parameters related to fine PM were included in the output, including the species[26]: FCRS, FPRM, PSO4, PNO3, PNH4, PH2O, NA, PCL, PEC, POA, SOA1 to 7 and SOAH. The simulated results were combined in the following way,

- Total $PM_{2.5}$: combined FCRS, FRPM, PSO4, PNO3, PNH4, NA, PCL, PEC, POA, SOA1 to 7 and SOAH;
- Primary $PM_{2.5}$: combined FCRS, FRPM, NA, PCL, POA and PEC; and
- Secondary $PM_{2.5}$: combined PSO4, PNO3, PNH4, SOA 1 to 7 and SOAH.

Although, secondary particulates are formed downwind from the source of precursors gases, coal-fired power plant flue gas also contains sulphates, nitrates, ammonium and organic carbon (Table 2, Chow *et al.*, 2004; Watson *et al.*, 2001), while SO_3 may be converted to sulphuric acid (H_2SO_4) before (in-stack) or when emitted directly to the atmosphere (Corio & Sherwell, 2000; Malfroy *et al*., 2005). Within the model setup, the CAMx output species PSO4 and PNO3 include both particulates formed in the stack from precursor gases (derived as part of particulate emissions) and the particulates formed downwind of the stack (due to ambient chemistry). For this study, secondary particulates include the secondary particulates formed within the stack due to how the model treats these emissions.

The CAMx model set up was defined to output data into 24-hour files per day, totalling a number of 366 files per scenario for 2016 (leap year). The CAMx model outputs for a single year were converted to 366 hourly NetCDF files containing the near-surface concentrations of all the species for both the baseline- and the concept scenario. The combined hourly files for the baseline- and concept scenario were then combined into one file for each of the scenarios. These combined files, containing the various species for each scenario were then averaged for the year 2016. To estimate the annual average concentrations attributable to the large coal-fired power plants, the annual average for the concept scenario was subtracted from the annual average of the baseline scenario.

3.1.3 Model performance evaluation

Air quality models use mathematical formulas to simulate the dispersion of air pollution in the atmosphere. These models all have limitations and uncertainties and cannot replicate real life. The objective of the model performance evaluation is to assess how well the air quality model simulation of $PM_{2.5}$ matches the ground-level observations at specific locations within the Highveld nest domain. Unfortunately, vertical profile measurements along plume paths were not available

[26] Abbreviations are given capitalised as reported in CAMx output CCRS - Coarse crustal, CPRM - Coarse primary, FCRS - Fine crustal, FPRM - Fine primary, NA – Sodium, PCL - Particulate Chloride, PEC - Primary Elemental Carbon, PH_2O - Aerosol Water Content, PNH4 - Particulate Ammonium, PNO3 - Particulate Nitrate, POA - Primary Organic Aerosol, PSO4 - Particulate Sulphate, SOA - Secondary Organic Aerosols.

for the study region and period. The evaluation therefore did not assess the model performance in simulating the transport and transformation of tall stack emissions in the complex Highveld atmosphere.

Ambient air quality data monitored within the Highveld domain in 2016 was requested from the data owners: the DFFE, Eskom and Sasol. The DFFE allowed the use of its observed ambient air quality data, which was made available by the data custodian, i.e. the South African Weather Service. The evaluation was based on $PM_{2.5}$ data from the monitoring stations in Diepkloof, Three Rivers, Ermelo, Secunda, Hendrina, Middelburg and Witbank (Emalahleni) (Locations shown in Figure 17 in section 3.1.1 and data availability in Table 8 in section 4.1). These are regulatory sites that use instruments that adhere to the EN 14907 reference method specified in the NAAQS for $PM_{2.5}$. The hourly $PM_{2.5}$ near-surface concentrations for the baseline scenario were extracted from corresponding locations within simulated grids (resolution ~ 2 km x 2 km).

Exploratory data analysis

An exploratory data analysis of the observed and modelled data was first conducted to better understand the patterns and identify any outliers or obvious errors.

Data quality

The observed data were evaluated for false positive and negative recordings, and where appropriate, this data was removed. It is good practice not to remove negative or positive monitoring data spikes before evaluating if they are real or false (Ministry for the Environment, 2009).

Time series

Times series graphs were evaluated by comparing the variability and values of the observed and modelled data sets.

Data outliers and and values below 1 µg/m^3

The observed and modelled data were analysed for intermittently occurring high concentrations and extremely low concentrations. Eq. (1) and Eq. (2) were used to estimate the number of high outliers in the datasets. Extremely low concentrations and zero values were defined as those below 1 µg/m^3, which is the limit of detection of the standard gravimetric measurement method (EN 14907) of $PM_{2.5}$.

$$IQR = Q3 - Q1 \quad (1)$$

$$Upper\ fence = Q3 + (1.5 \times IQR) \quad (2)$$

$Where$:

$IQR = Interquartile\ range$

$Q = Quartile$

Number of outliers = Values > Upper fence of IQR

Statistical performance evaluation

Following the exploratory data analysis, several statistical criteria were applied to evaluate the model performance. In its comparison, the observed and modelled data sets were paired in time (i.e., date match) and space (i.e., same coordinates). No single metric for model evaluation is completely applicable to all conditions and each metric has advantages and disadvantages (Chang & Hanna, 2004). The linear measures such as Fractional Bias (FB) and Normalised Mean Square Error (NMSE) can become overly affected by intermittently occurring high concentrations in both the observed and modelled dataset. Logarithmic measures such as Geometric Mean Bias (MG) and Geometric Variance (VG) can provide a more reasonable treatment of extreme highs and lows. MG and VG can become overly affected by extremely low concentrations (nearing limit of detection) and are undefined for zero values (Chang & Hanna, 2004).

Therefore, several metrics were used to evaluate the model performance. These included Absolute Fractional Bias (|FB|), MG, VG, NMSE and FAC2. FAC2 is the Fractions of Predictions within a Factor of Two of the observations. It is the most robust of these measures as it is not overly affected by either low or high outliers (Chang & Hanna, 2004; Chang & Hanna, 2005). No minimal thresholds were applied in the calculation of MG and VG. However, the exploratory analysis found the number of measurements below 1 µg/m^3, were less than 5% at each of the seven sites. The observed data set for Three Rivers had the most measurements below 1 µg/m^3 (3%). Where there existed ambiguity in the statistical results, the more robust FAC2 criteria was used to make the final determination.

$$|FB| = \frac{\left|\overline{C_o} - \overline{C_p}\right|}{0.5\ \left(\overline{C}_o + \overline{C_p}\right)} \quad (3)$$

$$NMSE = \frac{\overline{\left(C_o - C_p\right)^2}}{\overline{C_o}\,\overline{C_p}} \quad (4)$$

$$MG = \exp\left(\ln \overline{C}_o - \ln \overline{C_p}\right) \quad (5)$$

$$VG = exp\left[\overline{\left(\ln C_o - \ln C_p\right)^2}\right] \quad (6)$$

$$FAC2 = fraction\ of\ data\ that\ satisfy$$

$$0.5 \leq \frac{C_o}{C_p} \leq 2.0 \quad (7)$$

$Where$:
$C_p = Model\ predictions$
$C_o = Observations$
$overbar(\overline{C}) = Average\ over\ the\ dataset$

The following criteria were used as guidelines to evaluate if the model performed acceptably:

- A fraction of predictions within a factor of two of observations is approximately 50% (i.e., 0.5< FAC2<2);
- The mean bias is within approximately 30% of the mean (i.e., roughly |FB|<0.3 or 0.7<MG<1.3); and
- The random scatter is approximately a factor of two to three of the mean (i.e., roughly NMSE<1.5 or VG<4).

These model acceptance criteria were taken from the Technical Descriptions and User's Guide for the BOOT Statistical Model Evaluation Software Package, Version 2.0 (Chang & Hanna, 2005). It should be noted that these model acceptance criteria are not firm specifications. It is expected that the model performance will be affected by a decrease in the quality of input data.

3.2 Determining $PM_{2.5}$ attributable to coal-fired power

As previously mentioned, the change in $PM_{2.5}$ concentrations was estimated by calculating the difference between the simulated baseline scenario ("Coal-fired power on") and a concept scenario where all large coal-fired power plants in the domain were excluded ("Coal-fired power off"). By subtracting the concentrations simulated in the concept scenario from those simulated in the baseline, the full impact of the large coal-fired power plants on the concentrations and distribution of $PM_{2.5}$ over the Highveld could be isolated. A positive number would indicate that $PM_{2.5}$ concentrations were higher in the baseline scenario than in the concept scenario. In terms of source attribution, this is deemed a brute force or zero-out approach (Thunis *et al.,* 2019). It is considered appropriate for use here, where there is a lone source sector, secondary pollutants, conceptual scenario (i.e., no realistic investigation of mitigation) and adequate computational resources for multiple full-year simulations.

3.3 Determining the impact of $PM_{2.5}$ attributable to coal-fired power

3.3.1 Avoidable premature mortality

The formula for estimating the health impact attributed to $PM_{2.5}$ is referred to as a health impact function (Sacks *et al*., 2018). The health impact function used in this study is defined as Eq. (8):

$$\Delta Y = Y_0 \left(1 - e^{-\beta \Delta PM}\right) \times Pop \quad (8)$$

$Where$:
ΔY $= Estimated\ health\ impact\ attributed\ to\ the\ air\ pollution$
Y_0 $= Baseline\ incidence\ for\ the\ health\ effect\ of\ interest$
β $= Beta\ coefficient\ derived\ from\ epidemiologic\ study$
$\Delta PM = Change\ in\ annual\ average\ PM2.5\ (\mu g/m3)$
Pop $= Population\ exposed\ to\ the\ air\ pollution$

The WHO recommended concentration-response functions for cost-benefit analysis for its (HRAPIE) project (WHO, 2013). The relative risk for "All-Cause" for a 10 µg/m^3 change in annual $PM_{2.5}$ recommended by the WHO and used in this study is based on a meta-analysis of thirteen cohort studies (Hoek *et al.*, 2013). The β coefficient is determined by the natural logarithm of the relative risk (RR) divided by the exposure change (Table 6).

Table 6: Hazard ratio for all-cause mortality for a 10 µg/m^3 change in $PM_{2.5}$ (WHO, 2013; Hoek et al., 2013).

Relative Risk (RR)	Min RR	Max RR	Exposure Δ	Beta[27]	Standard Error
1.062	1.040	1.083	10 µg/m^3	0.0060	0.0010

[27] B = LN(RR)/ ΔExposure = LN (1.062)/10 = 0.0060

The all-cause mortality numbers were obtained from the Statistics South Africa 2018 statistical release “Mortality and causes of death in South Africa, 2016: Findings from death notification” for the areas within the modelling domain. The thirteen cohort studies analysed by Hoek *et al*. (2013) were based on adults. The baseline incidence (Y_0) was determined by dividing the “All-cause” mortality (≥25 years) within each municipal area by the population (≥25 years) within each municipal area. The health impact however was on the total population exposed. The mortalities between ages 15 and 24 were estimated using the age specific mortality rates for 2016 taken from Appendix F in Stats SA (2018a). The mortality rates for ages 15 and 24 amounted to 4 mortalities per 1000 population. The mortalities estimated between ages 15 and 24 were then deducted from the mortality numbers provided for ages 15 to 44 in Appendix I in Stats SA (2018a). The all-cause mortalities estimated for 25 to 44 were then added to the mortalities for 45 to 64 and 65+ for each municipal area taken from Stats SA (2018a). Population numbers were obtained from the Statistics South Africa provincial profiles for Gauteng, North-West, Limpopo, Mpumalanga, Free State and Kwazulu-Natal. The percentage of the population aged 0 to 24 for each municipal area was estimated based on age distribution numbers for each province. The population aged 25 and older was determined by subtracting the estimated population aged 0 to 24 from the total population. The municipal boundaries for 2016 were obtained from Statistics South Africa (Table 7).

Table 7: Population and all-cause mortality for 2016 (Stats SA. 2018a to g).

Province	**Municipality**	**GEO ID**	**Total Pop.**	**Pop. (≥25)**	**Area (km^2)**	**Mortality ≥25, excl. unspecified**
Gauteng	City of Tshwane MM[28]	TSH	3 275 152	1950163	6 298	19 987
	City of Johannesburg MM	JOH	4 949 347	2947050	1 645	26 808
	Ekurhuleni MM	EKU	3 379 104	2012061	1 975	23 373
	West Rand DM[29]	WES	838 594	499334	4 087	9 016
	Sedibeng DM	SED	957 528	570152	4 173	9 739
Limpopo	Waterberg DM	WAT	745 758	567730	44 913	4 437
	Greater Sekhukhune DM	GRE	1 169 762	890515	13 528	8 864
North West	Bojanala DM	BOJ	1 657 148	1432985	18 333	11 652
Mpumalanga	Ehlanzeni DM	EHL	1 754 931	1465408	27 896	12 612
	Gert Sibande DM	GER	1 135 409	948093	31 841	8 030
	Nkangala DM	NKA	1 445 624	1207130	16 758	9 543
Kwa-Zulu Natal	Zululand DM	ZUL	892 310	492753	14 799	5 433
	Amajuba DM	AMA	531 327	293411	7 102	4 316
Free State	Thabo Mofutsanyane	THA	779 330	701192	32 734	7 997
	Fezile Dabi DM	FEZ	494 777	445169	20 668	4 520

[28] MM: Metropolitan Municipality
[29] DM: District Municipality

3.3.2 Valuation of reductions in premature mortality risks

The benefit of reducing exposure to ambient $PM_{2.5}$ from coal-fired power plants was estimated using a welfare-based method that monetises the increased risk of mortality from air pollution corresponding to individuals' willingness to pay (WTP) (Markandya, 2019; OECD, 2012; World Bank, 2016). The WTP captures the compromise individuals are willing to make to lessen their mortality risk. The value of statistical life (VSL) constitutes the sum of many individuals' WTP for slight changes to this risk (OECD, 2012; World Bank, 2016), it is a local trade-off rate between mortality risk and capital (Kniesner & Viscusi, 2019). It is crucial to remember that a VSL does not constitute the value of any single human life or death or represent social judgement on what that value should be. The WTP has become a standard method in high-income countries to value the risk of air pollution mortality. However, WTP studies are still lacking in many other countries, including South Africa (World Bank, 2016). Eq.(9) provides a practical method to adjust a "base VSL" from the original situation in which it was developed to the context of another country. This adjustment considers the most salient characteristic to influence individuals under different circumstances, the income elastic (i.e., the percentage change in the WTP per percentage change in income) (World Bank, 2016). The value of the health impact was calculated by multiplying the estimated avoided premature mortality with the Value of Statistical Life (VSL) (Eq. (10)). The base VSL of \$3.83 million[30] represents a mean VSL estimation for high-income member countries of the Organisations for Economic Co-operations and Development (OECD) (World Bank, 2016). These countries have an average gross domestic product (GDP) per capita of approximately \$37 000 (World Bank, 2016). The OECD VSL is expressed in US2011\$ at purchasing power parity (PPP). The SA GDP per capita, PPP (constant 2017 international \$) for 2016 (\$12 702.92) was taken from the World Development Indicators database last updated on 30 June 2021 (World Bank, n.d). An income elasticity value of 1.2 for low- to middle-income countries was assumed, with an elasticity range of 1 to 1.4 for sensitivity evaluation (World Bank, 2016). In this study, the $VSL_{SA,2016}$ of \$1.06 million was estimated based on an income elasticity of 1.2. This is similar to the $VSL_{SA,2017}$ of \$1.046 million calculated by Viscusi *et al*. (2017) using a base U.S. VSL of \$9.631 million and an income elasticity of 1.

$$VSL_{c,n} = VSL_{OECD} \times \left(\frac{Y_{c,n}}{Y_{OECD}}\right)^{\varepsilon} \quad (9) \qquad Valuation = \Delta Y \times VSL_{c,n} \quad (10)$$

$Where$:

ΔY = $Estimated\ health\ impact\ attributed\ to\ the\ air\ pollution$

$VSL_{c,n}$ = $Value\ of\ a\ Statistical\ Life\ for\ country\ c\ in\ year\ n$

VSL_{OECD} = $Value\ of\ a\ Statistical\ Life\ for\ base\ sample\ of\ OECD\ countries$

$Y_{c,n}$ = $is\ the\ GDP\ per\ capita\ for\ country\ c\ in\ year\ n$

Y_{OECD} = $is\ the\ average\ GDP\ per\ capita\ for\ base\ sample\ of\ OECD\ countries$

ε = $Income\ elasticity$

[30] In terms of constant 2011 U.S. dollars at purchasing power parity (PPP) adjusted rates.

CHAPTER 4: RESULTS AND DISCUSSIONS

Chapter 4 presents the results of the model performance evaluation and the relationship between the ambient $PM_{2.5}$, particularly secondary $PM_{2.5}$, attributable to coal-fired power plants and its impact on human health in the Highveld.

4.1 Model performance evaluation

The model performance evaluation aimed to assess how well the air quality model simulation of $PM_{2.5}$ matched ground-level observations at specific locations within the Highveld nest domain. The simulated hourly $PM_{2.5}$ near-surface concentrations for the baseline scenario were extracted from the gridded model output (resolution ~ "2 km x 2 km"). The observed data were evaluated for false positive and negative recordings, and where appropriate, this data was removed. The observed and modelled data were then analysed by looking at graphical displays of time series at each site, as well as considering the number of outliers and low concentrations (<1 µg/m^3) within each data set. Following the exploratory data analysis of the observed and modelled data, several statistical criteria were applied to evaluate the model performance. For the statistical performance evaluation, the observed and modelled data sets were paired in time (i.e., date match). The statistical performance evaluation calculations were formulated to ignore points where the observational data was missing.

Exploratory data analysis

Data quality

Only the Diepkloof observed data (field measurements) contained negative values. Seventeen (17) negative data points were found, all within March 2016. The meta-data for these stations were not available and the reason for the negative values could not be determined. Looking at the values (average 18.81 µg/m^3) immediately before and after the negative recordings, the negative values were found anomalous and removed. No strange (e.g. 9999) or repeating positive values were flagged. Table 8 gives the data availability for 2016 for each ambient monitoring station used in the study.

Table 8: Data availability of DFFE ambient air quality monitoring stations used in the study.

Site	Coordinates (lat, lon; degrees)	Site Description	Data points before QC	Data points after QC	Data availability
Diepkloof	-26.25, 27.95	Urban	8 784	8 115	92%
Three Rivers	-26.65, 27.99	Urban	8 095	6 935	79%
Ermelo	-26.49, 29.96	Residential (Low income)	8 784	6 482	74%
Secunda	-26.55, 29.07	Residential (Low income)	8 103	5 288	60%
Hendrina	-26.15, 29.71	Residential(Medium/Upper)	8 784	8 309	95%
Middelburg	-25.79, 29.46	Residential(Medium/Upper)	7 364	7 152	81%
Witbank (Emalahleni)	-25.87, 29.18	Residential (Low income)	8 784	8 225	94%

Time series

The times series in Annexure A were evaluated by comparing the variability and values of the hourly, monthly, monthly-diurnal and diurnal observed and modelled data sets. The graphs for Diepkloof show that the the observed and modelled data compared better during winter (May, June, and July), while the observed and modelled trends appear similar. However, the model underestimated $PM_{2.5}$ from January to April 2016 and October to December 2016. The graphs for Ermelo show significant gaps in the observational data from June to August 2016. The observed and modelled trends appear similar. The data sets compare well during 00:00-04:00 and 09:00-16:00. However, the model overestimated $PM_{2.5}$ between 04:00 to 09:00 and 17:00 to 23:00. The graphs for Hendrina show the observed and modelled variations compare well throughout the year, while the observed and modelled trends appear similar. The model overestimated the daily $PM_{2.5}$ from 18:00 to 22:00 at Hendrina. The graphs for Middelburg show the observed and modelled variations compare well from January to May 2016. The model overestimated $PM_{2.5}$ from May 2016. The observational data for Middelburg has a large gap between November to December 2016. The observational data for Secunda only starts April 2016. There is also a large gap from October to November and the measurements stop at the start of December 2016. The observed and modelled trends appear similar, while the model underestimated $PM_{2.5}$ at Secunda. Three Rivers has no observational data for November 2016. The observed and modelled appear similar. The model underestimated $PM_{2.5}$ at Three Rivers. The graphs for Emalahleni show that the model underestimated $PM_{2.5}$ at this site. In general, the observed and modelled hourly, monthly, and monthly-diurnal variations compare relatively well throughout the year, while similar trends were observed.

Data outliers and values below 1 $\mu g/m^3$

As mentioned in section 3.1.3, the statistical criteria Fractional Bias (FB) and Normalised Mean Square Error (NMSE) can become overly affected by intermittently occurring high concentrations in either the observed or modelled dataset. The criteria Geometric Mean Bias (MG) and Geometric Variance (VG) may be overly affected by extremely low concentrations (nearing limit of detection) and are undefined for zero values (Chang & Hanna, 2004). The upper fence of the interquartile range (IQR), as described in Eq. (1) and Eq. (2) in section 3.1.3, was used to estimate the number of high outliers to evaluate the likelihood of FB and NMSE being affected by intermittently occurring high concentrations in the datasets. The limit of detection (1 $\mu g/m^3$) of the standard gravimetric measurement method (EN 14907) of $PM_{2.5}$ was used to define extremely low concentrations and zero values. The number of values below 1 $\mu g/m^3$ were used to evaluate the likelihood of MG and VG being affected by extremely low and zero values. Table 9 gives the values of the first quartile, the third quartile (Q3), the IQR, the upper fence and the number of outliers and values below 1 $\mu g/m^3$. Table 9 shows that combined, the datasets for Ermelo contain

the highest number of outliers (1598) and the highest number of values below 1 µg/m^3 (269). Three Rivers has the second highest number of values below 1 µg/m^3 (252).

Table 9: The number of outliers exceeding the upper fence of the IQR and the number of values below than 1 µg/m^3, The limit of detection of method EN 14907).

Observed data						
Site	**Q1**	**Q3**	**IQR**	**Upper fence**	**Number of outliers**	**< 1 µg/m^3**
Diepkloof	10.73	31.41	20.68	62.43	409.00	202.00
Three Rivers	10.85	39.71	28.86	82.99	196.00	228.00
Ermelo	5.16	18.91	13.75	39.53	509.00	217.00
Secunda	14.20	51.51	37.32	107.49	567.00	4.00
Hendrina	6.05	17.11	11.06	33.69	378.00	124.00
Middelburg	4.26	13.62	9.36	27.67	412.00	132.00
Witbank (Emalahleni)	8.10	26.08	17.98	53.04	730.00	14.00
Modelled data						
Site	**Q1**	**Q3**	**IQR**	**Upper fence**	**Number of outliers**	**< 1 µg/m^3**
Diepkloof	6.39	13.83	7.45	25.00	707.00	14.00
Three Rivers	6.43	14.18	7.75	25.81	666.00	24.00
Ermelo	8.57	36.94	28.37	79.49	1089.00	52.00
Secunda	9.40	31.40	21.99	64.39	830.00	13.00
Hendrina	7.21	16.93	9.72	31.51	612.00	55.00
Middelburg	6.49	14.80	8.32	27.28	611.00	41.00
Witbank (Emalahleni)	7.31	17.06	9.75	31.68	726.00	14.00

Statistical performance evaluation

Several metrics were used to evaluate the model performance. These included absolute FB, MG, VG, NMSE and FAC2 (Fractions of Predictions within a Factor of Two of the observations). The equations for these metrics can be found in section 3.1.3. FAC2 is the most robust of these measures. Unlike FB, MG, VG and NMSE, FAC2 is not overly affected by either low or high outliers (Chang & Hanna, 2004; Chang & Hanna, 2005). The software used for the model performance evaluations was formulated to ignore blanks or missing data. Figure 18 presents the results of the model performance evaluation in terms of |FB|, NMSE, MG, VG & FAC2. Figure 18 shows that at Diepkloof, the model performed well in terms of VG and relatively well in terms of NMSE. The model performed poorly at Ermelo in terms of VG, MG, |FB| and NMSE. However, the model's performance came close to meeting the FAC2 criteria. The model performance at Ermelo could have been affected by the low availability (74%) of observed data or by the poor comparison in diurnal data (Annexure A). It is also possible that the model performance at Ermelo could have been affected by intermittently occurring high concentrations and extremely low concentrations (Table 9). The model performed best at Hendrina and Middelburg, meeting the VG, MG, |FB| and NMSE performance criteria. The model also performed well at Witbank (Emalahleni), meeting the criteria for VG and MG, and coming close to meeting the criteria for |FB| (<0.3) and NMSE (<1.5) with an |FB| of 0.43 and an NMSE of 1.76. At Secunda, the model

performed well in terms of VG. However, it performed poorer in terms of MG, |FB| and NMSE. The low availability (60%) of observed data at Secunda could have affected the outcome of the model performance evaluation. The evaluation at Three Rivers did not meet the criteria for VG, MG, |FB| and NMSE. The low availability (79%) of observed data for or the poor comparison in diurnal data (Annexure A) could have affected the results for Three Rivers. Another possible reason for the poorer performance in terms of VG and MG could be the relatively high number of values below 1 µg/m^3 (Table 9). Three Rivers, however, at 0.4, came close to meeting the FAC2 criteria (0.5<FAC2>2).

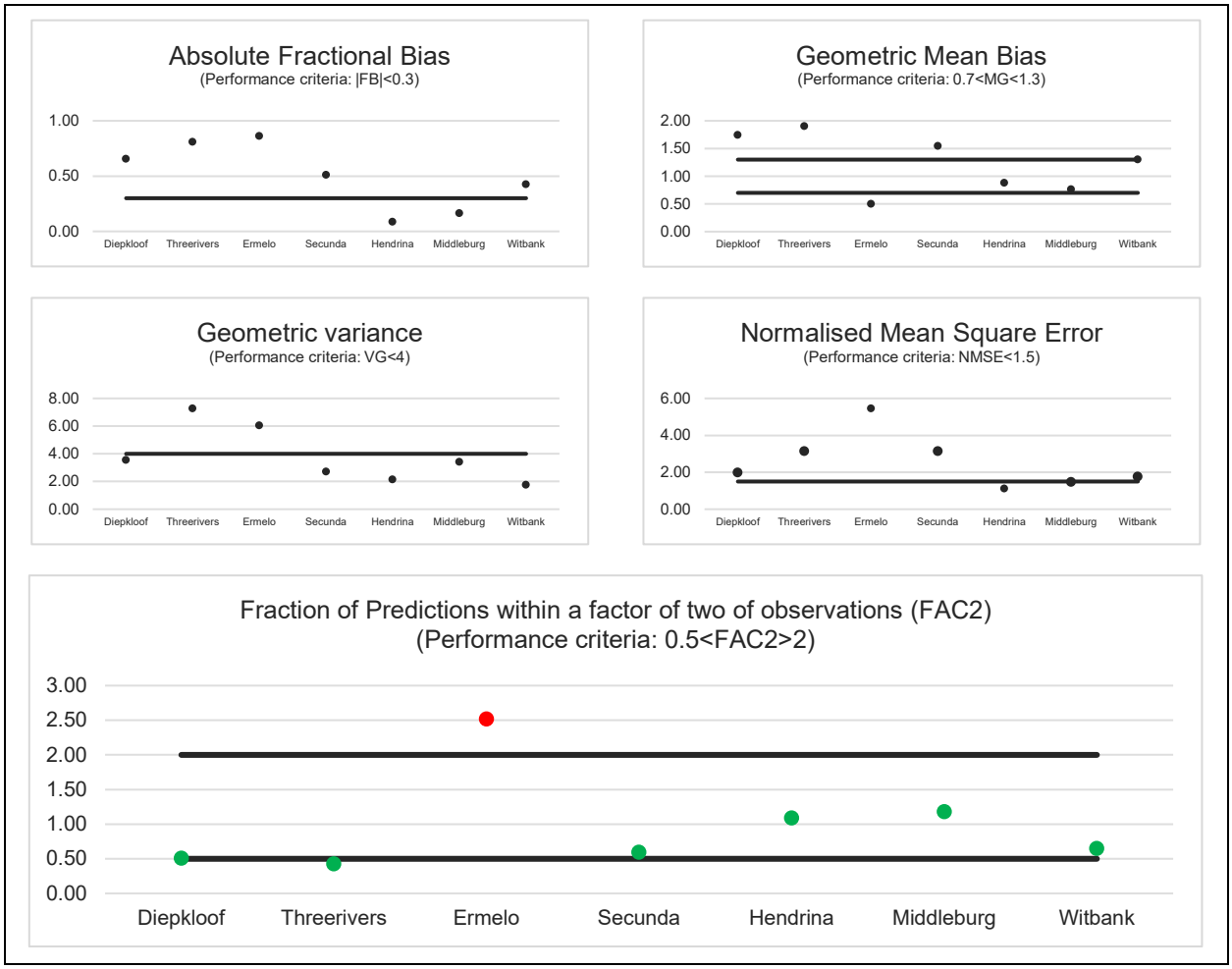

Figure 18: A graph illustrating the results of the metrics |FB|, NMSE, MG, VG & FAC2 used in the model performance evaluation. FAC2 was used as the determining criteria. Markers with acceptable performance were highlighted in green, and poorer model performance was highlighted in red.

Discussion

All air quality models have limitations and uncertainties and cannot replicate real life. In addition, most of the ambient air quality monitoring sites selected for the model performance evaluation are located within low-income settlements with significant local sources (such as residential fuel burning). These local sources and wind-blow dust (not included in the emission inventory) could lead to local air quality that is significantly different from that simulated for a grid with a resolution of approximately 2 km x 2 km. This study focused on annual and regional air quality, as it is not as strongly influenced by such local sources. However, it is important to be aware of these sources as they can affect the comparison of observed and modelled data. Similar to the findings made by Hersey *et al.* (2015) for $PM_{2.5}$ in the Vaal Triangle Airshed Priority Area (VTAPA) and Johannesburg (Buccleuch), and Govender & Sivakumar (2019) for $PM_{2.5}$ in the VTAPA, the variation graphs show the highest concentrations early in the morning, early in the evening and during the winter months. Hersey *et al.* (2015) found that most of the sites in the VTAPA were influenced by domestic fuel burning. Govender & Sivakumar (2019) attributed the $PM_{2.5}$ trends they found to windblown dust, domestic fuel burning, and the dissolving of the boundary layer around midmorning.

A comparison of the times series of the observed and modelled data found that the model overestimated $PM_{2.5}$ concentrations at Ermelo and Middelburg and underestimated $PM_{2.5}$ at the rest of the sites. The hourly variations in modelled and observed data are only comparable for parts of the year for Diepkloof, Ermelo, Middleburg and Secunda. The hourly variations in modelled and observed data for Hendrina and Emalahleni compare relatively well throughout the year. The observed and modelled monthly, monthly-diurnal, and diurnal trends appear similar for Diepkloof, Hendrina, Secunda, and Emalahleni. At Ermelo and Three Rivers, the monthly and monthly-diurnal trends of the observed and modelled data appear similar. However, the diurnal trends do not correspond well.

The model acceptance criteria applied in the statistical evaluation are not firm specifications and are generally used to compare maximum concentrations on sampling sites unpaired in space. The comparisons of observed and modelled data sets in this study were robust in that they were paired in time (i.e., date match) and space (i.e., same coordinates). The statistical model performance evaluation found that the model performance at each site, except for Ermelo and Three Rivers, met at least one of the performance criteria. FAC2 was used as the determining criteria because it is the most robust and not overly affected by either low or high outliers. The model performance met the criteria for FAC2 at all sites except Ermelo and Three Rivers. However, the model performance at Ermelo (FAC2 of 2.52) and Three Rivers (FAC2 of 0.4) come close to meeting the FAC2 criteria (0.5<FAC2>2). It was therefore concluded that the model performed adequately for this study.

4.2 The effect of coal-fired power plant emissions on secondary particulate chemistry in the atmosphere over the Highveld.

As previously mentioned, two simulations were run with the Eulerian chemical transport model, CAMx, i.e. a baseline scenario with all the significant sources within the Highveld, and a concept scenario where the emissions from large (≥1 000 MW) coal-fired power plants in the Highveld Priority Area (HPA) and VTAPA were excluded. The residual annual average concentrations attributable to the large coal-fired power plants were determined by subtracting the annual averages for the concept scenario from the annual averages for the baseline scenario. A positive number indicates the concentrations were higher in the baseline scenario (i.e., that included large coal-fired power plant emissions) than in the concept scenario.

Precursor gases

The results of the simulated annual average near-surface concentrations of the precursor gases (SO_2, NO, NO_2 and NH_3) are presented in Table 10 and Figure 19. The results are shown for the baseline scenario, the concept scenario and those attributed to the large coal-fired power plants. Table 10 gives the spatial 99th percentile and Figure 19 presents the distribution of the annual average near-surface concentrations of the precursor gases. For ease of reference the plants are numbered alphabetically in the first map in Figure 19.

Map (a) and map (b) in Figure 19 shows that the simulated annual average of SO_2 ranges from 0 to ~65.7 ppb for the baseline scenario and 0 to ~42.6 ppb for the concept scenario. Table 10 shows a significant decrease in the spatial 99th percentile of SO_2 (droping from 17.11 ppb to 4.39 ppb) when the large coal-fired power plants are excluded. Map (c) shows the annual average SO_2 attributed to the large coal-fired power plants ranges from ~0 to 64.4 ppb. The annual SO_2 NAAQS limit (19 ppb) is exceeded in all three instances (starting from moss green colour). In the baseline scenario, the annual SO_2 NAAQS is exceeded at Sasolburg, Secunda and all the Eskom coal-fired power plants. In the concept scenario, the annual SO_2 NAAQS is exceeded at Sasolburg and Secunda. The Sasol facility in Secunda has a boiler plant, with similar boiler technology to that of Eskom, which supplies steam to the Sasol facility (Grobler, 2016). The ambient SO_2 attributed to the large coal-fired power plants exceed the annual SO_2 NAAQS at or in proximity to all coal-fired power stations except Grootvlei. Figure 20 gives the percentage contributions of each plant to the total SO_2 emitted by all the large coal-fired power plants. Grootvlei and Komati each contributed approximately 2% to the total SO_2 emitted by the large coal-fired power plants (Figure 20). The annual SO_2 NAAQS was exceeded over an area of approximately 6 km^2 in proximity to Komati. However, no exceedances were modelled at or in proximity to the Grootvlei power plant. The simulation is interesting, because although its contribution to SO_2 emissions is low compared to the other plants, the Grootvlei power plant does not comply with the new plant

MES for SO_2 (Table 3). The cumulative simulated impact of the coal-fired power plants greatly increases the extent to which the NAAQS for SO_2 is exceeded. For instance, in the concept scenario, ambient SO_2 exceeded the annual NAAQS over an area of approximately 39.9 km^2 over the Sasol Secunda Synfuel operations. When the large coal-fired power plants are included, this area of exceedance increases by approximately 36.5% to 62.9 km^2.

Map (d) and map (e) in Figure 19 shows that the simulated annual average NO_2 ranges from 0 to ~35.0 ppb for the baseline scenario and 0 to ~33.5 ppb for the concept scenario. The spatial 99th percentile of NO_2 drops significantly from 10.93 ppb to 7.35 ppb when the large coal-fired power plants are "turned of" (Table 10). Map (f) shows annual average NO_2 attributed to the coal-fired power plants ranges from ~0 to 20.8 ppb. The annual NO_2 NAAQS (21 ppb; starting from forest green colour) is exceeded in the baseline and concept scenario. In both scenarios, the annual NO_2 NAAQS is exceeded over parts of Sasolburg, Johannesburg, and the Secunda Synfuel operations. The results correspond to the NO_2 hotspots identified by Lourens *et al*. (2012) and the HPA AQMP (SA DEA, 2012a). The ambient NO_2 exceeds its annual NAAQS near the Majuba coal-fired power plant in the baseline scenario.

NO and NH_3 do not have NAAQS, however, they are also important precursor gases to $PM_{2.5}$. Map (g) and map (h) in Figure 19 shows that the simulated annual average NO ranges from 0 to ~56.5 ppb for the baseline scenario and 0 to ~52.1 ppb for the concept scenario. When the large coal-fired power plants are "turned of" the spatial 99th percentile of NO drops significantly from 9.14 ppb to 4.12 ppb (Table 10). Map (i) shows the annual average NO attributed to the large coal-fired power plants ranges from ~0 to 56 ppb. Map (j) and map (k) in Figure 19 shows that the simulated annual average NH_3 is slightly higher in the concept scenario (Ranging from 0 ppb to 3.54 ppb) than in the baseline scenario (Ranging from 0 ppb to 3.07 ppb). The spatial 99th percentile of NH_3 increasing from 2.25 ppb in the baseline scenario to 2.75 ppb in the concept scenario (Table 10).

Table 10: The spatial 99th percentile of the annual averages of precursor gases (ppb) within the Highveld study area.

Scenario	SO_2	NO_2	NO	NH_3
Baseline (Coal-fired Power On)	17.11	10.93	9.14	2.25
Concept (Coal-fired Power Off)	4.39	7.35	4.12	2.75
Difference (Attributable to coal-fired power plants)	14.89	7.69	6.51	0.00

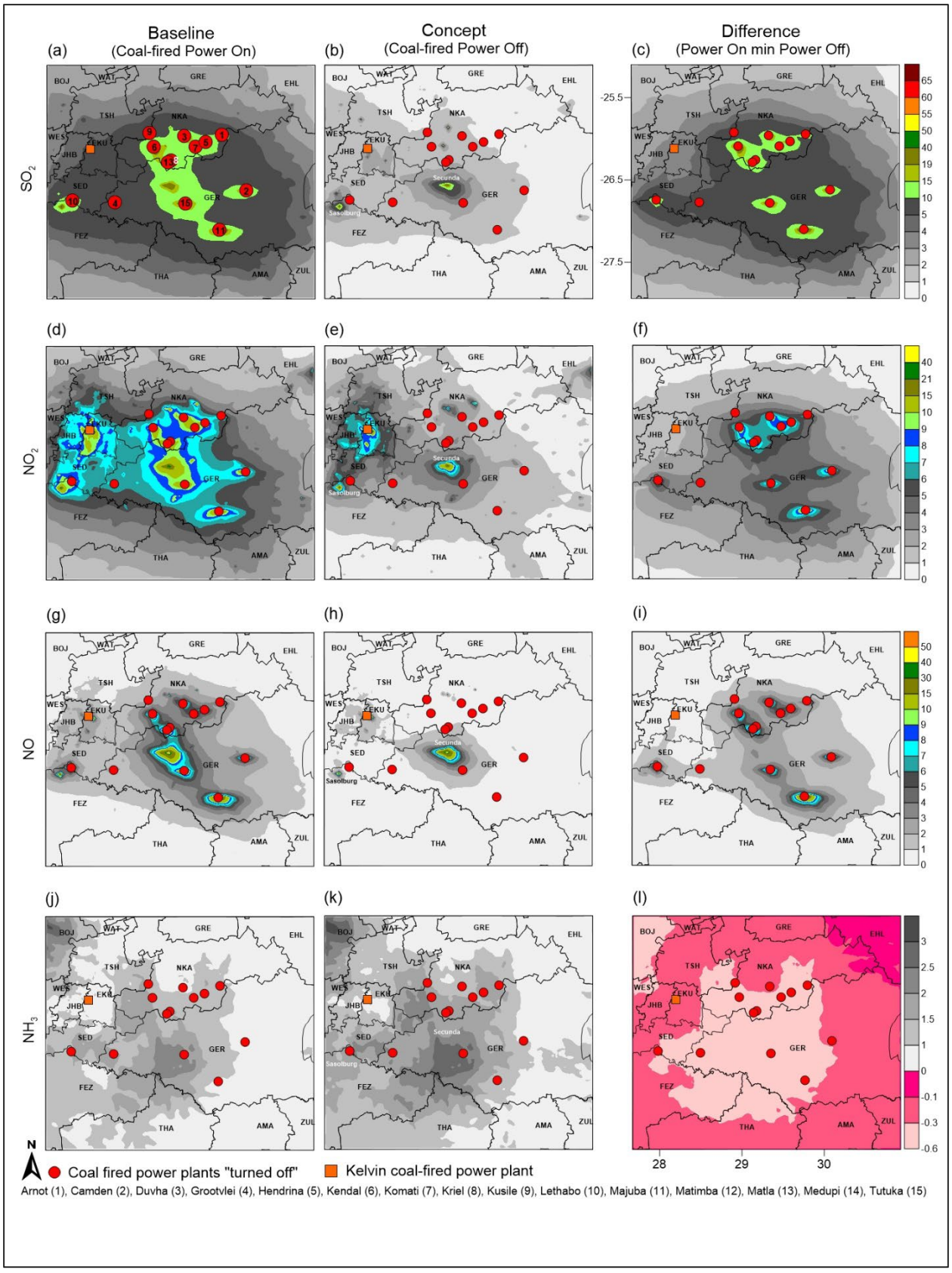

Figure 19: The simulated annual average near-surface concentrations (ppb) of SO_2, NO, NO_2 and NH_3 of the baseline scenario ("Coal-fired power on"), the concept scenario ("Coal-fired power off") and the residual concentrations attributed to the large coal-fired power plants. A positive number indicates gas concentrations were higher in baseline scenario than the concept scenario. The acronyms on the map refer to the different municipal areas (Table 7).

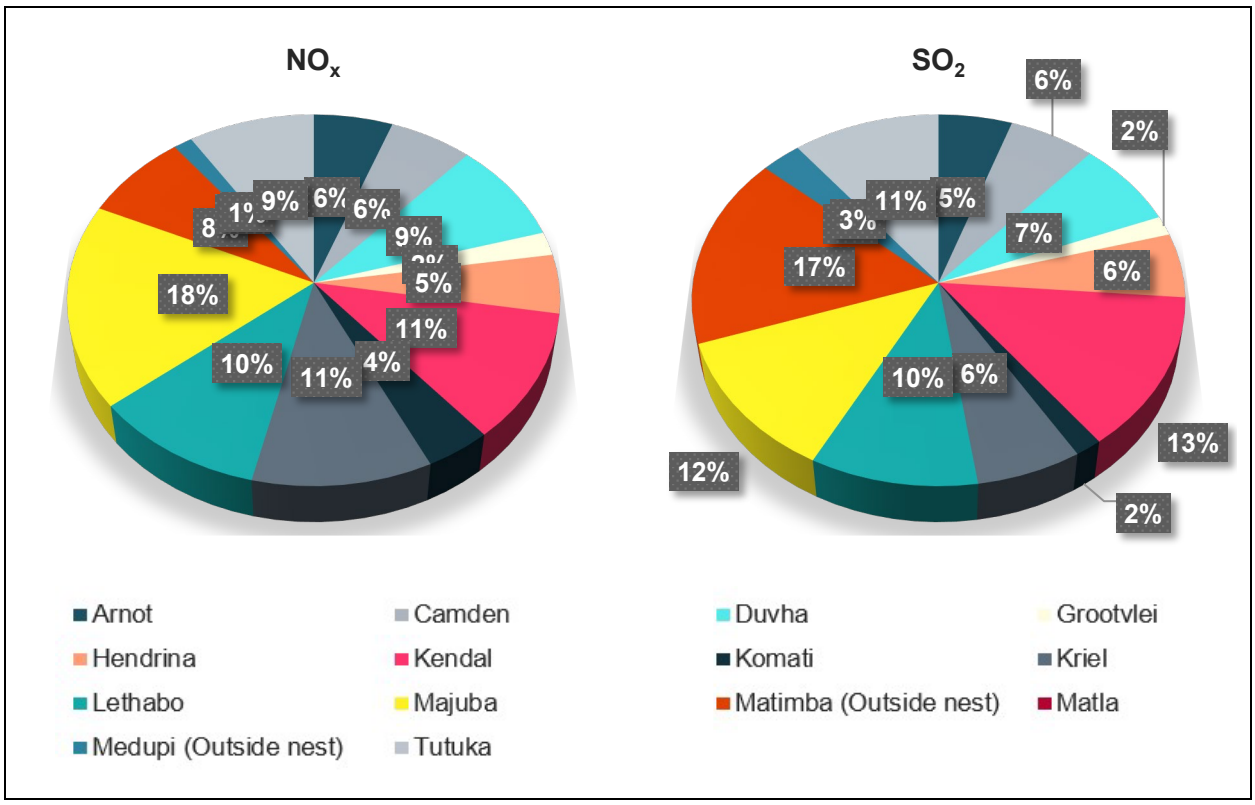

Figure 20: The percentage contribution of each plant to the total NO_x and SO_2 emitted by the all the large (≥1 000 MW) coal-fired power plants (Adapted from the values in Table 5).

Secondary fine particulates

Table 11 gives the spatial 99th percentile of the annual average near-surface concentrations of the secondary fine particulate species (Particulate Sulphate (PSO4), Particulate Nitrate (PNO3) and Particulate Ammonium (PNH4)). Figure 21 presents the distribution of the annual average near-surface concentrations of these species. Table 11 and Figure 21 show the results for the different senarios and those attributed to the large coal-fired power plants.

Map (a) and map (b) in Figure 21 shows that the simulated annual average PSO4 ranges from ~2.4 to 30.6 µg/m^3 for the baseline scenario and ~1 to ~29.3 µg/m^3 for the concept scenario. The spatial 99th percentile of 4.56 µg/m^3 to 2.71 µg/m^3 when the large coal-fired power plants are excluded (Table 11). Map (c) shows the annual average PSO4 attributed to the coal-fired power plants ranges from ~0 to 2.5 µg/m^3. The highest PSO4 concentrations, attributable to the large coal-fired power plants, (dark grey colour in row one, right column) are seen near the Camden and Majuba coal-fired power plants[31] in the Gert Sibande (GER) district municipality. Figure 20 gives the percentage contributions of each plant to the total SO_2 emitted by all the large coal-fired power plants. High PSO4 concentrations around Majuba is expected because it was the second highest coal-fired power emitter of SO_2 within this domain. Kendal was the highest emitter of SO_2

[31] For the locations of Camden and Majuba, reference can be made to the numbering in the first map in Figure 19 (first row, left column). Camden is numbered as 2 and Majuba is numbered as 11.

within this domain, emitting ~13.4% of the total SO_2 emitted by the large coal-fired power plants. Interestingly, no high PSO4 concentration are visible around Kendal but are near Camden. However, Camden emitted far less SO_2 than Kendal (~6% of total SO_2 emitted by large coal-fired power plants).

Map (d) and map (e) in Figure 21 shows that the simulated annual average PNO3 ranges from ~0.05 to 1.2 µg/m^3 for the baseline scenario and ~0.05 to ~0.7 µg/m^3 for the concept scenario. Table 11 shows a significant decrease in the spatial 99th percentile of PNO3 (1.11 µg/m^3 to 0.67 µg/m^3) when there are no emissions from the large coal-fired power plants. Map (f) shows the annual average PNO3 attributed to the large coal-fired power plants ranges from <0 to 0.5 µg/m^3. The highest PNO3 concentrations were simulated over the Standerton area in the GER. The average annual PNO3 simulated for the concept scenario were slightly higher in some areas along the northern boundary of the study area than those simulated for the baseline scenario, seen in the negative values in map (f) in Figure 21.

Map (g) and map (h) in Figure 21 shows that the simulated annual average PNH4 ranges from ~0.6 to 1.46 µg/m^3 for the baseline scenario and ~0.6 to ~1.1 µg/m^3 for the concept scenario. When the large coal-fired power plants are excluded, the spatial 99th percentile of PNH4 drops significantly from 1.39 µg/m^3 to 0.93 µg/m^3 (Table 11). Map (i) shows the annual average PNH4 attributed to the large coal-fired power plants ranges from 0 to 0.5 µg/m^3. The highest PNO3 concentrations were mostly in the GER.

Map (j) and map (k) in Figure 21 shows that the average SOA simulated for the concept scenario (~0.15 to 0.780 µg/m^3) is higher than the average SOA simulated for the baseline scenario (~0.15 to 0.783 µg/m^3, though the concentrations are low. No change in seen in the spatial 99th percentile of Secondary Organic Aerosols (SOA) between the baseline scenario and the concept scenario (Table 11). Map (l) in Figure 21 shows that the simulated annual average SOA attributable to the large coal-fired power plants ranges from ~ -0.002 to 0.012 µg/m^3. The average SOA simulated for the concept scenario was slightly higher over most of the study area than those simulated for the baseline scenario, though the differences were small (~0-0.002 µg/m^3) and can most likely be considered negligible.

Table 11: The spatial 99th percentile of the annual averages of secondary particulates (µg/m^3) within the Highveld study area.

Scenario	PSO4	PNO3	PNH4	SOA
Baseline (Coal-fired Power On)	4.65	1.11	1.39	0.65
Concept (Coal-fired Power Off)	2.71	0.67	0.93	0.65
Difference (Attributable to coal-fired power plants)	2.27	0.45	0.46	0.01

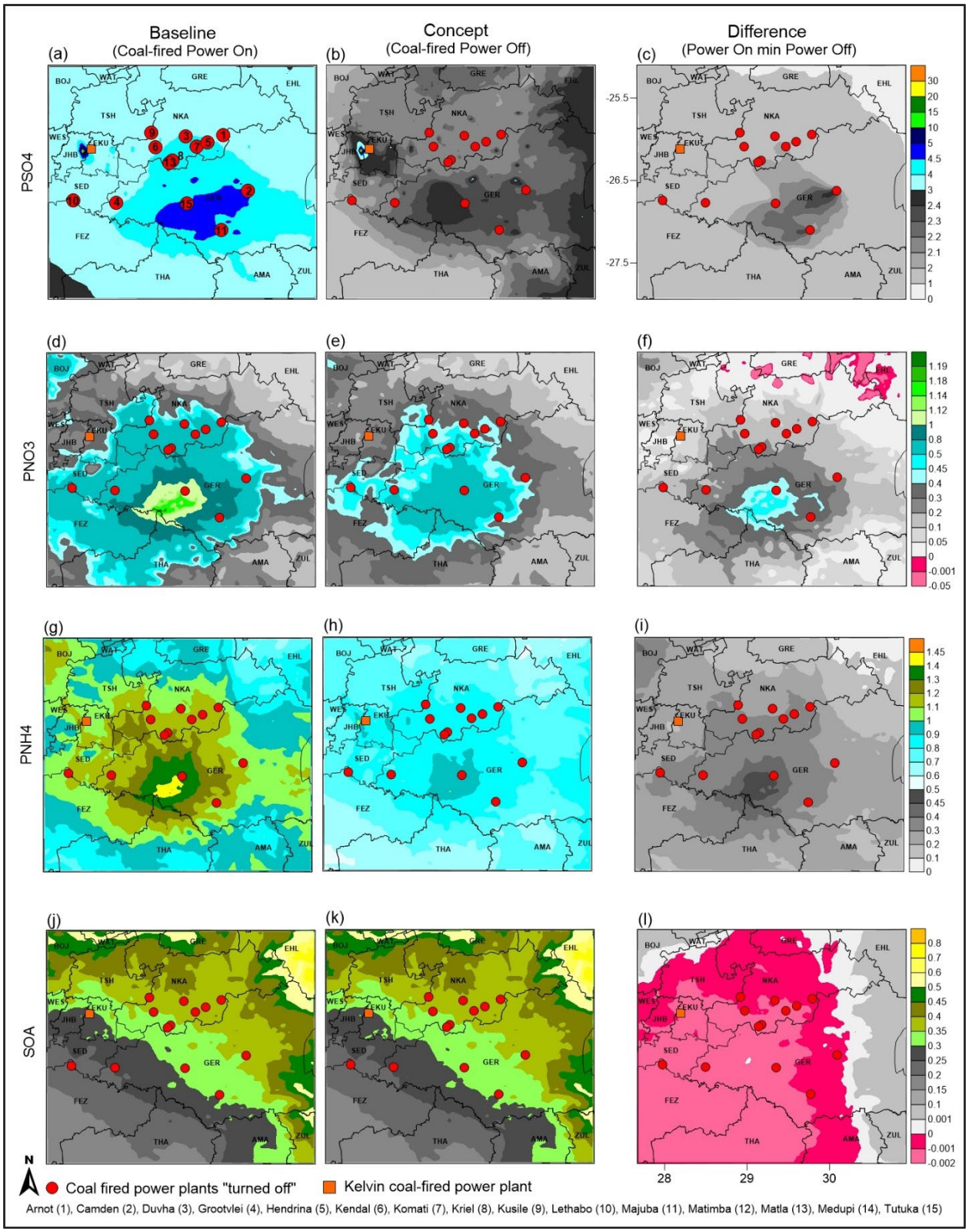

Figure 21: The simulated annual average near-surface level concentrations (µg/m^3) of PSO4, PNO3, PNH4 and SOA for the baseline scenario ("Coal-fired power on"), the concept scenario ("Coal-fired power off") and the residual concentrations attributed to the large coal-fired power plants. A positive number indicates gas concentrations were higher in baseline scenario than the concept scenario. The acronyms on the map refer to the different municipal areas (Table 7).

Primary fine particulates

Figure 22 gives a spatial representation of the annual average near-surface concentrations of the primary $PM_{2.5}$ species (Fine crustal (FCRS), Fine primary (FPRM), Primary Organic Aerosol (POA), Primary Elemental Carbon (PEC), Particulate Chloride (PCL) and Sodium (NA)) simulated for the baseline and concept scenario and those attributed to the large coal-fired power plants. It is evident that the difference between primary $PM_{2.5}$ in baseline and concept scenarios is insignificant across all simulated components. For both the baseline scenario and concept scenario, the greatest range in fine particulates is simulated for FPRM (0 to ~176 µg/m^3), followed by POA (0 to ~25 µg/m^3), PEC (0 to ~9 µg/m^3), FCRS (0 to ~2 µg/m^3) and NA (0 to ~0.06 µg/m^3).

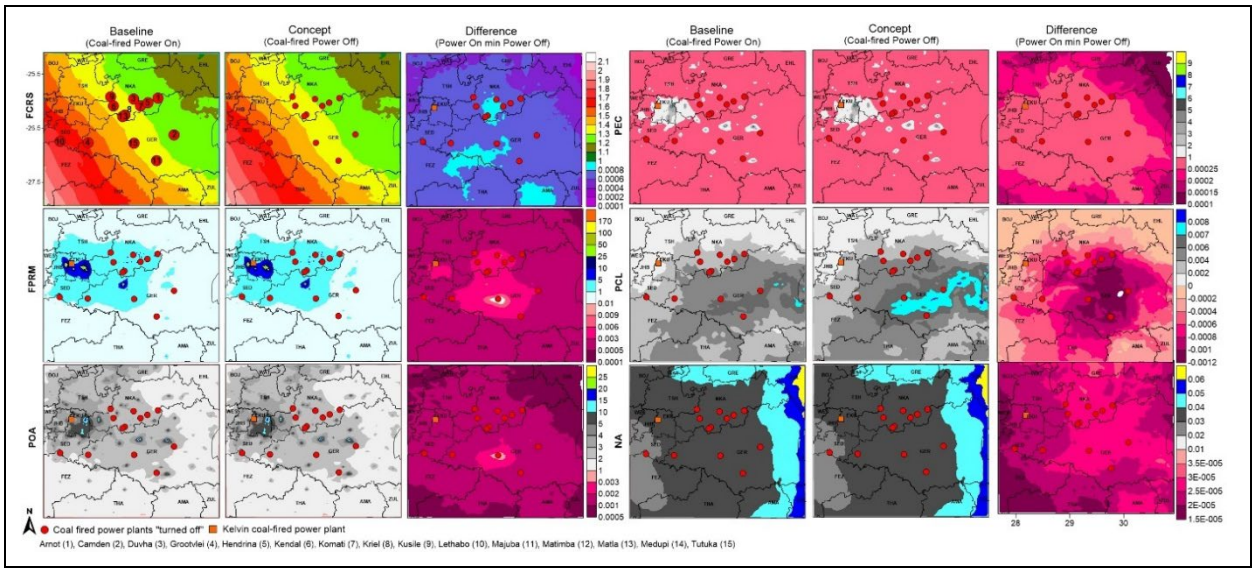

Figure 22: The simulated annual average near-surface concentrations (µg/m^3) of the components of primary $PM_{2.5}$ (FCRS, FPRM, POA, PEC, PCL and NA) for the baseline scenario ("Coal-fired power on"), the concept scenario ("Coal-fired power off") and the residual concentrations attributed to the large coal-fired power plants. A positive number indicates gas concentrations were higher in baseline scenario than the concept scenario. The acronyms on the map refer to the different municipal areas (Table 7).

Discussion

A significant decrease is seen in the annual average near-surface concentrations of SO_2, NO and NO_2 when the large coal-fired power plants are excluded from the baseline scenario. This shows that the large coal-fired power plants are the most significant contributors to the simulated ambient annual average SO_2, NO and NO_2, precursor gases of $PM_{2.5}$. This corresponds with the findings made by Scorgie & Thomas (2006) and those in the HPA AQMP (SA DEA, 2012a), that coal-fired power, is considered the highest contributor of $PM_{2.5}$ precursor gases (SO_2 and NO_x) on the Highveld.

Without any of the other sources, the SO_2 attributed to the large coal-fired power plants exceeded the annual SO_2 NAAQS. The cumulative impact of the coal-fired power plants greatly increased the extent to which the NAAQS for SO_2 and NO_2 were exceeded. For the annual average of SO_2,

the increase in the extent of the area of exceedance of the NAAQS was as much as 36.5% over the Sasol Secunda Synfuel operations.

An increase was seen in the NH_3 concentrations between the baseline scenario and the concept scenario. This means the model results found more simulated NH_3 when the coal-fired power plants were turned off than when they were operating. NH_3 is not emitted by the coal-fired power plants in the model, as no estimates were provided through the NAEIS. The primary source of NH_3 was agriculture. One reason for the decrease in NH_3 when coal-fired power plants operate is the reaction between NH_3 from sources such as agriculture and the precursor gases from the coal-fired power plants to form secondary particulates. Thus, the baseline scenario had this additional removal process for NH_3. This is further supported by the result that there was less PNH_4 in the concept scenario than in the baseline scenario.

It is not surprising that the model results found the large coal-fired power plants to be significant contributors to PSO4 and PNO3, considering coal fired power plants are significant sources of sulphates and nitrates (Zhao *et al.*, 2021; Chow *et al., 2004; Watson et al., 2001*) and that local studies have identified them as likely sources of secondary aerosols in the Highveld area (Altieri *et al*., 2022; Muyemeki *et al*., 2021; Walton *et al.*, 2021).

The negative PNO3 concentrations along the northern boundary of the study area suggest that the simulated PNO3 is slightly higher when the large coal-fired power plants are not operational. (i.e., more simulated PNO3 is formed when the large coal-fired power plants are “switched off”). However, these differences are very small (<0.05 µg/m^3) and may be considered negligible. Determining if this slight change is robust would require more simulations and using the CAMx source tracking feature.

The results show SOA and POA contributed little to the total ambient annual $PM_{2.5}$ attributable to the large coal-fired power plants. However, studies on coal-fired power plants in China (7.1% OC, Zhao *et al*., 2021) and the United States (~19.6% OC, Chow *et al*., 2004; Watson *et al*., 2001) show a significant contribution to OA. Previous studies have also found that SOA is important for particle growth (Vakkari *et al*., 2015). One reason for the possible underrepresentation of OA may include the omission of condensable PM[32] from the PM reported by coal-fired power plants on NAEIS (Refer to section 5.2 for the reasons condensable PM is underreported by coal-fired power plants). Particle emissions from coal-fired power plants consist of filterable and condensable PM. Several studies have found that condensable PM from coal fired power plants are 1.03 to 2.87 times higher than its filterable $PM_{2.5}$ (Yang *et al*., 2014; Li *et al*., 2017; Yang *et al*., 2018). In-stack measurements of several coal-fired boilers, done by Corio & Sherwell (2000), showed that

[32] Condensable PM: “Material that is a vapour in stack gas which condenses into a liquid or solid within a few seconds of leaving the stack when it cools in the atmosphere” (Corio & Sherwell, 2000; Huang *et al*, 2020; Li *et al.*, 2017).

approximately 76% of total PM_{10} comprised condensable PM. Condensable PM constitutes organic and inorganic compounds; however, there is some disagreement on the importance of inorganic or organic condensable PM from coal-fired power plants. Corio & Sherwell (2000) and Brewer *et al.* (2016) found that inorganic compounds (mainly sulphate) are the dominant contributors to condensable PM. Li *et al.* (2017) found that organic compounds are the most significant contributors to condensable PM. Condensable PM from combustion sources can contribute significantly to total $PM_{2.5}$ emissions (Morino *et al.*, 2018). Therefore, one reason for the possible underrepresentation of OA may include the omission of condensable PM[33] from the PM reported by coal-fired power plants on NAEIS (Refer to section 5.2 for the reasons condensable PM is underreported by coal-fired power plants). When Japanese emission inventories were modified to include condensable PM, emission rates of organic aerosols increased by a factor of seven over Japan (Morino *et al.*, 2018). The under reporting of condensable PM could be one reason for the disparity found when comparing the model results with the OC found near coal-fired power plants in the China and US studies.

The very small negative SOA over most of the study area suggests that the simulated SOA is slightly higher when the large coal-fired power plants are not operational. (i.e., More simulated SOA is formed when the large coal-fired power plants are "switched off"). The SOA could be affected by a change in oxidant chemistry and the types of emission sources in the area. However, the differences are very small (~0.002 µg/m^3) and can be considered negligible.

The model results found that the large coal-fired power plants contribute little to primary $PM_{2.5}$. Most of the primary $PM_{2.5}$ can be attributed to FPRM and POA. The highest concentrations of FPRM and POA, attributable to the large coal-fired power plants, were simulated over the Standerton area in the GER.

4.3 Ambient $PM_{2.5}$ concentrations attributable to the large coal-fired power plants in the Highveld.

The annual average concentrations of the different fine particulate species were summed for each scenario (baseline and concept) to determine the primary $PM_{2.5}$, secondary $PM_{2.5}$ and total $PM_{2.5}$ for the respective scenarios. These annual averages simulated for the concept scenario were then deducted from the baseline scenario to give the annual average $PM_{2.5}$ attributable to the large coal-fired power plants.The model results of primary $PM_{2.5}$ comprises FCRS, FRPM, NA, PCL, POA and PEC, while the model results of secondary $PM_{2.5}$ comprises PSO4, PNO3, PNH4, SOA 1 to 7 and SOAH.

[33] Condensable PM: "Material that is a vapour in stack gas which condenses into a liquid or solid within a few seconds of leaving the stack when it cools in the atmosphere" (Corio & Sherwell, 2000; Huang *et al*, 2020; Li *et al.*, 2017).

The results of the simulated annual average near-surface concentrations of $PM_{2.5}$ the different senarios and those attributed to the large coal-fired power plants are presented in Table 12 and Figure 23. Table 12 gives the spatial 99th percentile of the annual average near-surface concentrations of total $PM_{2.5}$, primary $PM_{2.5}$ and secondary $PM_{2.5.}$ Figure 23 presents the distribution of the annual average near-surface concentrations. Figure 23 is divided into three rows and columns. The rows differentiate the scenarios (baseline and concept) and the difference attributed to the large coal-fired power plants. The columns distinguish between the total-, primary- and secondary $PM_{2.5}$ for each scenario and the difference.

Table 12 shows a significant decrease in the spatial 99th percentile of total $PM_{2.5}$ (22.45 µg/m^3 to 20.62 µg/m^3) and secondary $PM_{2.5}$ (7.36 µg/m^3 to 4.36 µg/m^3) when the large coal-fired power plants are excluded. Almost no change is seen in the spatial 99th percentile of primary $PM_{2.5}$ between the baseline scenario and the concept scenario. The spatial 99th percentile of secondary $PM_{2.5}$ (3.07 µg/m^3) attributed to the large coal-fired power plants was close to that of total $PM_{2.5}$ (3.08 µg/m^3) attributed to the large coal-fired power plants.

It is evident from map (a) in Figure 23 that the baseline scenario ranged from ~6 µg/m^3 to 226.16 µg/m^3. The current NAAQS for annual average $PM_{2.5}$ (20 µg/m^3) is exceeded over the Johannesburg- (JHB) Ekurhuleni- (EKU), Nkangala- (NKA) and Gert Sibande- (GER) municipalities. A comparison between map (a) and map (d) in Figure 23 reveals a reduction in the spatial extent of total $PM_{2.5}$ simulated in the concept scenario. The simulated annual average total $PM_{2.5}$ for the concept scenario ranges from ~5 µg/m^3 to 224.68 µg/m^3. The current NAAQS for annual average $PM_{2.5}$ (20 µg/m^3) continues to be exceeded over JHB, EKU, NKA, and GER. However, the extent of the area experiencing concentrations above the NAAQS is less. Map (g) in Figure 23 shows the annual average total $PM_{2.5}$ attributed to the large coal-fired power plants range from ~0.05 µg/m^3 to 3.17 µg/m^3. There is no visible change between the map (g) (i.e. total $PM_{2.5}$) and map (i) (i.e. secondary $PM_{2.5}$) in Figure 23, indicating that most of the simulated total $PM_{2.5}$ from large (≥1 000 MW) coal-fired power plants comprises secondary $PM_{2.5}$.

Table 12: The spatial 99th percentile of annual averages of $PM_{2.5}$ (µg/m^3) within the Highveld study area.

Scenario	Primary	Secondary	Total
Baseline (Coal-fired Power On)	16.58	7.36	22.45
Concept (Coal-fired Power Off)	16.58	4.36	20.62
Difference (Attributable to coal-fired power plants)	0.01	3.07	3.08

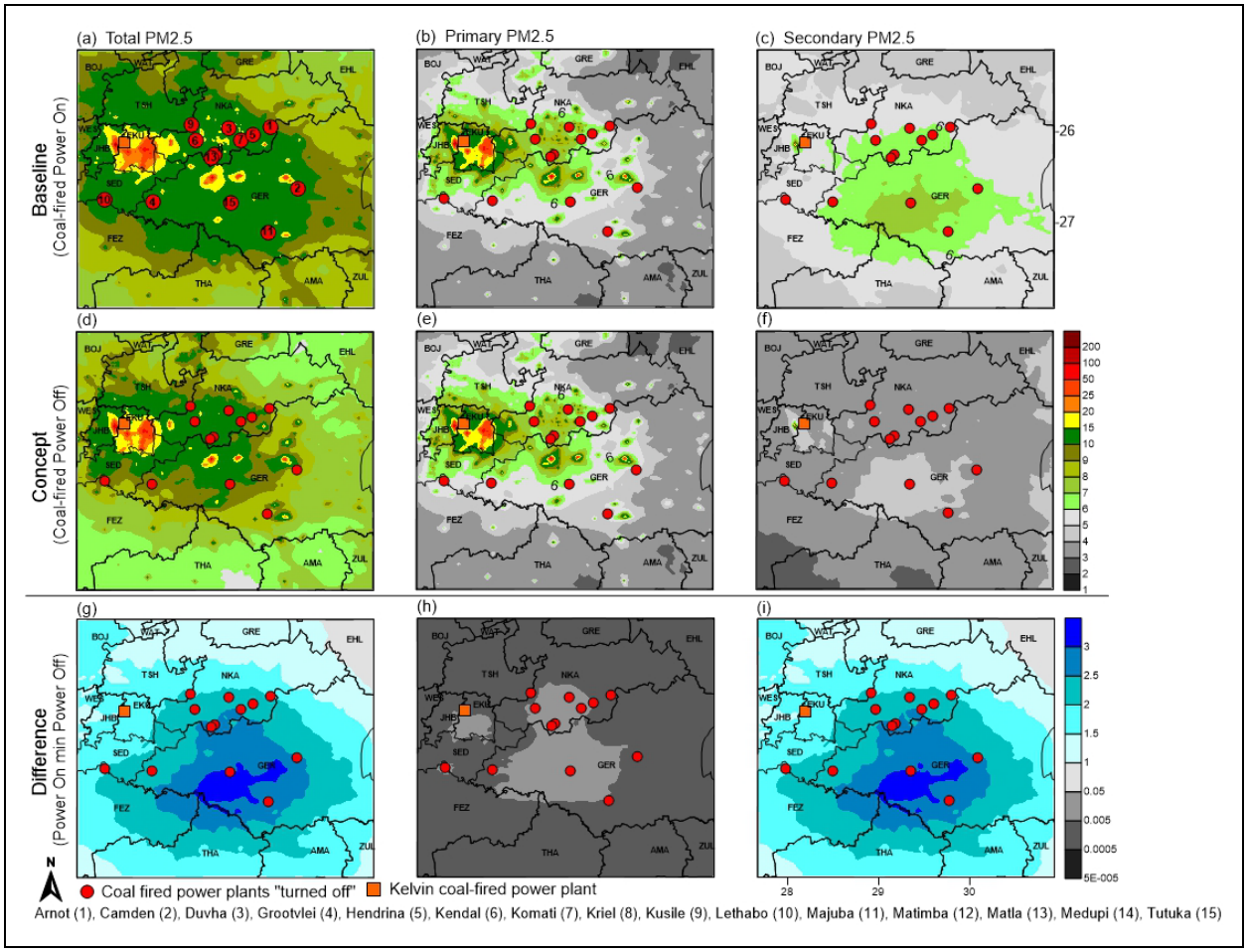

Figure 23: The first two rows of this figure give the simulated annual average $PM_{2.5}$ near-surface concentrations (µg/m³) for the baseline scenario ("Coal-fired power on") and the concept scenario ("Coal-fired power off"). The third row gives the residual annual average near-surface concentrations (µg/m³) of $PM_{2.5}$. A positive number indicates $PM_{2.5}$ concentrations were higher in baseline scenario than the concept scenario. The acronyms on the map refer to the different municipal areas (Table 7).

Table 13 gives the annual average $PM_{2.5}$, attributable to the large coal-fired power plants for each municipal area. Table 13 shows that the greatest change in annual average $PM_{2.5}$ (2.32 µg/m³) when the large coal-fired power plants are excluded occurs over the GER. Figure 24 presents the range of annual average $PM_{2.5}$ attributable to the coal-fired power plants for each municipality in the study area.-The first quartile (i.e., 25% of the values fall below this value) is represented by a black circle marker. The median is represented by a pink line. The third quartile (i.e., 75% of the values fall below this value) is represented by a black cross marker. The box covers the area where 50% of the data found. The wisker lines show the minimum and maximum values. Figure 24 shows the JOH, West Rand- (WES) and Greater Sekhukhune- (GRE) municipal areas to have the most concentrated distributions. Ehlanzeni (EHL) has the lowest distribution (50% of the $PM_{2.5}$ ranges between 0.85 - 1.02 µg/m³) and GER has the highest (50% of the $PM_{2.5}$ ranges between 1.97 – 2.72 µg/m³).

Table 13: The average per municipality of the annual average $PM_{2.5}$ ($\mu g/m^3$), attributable to large coal-fired power plants. Refer to Table 7 for the GEO ID definitions.

GEO ID	Pop.	$\Delta PM_{2.5}$	GEO ID	Pop.	$\Delta PM_{2.5}$	GEO ID	Pop.	$\Delta PM_{2.5}$
TSH	3 275 152	1.6	WAT	745 758	1.4	NKA	1 445 624	1.7
JOH	4 949 347	1.5	GRE	1 169 762	1.2	ZUL	892 310	1.6
EKU	3 379 104	1.7	BOJ	1 657 148	1.6	AMA	531 327	1.9
WES	838 594	1.5	EHL	1 754 931	0.9	THA	779 330	2.0
SED	957 528	1.9	GER	1 135 409	2.3	FEZ	494 777	2.1

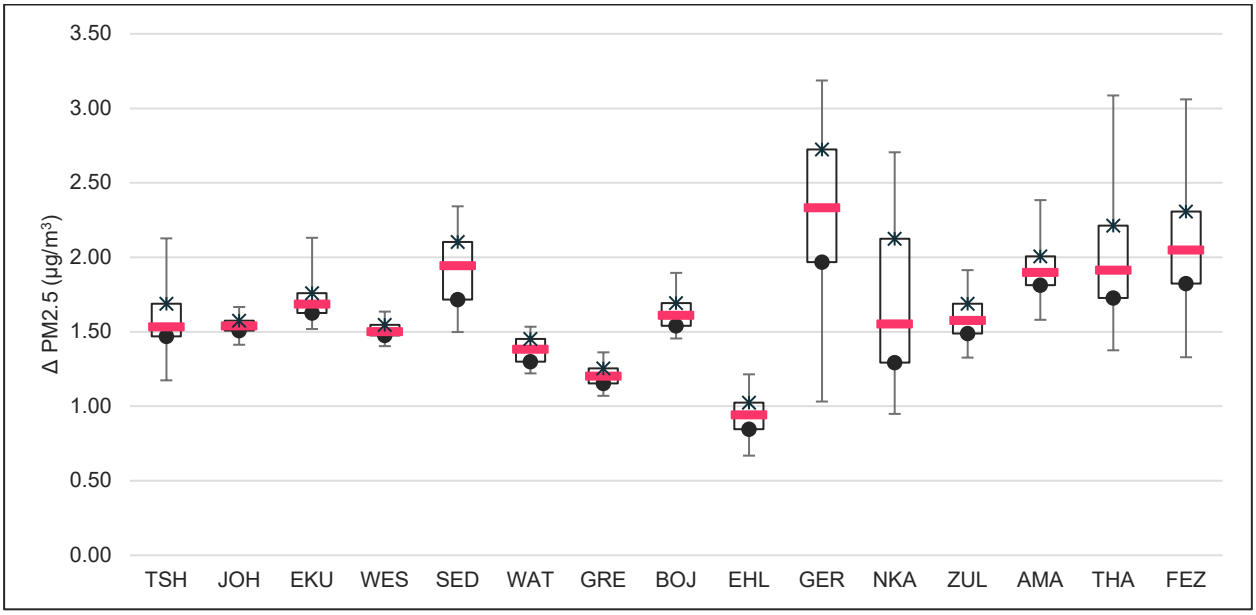

Figure 24: The range of the annual average $PM_{2.5}$ ($\mu g/m^3$) attributable to large coal-fired power plants for each municipality (Figure 23). The first quartile is represented by a black circle marker. The median is represented by a pink line. The third quartile is represented by a black cross marker. The box covers 50% of the data. The parallel lines from the boxes indicate the minimum and maximum values. The acronyms on the figure refer to the different municipal areas (Table 7).

Discussion

The model simulations show that the large coal-fired power plants are a significant source of ambient annual average $PM_{2.5}$, particularly secondary $PM_{2.5}$. The highest values for annual average total and secondary $PM_{2.5}$, attributable to the coal-fired power plants, were simulated within GER. It is expected as most of the PSO4, PNO3 and PNH4, attributable to the large coal-fired power plants, were simulated over this municipality as discussed in Section 4.2. It should be noted that the study did not account for the fine $PM_{2.5}$ from the ash dumps or dams.

4.4 The impact of the $PM_{2.5}$ attributable to the large coal-fired power plants in the Highveld on human health.

The impact that $PM_{2.5}$, attributable to the large coal-fired power plants in the Highveld, has on human health was evaluated in terms of avoidable premature mortality and the willingness to pay for marginal changes to lower mortality risk. The health impact function defined in Eq.(8) with inputs as described in section 3.3.1 was used to estimate avoidable premature mortality. The VSL for South Africa, a monetary value that a group of individuals would be willing to pay for a minimal reduction in their risk of premature death, was calculated using Eq.(9) with inputs as described in section 3.3.2.

Table 14 shows the avoidable premature mortality for each municipal area in the Highveld, estimated from the change in simulated annual average $PM_{2.5}$ ($\mu g/m^3$) attributable to the large coal-fired power plants. The most significant avoidable premature mortality numbers are seen in the JHB- (416), EKU- (402) and Tshwane- (TSH, 317) municipal areas. Approximately 2 409 premature mortalities are ascribed to the total ambient $PM_{2.5}$ attributed to the large coal-fired power plants in 2016.

Table 14: The avoidable premature mortality (All-cause) for each municipal area within the Highveld domain. The baseline incidence was based on the mortality and population numbers aged 25 and older. The health impact was based on the total population exposed. Population numbers were taken from Stats SA. 2018b to g. Mortality numbers were taken from Stats SA. 2018a. Refer to Table 7 for the GEO ID definitions.

GEO ID	Total Pop (Million).	$\Delta PM_{2.5}$ ($\mu g/m^3$)	Baseline incidence	Avoidable premature mortality
TSH	3.3	1.6	0.010	317
JOH	4.9	1.5	0.009	416
EKU	3.4	1.7	0.012	402
WES	0.8	1.5	0.018	136
SED	1.0	1.9	0.017	188
WAT	0.7	1.4	0.008	48
GRE	1.2	1.2	0.010	84
BOJ	1.7	1.6	0.008	131
EHL	1.8	0.9	0.009	85
GER	1.1	2.3	0.008	133
NKA	1.4	1.7	0.008	116
ZUL	0.9	1.6	0.011	94
AMA	0.5	1.9	0.015	89
THA	0.8	2.0	0.011	106
FEZ	0.5	2.1	0.010	62
Total	24.0		**Total**	2 409

Table 15 shows the monetary value associated with the health impacts ascribed to the $PM_{2.5}$ attributed to the large coal-fired power plants. The value in Table 15 is based on an income elasticity value of 1.2 for low- to middle-income countries with an elasticity range of 1 to 1.4 for sensitivity evaluation. Based on an average exchange rate in 2016 of 14.7049 R/US dollar

(Exchange Rates.org.uk., n.d.), this impact equates to a total valuation of R37.6 billion (ranging between R19.83 billion to R61.63 billion due to uncertainty in assigning the VSL method) (SA2016R) (Table 15).

Table 15: The monetary value (in USD and ZAR) associated with removing $PM_{2.5}$, primarily secondary $PM_{2.5}$, attributable to the large coal-fired power plants based on a $VSL_{sa\ (2016)}$ of 1.06 million$ (0.86-1.31 million$). Refer to Table 7 for the GEO ID definitions.

GEO ID	Avoidable premature mortality	Value (Billion $)	Value (Billion Rand)
TSH	317	0.3 (0.18-0.55)	5.0 (2.61-8.12)
JOH	416	0.4 (0.23-0.72)	6.5 (3.42-10.64)
EKU	402	0.4 (0.23-0.70)	6.3 (3.31-10.29)
WES	136	0.1 (0.08-0.24)	2.1 (1.12-3.49)
SED	188	0.2 (0.11-0.33)	2.9 (1.55-4.81)
WAT	48	0.05 (0.03-0.08)	0.8 (0.40-1.23)
GRE	84	0.1 (0.05-0.15)	1.3 (0.69-2.16)
BOJ	131	0.1 (0.07-0.23)	2.0 (1.08-3.35)
EHL	85	0.1 (0.05-0.15)	1.3 (0.70-2.17)
GER	133	0.1 (0.07-0.23)	2.1 (1.10-3.40)
NKA	116	0.1 (0.07-0.20)	1.8 (0.96-2.97)
ZUL	94	0.1 (0.05-0.16)	1.5 (0.77-2.40)
AMA	89	0.1 (0.05-0.16)	1.4 (0.73-2.28)
THA	106	0.1 (0.06-0.19)	1.7 (0.88-2.72)
FEZ	62	0.1 (0.03-0.11)	1.0 (0.51-1.59)
Total	2 409	2.6 (1.35-4.19)	37.6 (19.83-61.63)

Discussion

The GER (2.32 µg/m^3), followed by Thabo Mofutsanyane (THA, 2.00 µg/m^3) and Fezile Dabi (FEZ, 2.07 µg/m^3) district municipalities experienced the greatest change in annual average $PM_{2.5}$ when the large coal-fired power plant source is "removed". However, the number of avoidable premature mortality is lower for these areas due to their comparatively lower populations. Due to their greater populations, metropolitan municipalities benefit most from removing $PM_{2.5.}$ The model results reveal a potential to reduce the number of "All-cause" mortalities by approximately ~1.32%[34] by reducing $PM_{2.5}$, most significantly secondary $PM_{2.5}$ attributable to the large coal-fired power plants. The spatial 99th percentile of the secondary $PM_{2.5}$ comes close to that of the total $PM_{2.5,}$ attributed to large coal-fire power plants. Since most of the $PM_{2.5}$ attributed to the large coal-fired power plants comprises of secondary $PM_{2.5}$ and because we know most of this is a result of SO_2 and NO_x, it is safe to say that reducing the SO_2 and NO_x emissions from the large coal-fired power plant has the potential to reduce the number of "All-cause" mortalities by approximately ~1.32%. Avoiding the ~1.32% mortality could amount to an estimated economic benefit of R37.6 billion (SA2016R) as mentioned above.

[34] Based on the estimated total avoidable premature mortality (2 409) and the total 2016 all-cause mortality (181 872).

4.5 Previous studies

4.5.1 Comparison with methods and scope of previous studies

Table 16 provides a breakdown of previous studies that considered air pollution from coal-fired power plants in South Africa. Several studies (Gray, 2019; Marais *et al.*, 2019; Myllyvirta, NEC, 2018; PAC, 2018; 2014; Pretorius *et al.*, 2017; Scorgie & Thomas, 2006; Steyn & Kornelius, 2018; Van Horen, 1996) have used modelling to look at the impact of air pollution from South African coal-fired power plants and on human health. Except for van Horen (1996), Marais *et al.* (2019) and Myllyvirta (2014), the other studies used a Lagrangian model called CALPUFF (Gray, 2019; NEC, 2018; PAC, 2018; Pretorius *et al*., 2017; Scorgie *et al*., 2004; Scorgie & Thomas, 2006; Steyn & Kornelius, 2018). The emission inventory used in this study is different from all previous modelling studies. Thus, a quantitative model intercomparison cannot be performed. However, as these studies consider the impacts of coal-fired power plants, the results will be discussed and compared.

Table 16: Comparison with previous studies.

Scope	van Horen (1996)	Scorgie & Thomas (2006)	Myllyvirta (2014)	Pretorius *et al*. (2017)	Steyn & Kornelius (2018) based on Grobler (2016)	Eskom 2019 MES applications supporting documents NEC (2018) PAC (2018)	Marais *et al.* (2019)	Gray (2019)	This study
Models	EXMOD model embedded air quality dispersion models (ISC2, SLIM3 and SCREEN2)	CALPUFF	Regression models derived from single source CTM (CAMx and CALPUFF[35]) model runs	CALPUFF	CALPUFF	CALPUFF NEC (2018)	GEOS-Chem CTM (version 10−01	CALPUFF	CAMx
Geographical domain	South Africa	Highveld	South Africa (Langerman & Pauw, 2018)	Highveld	Highveld	Highveld NEC (2018)	Africa & South Africa	Highveld	Highveld
Exposed population	36.2 million (Langerman & Pauw, 2018)	10.83 million (Langerman & Pauw, 2018)	~50 million (Langerman & Pauw, 2018)	Not stated Population density provided on map	Not stated	~20.3 million exposed to air pollution in modelling domain. PAC (2018) ~17.7 million people exposed to > additional 1 mean annual average of $PM_{2.5}$ µg/m^3. PAC (2018)	~7 million Change in population from 2012 to 2030	~20.62 million in 2016	~24 million

[35] Baker & Foley (2011) model based on CAMx modeling of stack emissions of large U.S. air pollution emission sources and Zhou et al (2006) model based on CALPUFF modeling of power plants in China.

Scope	van Horen (1996)	Scorgie & Thomas (2006)	Myllyvirta (2014)	Pretorius *et al*. (2017)	Steyn & Kornelius (2018) based on Grobler (2016)	Eskom 2019 MES applications supporting documents NEC (2018) PAC (2018)	Marais *et al.* (2019)	Gray (2019)	This study
Power plants considered (Sources underlined are either not coal-fired power plants or are not part of Eskom)	Arnot, Duvha, Hendrina, Kendal, Kriel, Lethabo, Matimba, Matla, Tutuka	Arnot, Duvha, Hendrina, Kendal, Kriel, Lethabo, Majuba, Matla, Tutuka	Arnot, Camden, Duvha, Grootvlei, Hendrina, Kendal, Komati, Kriel, Lethabo, Majuba, Matimba, Matla, Medupi, Tutuka	Arnot, Camden, Duvha, Grootvlei, Hendrina, Kendal, Komati, Kriel, Lethabo, Majuba, Matla, Tutuka, Kelvin Secunda Station 1, Secunda station 2, Sasol station 1, Sasol station 2	Arnot, Camden, Duvha, Grootvlei, Hendrina, Kendal, Komati, Kriel, Majuba, Matla, Tutuka and Sasol Synfuels steam plants (Langerman & Pauw, 2018 & Grobler 2016)	Arnot, Camden, Duvha, Grootvlei, Hendrina, Kendal, Komati, Kriel, Kusile, Lethabo, Majuba, Matla, and Tutuka. NEC (2018)	Power plants (coal, natural gas & bunker fuel) and vehicle emissions	Arnot, Camden, Duvha, Grootvlei, Hendrina, Kendal, Komati, Kriel, Majuba, Matla, Tutuka, Sasol Synfuels & Natref Refinery	Arnot, Camden, Duvha, Grootvlei, Hendrina, Kendal, Komati, Kriel, Lethabo, Majuba, Matimba, Matla, Medupi, and Tutuka
Emissions year	Based on 1994 emissions	Based on 2003 emissions	Based on "Current" emissions in the 2013 Atmospheric Impact Reports as part of Eskom MES postponement applications.	Emission year(s) unclear. Modelled for 2011 to 2013	Emission year(s) unclear. Taken from Eskom and Sasol 2014 MES applications. Modelled for 2010 to 2012	Emission year(s) unclear. Report provides "Current" emissions. Emissions for Kusile were averaged from June 2017 to December 2017. Report dated 2018. NEC (2018)	Based on 2012 emissions and projected 2030 emissions	Baseline is based on 2016 emissions	Based on 2016 emissions

Scope	van Horen (1996)	Scorgie & Thomas (2006)	Myllyvirta (2014)	Pretorius *et al*. (2017)	Steyn & Kornelius (2018) based on Grobler (2016)	Eskom 2019 MES applications supporting documents NEC (2018) PAC (2018)	Marais *et al.* (2019)	Gray (2019)	This study
Ambient concentrations & Averaging period	Concentrations not stated Annual averaging period	Annual average contributions by coal-fired power plants: SO_2: 44 µg/m^3 NO_2: 8.1 µg/m^3 PM_{10}: 5.5 µg/m^3	Annual average contributions by coal-fired power plants over South Africa: $PM_{2.5}$: 0.1 to 3.4 µg/m^3 (Baker&Foley model) $PM_{2.5}$: <0.45 to 1.81 µg/m^3 (Zhou *et al.* model) (Taken from a map)	Three-year average contributions by coal-fired power plants: SO_2: ~2 to ~7 µg/m^3 NO_x: ~0.5 to ~2 µg/m^3 PM_{10}: ~1.2 to ~2.6 µg/m^3 (Taken from a map)	Three-year average for baseline conditions: SO_2: ~2 to ~28 µg/m^3 (Taken from map)	Maximum predicted annual average for "current emissions": SO_2: 22 µg/m^3 NO_2: 7.0 µg/m^3 PM_{10} or $PM_{2.5}$: 1.1 µg/m^3 Secondary particulates: 4.2 µg/m^3 NEC (2018) $PM_{2.5}$: >1 µg/m^3 attributed to coal fired power plants PAC (2018) Annual average & 99th percentile of 24-hour and 1-hour concentrations	Annual average contributions by power plants and vehicle emission: 2012 $PM_{2.5}$ (No dust of sea salt): 0 to 40 µg/m^3 Difference in $PM_{2.5}$ between 2012 & 2030: 1.41 µg/m^3	Annual average contributions by coal-fired power plants and Sasol Synfuels and Natref: SO_2: 19 µg/m^3 NO_2: 8.76 µg/m^3 PM_{10}: 3.7 µg/m^3 o$PM_{2.5}$: 3.2 µg/m^3	Annual average contributions by coal-fired power plants: SO_2: ~ 0 to 168.62 µg/m^3[36] NO_2: 0 to 54.18 µg/m^3 $PM_{2.5}$: ~0.05 µg/m^3 to 3 µg/m^3
Health Impact (Mortality)	56 (174-266) from TSP, SO_2 and NO_x	16.6 due to SO_2 from coal-fired power plants.	2 238 (729-4 237) (Baker & Foley model)	-	Benefit of reducing SO_2: Sulphates: 32	Health impacts attributed to $PM_{2.5}$ is unclear without	Exposure to $PM_{2.5}$ from 2030 fossil-fuel use:	Exposure to $PM_{2.5}$ from coal-fired power, Sasol	2 409 (β = 0.0060 based on RR 1.062 for All-cause

[36] Results in ppb were converted to µg/m^3 using the equation: µg/m^3 = (ppb) x (12.187) x (M) / (273.15 + °C). The conversion assumes an ambient pressure of 1 atmosphere and a temperature of 25 degrees Celsius.

Scope	van Horen (1996)	Scorgie & Thomas (2006)	Myllyvirta (2014)	Pretorius *et al*. (2017)	Steyn & Kornelius (2018) based on Grobler (2016)	Eskom 2019 MES applications supporting documents NEC (2018) PAC (2018)	Marais *et al.* (2019)	Gray (2019)	This study
		Zero attributed to PM_{10} and NO_3 from coal-fired power plants.	2 731 (890-5 171) (Zhou *et al*. model) From "current" annual mortality attributed to $PM_{2.5}$ and precursor emissions. Not based on "All-cause," estimated per cause (Lung cancer, IHD, COPD, stroke and includes lower respiratory infections for children under 5).		SO_2: 25 (Langerman & Pauw, 2018 & Grobler, 2016)	doing further calculations. Not based on "All-cause," estimated per cause (Respiratory mortality using SO_2, Cardiovascular mortality using NO_2 and Cerebrovascular and Diabetes mellitus mortality using $PM_{2.5}$.	10 400 (2 000-18 300)	Synfuels & Natref: 454.7 (302.5-650.2) Exposure to $PM_{2.5}$ attributed to coal-fired power: 471.2 (315.3-673.6)[37] Not based on "All-cause," estimated per cause (IHD, Lung cancer, stroke, COPD and includes lower respiratory infections for children under 5).	mortality). The baseline incidence was based on mortality- and population numbers ages ≥25.
VSL	Low estimate R800 000 Central estimate: 1.2 million Rand	-	Estimated $VSL_{SA\ (2012)\ adults}$: 12.1 million Rand based on an income	-	Estimated $VSL_{SA\ (2020)}$ of 53 million rand based on an income elasticity of 1.	$VSL_{SA\ (2018)}$: ~48-million-rand PAC (2018)	-	-	$VSL_{SA\ (2016)}$: 1.06 million US dollar (~15.61 million Rand)[38] based on an income

[37] The total for coal-fired power plants was based on the sum of the estimated annual mortality by source in Table 4 of Gray (2018). Note that the totals summed for coal-fired power plants are higher than the total for all sources in Table 4 of Gray (2018). The reason for this is unclear.
[38] Based on an average exchange rate in 2016 of 14.7049 R/US dollar.

Scope	van Horen (1996)	Scorgie & Thomas (2006)	Myllyvirta (2014)	Pretorius *et al*. (2017)	Steyn & Kornelius (2018) based on Grobler (2016)	Eskom 2019 MES applications supporting documents NEC (2018) PAC (2018)	Marais *et al.* (2019)	Gray (2019)	This study
	High estimate: 1.9 million Rand		elasticity of 0.8. Estimated $VSL_{SA\ (2012)\ children}$: 24.2 million Rand based on an income elasticity of 0.8.						elasticity of 1.2.
Valuation	Air pollution: 0.62 (0.85-1.05) billion Rand[39][40]	-	$PM_{2.5}$: (Baker&Foley 2011 model): 30 billion Rand[41]	-	Benefit of reducing SO_2: 115 billion Rand	Full compliance with new plant MES for SO_2, NO_2 and PM (considers $PM_{2.5}$) has an estimated health benefit of between 2.5 billion and 22.1 billion Rand over 16 years PAC (2018)	-	-	37.6 billion Rand[42]

[39] Based on 1995 Rand values.
[40] Does not consider pollution originating from ash dumps at power plants.
[41] Based on VSL, OECD 2005, and an estimated central VSL for South Africa for 2012 of 12.1 million Rand.
[42] Based on VSL, OECD 2011, and an estimated VSL for South Africa for 2016.

4.5.2 Comparison with results of previous studies

Van Horen (1996) used the EXMOD externalities model to estimate the health effects of coal-fired power plant air pollution (TSP, SO_2 and NO_2) and evaluate these health effects. The EXMOD air quality modelling component comprises the ISC2, SLIM3 and SCREEN2 Gaussian plume, dispersion models. The study does not account for the secondary particulates formed from the interaction of SO_2 and NO_2 from coal-fired power plants with precursor emissions from other sources within the region. The mortality and valuation estimated by van Horen (1996) are lower than the mortality and valuation estimated in this study. Reasons for this include that the van Horen (1996) study results are based on emissions from fewer coal-fired power plants and the 1995 Rand value. Scorgie & Thomas (2006) used a high threshold concentration ($PM_{2.5}$ = 15 $\mu g/m^3$) in their risk assessment. All simulated annual average PM_{10} ground-level concentrations fell below this high threshold concentration; therefore, zero mortality was attributed to PM_{10}.

Scorgie & Thomas (2006) used the CALPUFF dispersion modelling suite to simulate air pollution (PM_{10}, SO_2 and NO_2) from Eskom coal-fired power plants in the Highveld and estimated the health effects attributed to the air pollution. Emissions from other sources (industry, open cast coal mines and ash disposal sites, vehicle emissions and domestic fuel burning) were simulated to determine background air pollutant concentrations. The simulated PM_{10} results accounted for both primary and secondary particulates. The annual average SO_2 and NO_2 contributions by the large coal-fired power plants simulated in this study are higher, but in the same order of magnitude, than those simulated by Scorgie & Thomas (2006). The lower SO_2 and NO_2 values in Scorgie & Thomas (2006) may be partly due to the simulation of emissions from fewer (10) coal-fired power plants.

Pretorius *et al*. (2017) used the CALPUFF dispersion modelling suite to simulate a three-year average (primary and secondary) PM_{10} contribution by coal-fired power plants over the Highveld area. The study included coal-fired power plants operated by Eskom, Sasol, and City Power. The study simulated the coal-fired power plants with no background. It, therefore, did not account for the secondary particulate matter formed from the interaction of the SO_2 and NO_2 from coal-fired power plants with precursor emissions from other sources within the Highveld. The study considered the impact of fine particulates by estimating the intake fractions of NO_3 and SO_4 from the simulated (primary and secondary) PM_{10}. An important finding of the study is that the secondary particulate (NO_3 and SO_4) contribution to the intake value (kg per year) from total PM_{10} is more pronounced than that of primary PM_{10}. The SO_2 and NO_2 coal-fired power plant contributions in this study are also higher than those simulated by Pretorius *et al*. (2017), but in the same order of magnitude. Reasons for the lower SO_2 and NO_2 values in Pretorius *et al*. (2017) could be due to the differences in models used (Calpuff vs CAMx), emission inventories and domain boundaries. Pretorius *et al*. (2017), did not account for the secondary particulates formed

from the interaction of the precursor emissions of $PM_{2.5}$ from coal-fired power plants with precursor emissions from other sources within the region.

Of the previous studies that considered air pollution from coal-fired power plants in South Africa, Gray (2019), Marais *et al.* (2019), Steyn & Kornelius (2018), NEC & PAC (2018) and Myllyvirta (2014) considered the impact of secondary $PM_{2.5}$ from coal-fired power plants.

Marais *et al.* (2019) used the chemical transport model GEOS-Chem, to simulate the impact of $PM_{2.5}$ air pollution from the use of fossil-fuels for electricity generation and transport in Africa. GEOS-Chem is a global 3D model of atmospheric chemistry. The study looks at power generation from coal, natural gas and bunker fuel, and the impact of $PM_{2.5}$ includes vehicle emissions. The study also does not focus on the Highveld but reports the impact on Africa and South Africa.

Gray (2019) used the CALPUFF dispersion modelling suite to simulate air pollution (PM_{10}, $PM_{2.5}$, SO_2 and NO_2) from Eskom coal-fired power plants, Sasol Synfuels and Natref refinery. The study simulated the 2016 emissions and a 2020 MES compliance scenario. The study simulates the cumulative impact of three major source contributors and later attributes $PM_{2.5}$ mortality to each of the sources. Allowing for an estimation of $PM_{2.5}$ mortality attributed solely to coal-fired power plants. It is unclear if background conditions were considered, perhaps through the input of ambient values. The study does not explicitly account for air pollution transported across the boundary and does not explicitly account for other sources in the Highveld (e.g., biomass burning, other industries, biogenic VOCs and ammonia from agriculture, domestic fuel combustion and on-road vehicles) on the formation of secondary $PM_{2.5}$.

Steyn & Kornelius' 2018 compared a baseline scenario with compliance with the new plant MES scenario to assess the impact of reducing SO_2 emissions from Eskom and Sasol's solid fuel combustion installations. The study used the CALPUFF dispersion modelling suite and simulated ground-level concentrations over the Highveld Priority Area. Although it appears to be included, Steyn & Kornelius' (2018) published study does not contain results for secondary sulphate particulates, rather the results are presented in Grobler (2016). Cairncross (2018) commented that some of the mitigation costs not related to the emission sources were included in the cost-benefit estimates done by Steyn & Kornelius (2018) and that the benefits related to sulphate exposure were excluded. The study simulated the cumulative impact of SO_2 emissions from two significant source contributors, Eskom coal-fired power plants and the Sasol facility in Secunda. The study only considers sulphates. It is unclear if background conditions were considered, perhaps through the input of ambient values. The study does not explicitly account for pollution transported across the boundary and does not explicitly account for other sources in the Highveld (e.g., biomass burning, other industries, biogenic VOCs and ammonia from agriculture, domestic fuel combustion and on-road vehicles) on the formation of secondary PM.

NEC (2018) used the CALPUFF dispersion modelling suite to simulate air pollution (PM_{10}, $PM_{2.5}$, secondary PM, SO_2 and NO_2) from the Eskom coal-fired power plants for three scenarios. These scenarios simulated "current" emissions, compliance to new plant MES and emissions for a scenario where five of the coal-fired power plants are non-operational. The study simulates the cumulative impact of Eskom coal-fired power plants source on ambient $PM_{2.5}$ and considers secondary $PM_{2.5}$. It is unclear if background conditions were considered, perhaps through the input of ambient values. The study does not explicitly account for pollution transported across the boundary and does not explicitly account for other sources in the Highveld (e.g., biomass burning, other industries, biogenic VOCs and ammonia from agriculture, domestic fuel combustion and on-road vehicles) on the formation of secondary $PM_{2.5}$. PAC (2018) used the dispersion modelling results of in a cost benefit analysis, comparing the monetary value of the estimated health benefits to the capital and operational costs different scenarios.

Myllyvirta (2014) used statistical parameterisation to relate emissions from coal-fired power plants to $PM_{2.5}$ and estimated $PM_{2.5}$ emissions based on a ratio with PM10 of 4/9. The parameterisations were based on regression models derived from single-source chemical transport model (CAMx and CALPUFF) runs. These model runs were based on CAMx modelling stack emissions from significant air pollution sources in the United States (Baker & Foley, 2011) and the CALPUFF modelling of power plants in China (Zhou *et al*., 2006), not local sources.

The annual average SO_2 and NO_2 emissions attributed to the large coal-fired power plants in this study are higher, but in the same order of magnitude, than those simulated by Steyn & Kornelius (2018) and NEC (2018). The lower SO_2 and NO_2 values in Steyn & Kornelius (2018) and NEC (2018) could be due to the differences in models used (Calpuff vs CAMx), emission inventories and domain boundaries. The annual average $PM_{2.5}$ contributions by the large coal-fired power plants, simulated in this study, compare well with those estimated by Myllyvirta (2014) and simulated by NEC (2018) and Gray (2019).

Myllyvirta (2014) considered the following causes of mortality: Lung cancer, Ischemic Heart Disease (IHD), Chronic Obstructive Pulmonary Disease (COPD), stroke and lower respiratory infections. For a 10 $\mu g/m^3$ increase in annual average $PM_{2.5}$, the following relative risks were applied by Myllyvirta: 1.14 for lung cancer, 1.26 for IHD, 1.05 for COPD, 1.12 for stroke and 1.12 for lower respiratory infections in children under five. This study focused on all-cause mortality and used a relative risk of 1.062. The mortality results for Myllyvirta (2014) and this study are very similar although Myllyvirta (2014)'s study is based on a greater exposed population size as the domain was larger (~50 million, Langerman & Pauw, 2018). Reasons for this are that this study uses a chemical transport model in the estimation of $PM_{2.5}$ and the domain in this study contains the areas where the impacts from large coal-fired powered plant emissions are the greatest.

The valuation in Myllyvirta (2014) is lower than this study. One reason for the lower valuation is the lower 2012 VSL used in Myllyvirta (2014).

The paper by Steyn & Kornelius (2018) gives a valuation of the reduction of SO_2 from coal-fired power plants, however, it does not give the number of premature mortalities avoided. Numbers of the estimated premature mortality avoided attributable sulphates and SO_2, for the Steyn & Kornelius (2018) study, are given in Langerman & Pauw (2018) and Grobler (2016). Langerman & Pauw (2018) and Grobler (2016) provides that the reduction in SO_2 results in an estimated 32 premature mortalities from sulphates and 25 premature mortalities from SO_2. The study was based on a timeframe of 30 years from 2020 to 2050 when all current plants will reach end of life Grobler (2016). Steyn & Kornelius (2018) estimated health benefit of 115-billion-rand health benefit (adult mortality).

PAC (2018) used dispersion modelling results from the NEC (2018) study in a cost benefit analysis, comparing the monetary value of the estimated health benefits to the capital and operational costs different scenarios. Although the methodology for estimating health impacts is discussed in PAC (2018), without further calculations it is unclear what premature mortality was attributed to $PM_{2.5}$ from the Eskom coal-fired power plants.

The difference in $PM_{2.5}$ (1.41 µg/m^3) between the 2012 and 2030 simulated fossil-fuel emissions from power plants and vehicles in South Africa, applied in Marais *et al.* (2019) to determine the mortality is less than the annual average $PM_{2.5}$ this study attributes to the large coal-fired power plants (1.67 µg/m^3) in the Highveld. However, the mortality determined by Marais *et al.* (10 400) is greater than that estimated in this study (2 409), mainly due to the greater exposed population.

Gray (2019) attributed less (471.2) mortalities than this study (2 409) to the annual average $PM_{2.5}$ contributed by the large coal-fired power plants in the Highveld. Reasons for the differences include the differences in models, model chemistry, boundary conditions, other source considerations, the mortality cause and ages considered in the health impact estimates.

CHAPTER 5: CONCLUSION

Chapter 5 presents an overview of the study within the context of the study objectives and recommendations for future studies.

5.1 The impacts of coal-fired power plants on aerosol particles in the Highveld

Coal-fired power plants emit sulphur dioxide (SO_2) and nitrogen oxides (NO_x), known precursor gases of secondary $PM_{2.5}$ (particulate matter with an aerodynamic diameter ≤ 2.5μm) air pollution. $PM_{2.5}$ air pollution can travel far from its source or the area where it was formed, and once inhaled, it can penetrate deep into the respiratory system and cause adverse health impacts. Long-term exposure to ambient $PM_{2.5}$ may even lead to premature mortality. Most of the coal-fired power plants in South Africa are located within the industrialised Highveld region. This region has complex meteoroloigcal conditions that are often highly unfavourable for air pollution dispersion. To effectively manage ambient air quality in the Highveld, we must understand the relationship between ambient $PM_{2.5}$ and the contribution of significant sources, such as coal-fired power plants, to ambient $PM_{2.5}$ levels.

Four previous studies have attributed the annual average $PM_{2.5}$ solely to coal-fired power plants in the Highveld (Gray, 2019; Steyn & Kornelius, 2018; NEC & PAC, 2018; Myllyvirta, 2014). Myllyvirta (2014) used regression models derived from single-source chemical transport model (CAMx & CALPUFF) runs and estimated $PM_{2.5}$ emissions based on a ratio with PM10 of 4/9. The other three studies used chemical transport models (Gray, 2019; Steyn & Kornelius, 2018; NEC & PAC, 2018). It is unclear if background conditions were considered, perhaps through the input of ambient values. However, these studies did not explicitly account for air pollution transported across the boundary or all other major sources in the Highveld in the formation of secondary $PM_{2.5}$. Each of the four studies has limitations and does not represent a complete estimate of the secondary $PM_{2.5}$ attributable solely to coal-fired power plants in the Highveld.

This study used a Eulerian chemical transport model, CAMx, to simulate the atmospheric chemistry and the impact of air pollution from coal-fired power plants at a high spatial resolution over the industrial Highveld, to provide a more complete estimate of $PM_{2.5}$, particularly secondary $PM_{2.5}$ attributable to the coal-fired power plants. A model performance evaluation found the model simulations adequate for this study. By comparing the concept simulation, where all large coal-fired power plant emissions are excluded, with the baseline simulation of the Highveld atmosphere, the study can attribute a more complete simulated impact of the large coal-fired power emissions on the annual average $PM_{2.5}$ over the Highveld. The model simulations found that the large coal-fired power plants are the greatest contributors to ambient annual average SO_2, NO, and NO_2 and significant contributors to secondary particulate species PSO4, PNO3 and

PNH4. Therefore, it is no surprise that the model results also show that the large coal-fired power plants are a significant source of ambient annual average $PM_{2.5}$, particularly secondary $PM_{2.5}$.

The highest annual average total and secondary $PM_{2.5}$ concentrations, attributable to the large coal-fired power plants, were simulated within the Gert Sibande district municipality (GER). It is expected as most of the PSO4, PNO3 and PNH4 were simulated over the same municipal area. Although GER, followed by the Fezile Dabi (FEZ)- and Thabo Mofutsanyane (THA) district municipalities, experienced the greatest change in annual average $PM_{2.5}$ due to its greater population density, the metropolitan municipalities benefit most from removing $PM_{2.5}$. Most of the $PM_{2.5}$ attributable to the large coal-fired power plants comprises secondary $PM_{2.5}$.

Reducing the $PM_{2.5}$ precursor emissions, SO_2 and NO_x, from the large coal-fired power plant can reduce the number of "All-cause" mortalities in the study area by up to ~1.32%. A total reduction in the premature mortality attributed to $PM_{2.5}$ from the large coal-fired power plants is valued at an estimated R37.6 billion (SA2016R) in 2016.

5.2 Research limitations

The main research limitations include the following:

1. Uncertainties in emission inputs are one of the main contributors to significant errors in photochemical modelling (US EPA, 2019; Russel & Dennis, 2000). Every effort was made to develop an emission inventory representative of the emissions within the Highveld. There are still many improvements that are needed, such as:
    a. this study is subject to uncertainties in emission estimates from mining (particularly spontaneous combustion of underground coal mines), vehicle emissions, and agricultural ammonia;
    b. data on condensable PM emissions is limited because most countries do not require sources to measure it (Huang *et al*, 2020; Yang *et al*., 2014). The list of activities published in terms of Section 21 of NEM: AQA in GN 893 in GG 37054 on 22 November 2013 (as amended) do not specifically refer to condensable PM. The list defines PM as "*Means total particulate matter, which is the solid matter contained in the gas stream in the solid state as well as the insoluble and soluble **solid** matter contained in entrained droplets in the gas stream, as measured by the appropriate method listed in Annexure A of GN893*". The definition of PM is ambiguous; however, Annexure A provides for the US EPA Method 202 in the 2018 amendment[43]. It is therefore likely that the definition of PM in South Africa includes condensable PM. Thus, condensable PM should be included in the South African emission inventory,

[43] Published in GN 1207, GG 42013 on 31 October 2018.

or if it is included it should be noted as such, to improve the representation of coal-fired power stations.

c. Eskom uses opacity monitors to measure PM emissions from coal-fired power plants (Keir, 2014). Opacity[44] monitors measure PM using light (US EPA, 2000; LAND-AMETEK, 2008). The method used to measure condensable PM uses condensation by cooling the filtered gas to a temperature between 20 to 30 ºC (Huang *et al*, 2020; Yang *et al*., 2014). Continuous emission monitoring systems using light (e.g., light scattering or light extinction) may not be applicable in monitoring condensable PM (Beutner, 1974; US EPA, 2000)[45]. The PM emissions reported in NAEIS for the Eskom coal-fired power plant therefore do no account for condensable PM and the model results underrepresent primary condensable PM, particularly impacting PSO4 and POA.

d. the emission inventory does not account for wind-blown dust.

2. The $PM_{2.5}$ attributed to the coal-fired power plants does not include fine particulates from coal storage areas and ash dumps or dams. The study focused on the $PM_{2.5}$ attributed to precursor gases emitted from the coal-fired power plant stacks.
3. The model performance evaluation is based on limited observed ground-level data. Only ambient air quality data from seven monitoring stations owned by the Department of Forestry, Fisheries and the Environment could be obtained during the study.
4. Vertical profile measurements along plume paths were unavailable for the study region and period. Therefore, the model performance in simulating the transport and transformation of tall stack emissions in the complex Highveld atmosphere was not assessed. De Lange *et al.* (2021) have highlighted that the simulated dispersion of the plumes is dependent on the planetary boundary layer (PBL) scheme selected in WRF. As there are no vertical measurements, it is unclear which PBL scheme best simulates this dispersion.
5. Coal-fired power plants emit various air pollutants that can harm human health. This study only considers the health risks associated with the annual average $PM_{2.5}$. Further work could estimate the impact of coal-fired power plant emissions on 24-hr average $PM_{2.5}$ and other trace gas species (e.g., ozone).
1. The relative risk used to estimate the health impact was based on a pooled estimate from several cohort studies. These cohort studies cover a wide geographic area, including America, Europe, and Asia. None of these studies included South Africa. However, a study by Liu *et al*. (2019) shows that the percentage difference in daily all-cause mortality per 10

[44] Opacity is defined as the degree to which particle emissions reduce the intensity of transmitted photopic light (due to absorption, reflection, and scattering) and obscure the view of an object through ambient air, an effluent gas stream, or an optical medium, of a given pathlength (LAND-AMETEK, 2008).

[45] To account for condensable PM, continuous emission monitoring systems should be able to measure PM at the Reference Method filter temperature (<29.4ºC) (US EPA, 2000).

μg/m^3 increase in $PM_{2.5}$ estimated for South Africa (0.8%) is similar to that of the countries used in the cohort studies (i.e., 1.58% for the US, 1.7% for Canada, 0.79 for Switzerland, 0.41% for China and 1.42% for Japan).

2. The health impact for this study was estimated based on the total population numbers within the municipal areas. However, the relative risk used to estimate the health impact was based on cohort studies using adults aged ≥25 years. The baseline incidence used in the health impact function (Eq. (8)) was therefore based on the mortality- and population numbers for ages ≥25 years.
3. The results were not presented in population-weighted averages because the all-cause mortality data in the Stats SA statistical release (P0309.3) was given for metropolitan and district municipalities.
4. Willingness to pay (WTP) studies are still lacking in South Africa. The VSL for SA was estimated using a "base VSL" based on mean VSL estimates from WTP studies conducted in high-income countries. Transferring an economic valuation based on populations in more developed countries introduces uncertainty. The VSL for SA was adjusted by applying an income elasticity value of 1.2 for low- to middle-income. The $VSL_{sa,2016}$, estimated for this study compared well with a $VSL_{sa,2017}$, estimated for South Africa by Viscusi *et al*. (2017).

5.3 Contribution to the broader body of knowledge

- To date, this study is the most comprehensive application of a chemical transport model, looking at $PM_{2.5}$ from coal-fired power plants on the South African Highveld.
- To date, this study is the only application of a Eulerian chemical transport model, looking specifically at $PM_{2.5}$ solely from coal-fired power plants on the industrial Highveld and adjacent areas.
- Unlike previous studies, this study explicitly accounts for air pollution transported across the boundary and other sources in the Highveld (e.g., biomass burning, other industries, biogenic VOCs and ammonia from agriculture, domestic fuel combustion and on-road vehicles) on the formation of secondary $PM_{2.5}$.
- The study focuses on coal-fired power plants, one of the most significant emissions sources in South Africa. It is also a sector struggling to comply with minimum emission standards and is faced with difficult management questions.
- The study shows that coal-fired power plants are significant sources of $PM_{2.5}$ precursor gasses SO_2 and NO_2 and contribute significantly to ambient $PM_{2.5}$, particularly secondary $PM_{2.5}$ in the Highveld. Most of the $PM_{2.5}$ attributable to the coal-fired power plants comprise secondary $PM_{2.5}$. This is significant not only for the dangers of $PM_{2.5}$ but also because it can

be reduced by reducing SO_2 and NO_2 emissions. This is also significant as it highlights the importance of including secondary $PM_{2.5}$ in such assessments.

- The study shows a potential to reduce the number of “All-cause” avoidable premature mortality by ~1.32% by reducing the $PM_{2.5}$ precursor gasses SO_2 and NO_2 from the large coal-fired power plants. This reduction in avoidable premature mortality could amount to an estimated economic benefit of 37.6 billion Rand (SA2016R).
- This study was focused on a small portion of the greater Highveld area; however, its estimated economic benefit (37.6 billion $Rand_{SA2016}$) is more than the 30 billion $Rand_{SA2012}$ Myllyvirta estimated for the entire South Africa. This would be expected as a chemical transport model is used in the estimation of $PM_{2.5}$ and the domain in this study contains the areas where the impacts from large coal-fired powered plant emissions are the greatest.
- This study attributed an estimated 2 409 mortalities to the annual average $PM_{2.5}$ contributed by the large coal-fired power plants in the Highveld. This is higher than the 471.2 mortalities estimated by Gray (2019). This is expected due to the differences in model setup and the more complex chemical mechanism in the CAMx study. The difference in results could also be due to the differences in mortality estimations. The estimated mortalities in this study were based on “All-cause” mortality rates as opposed to the cause-specific estimates in Gray (2019). There are also differences in the ages considered in the estimations.
- By understanding the relationship between the levels of ambient $PM_{2.5}$, particularly secondary $PM_{2.5}$, and the emissions of primary $PM_{2.5}$ and precursor gases from coal-fired power plants, we can better investigate the impact of $PM_{2.5}$ attributable to coal-fired power plants on human health in the Highveld.
- This study presents a method for apportioning secondary particulate matter to various sources. Understanding this relationship can assist the government when allocating resources to air quality management, health and safety strategies and programs to improve air quality and, by extension, the health and well-being of communities in the Highveld.

REFERENCES

Africon Engineering International (Pty) Ltd (Africon). 2005. City of Tshwane Metropolitan Municipality State of Energy Report. Retrieved from: https://www.cityenergy.org.za/uploads/resource_99.pdf

Alfarra, M. R., 2004. Insights into atmospheric organic aerosols using an aerosol mass spectrometer. Manchester, UK. University of Manchester. (Thesis – PhD).

Altieri, K. E., Burger, J., Language, B., & Piketh, S. J. 2022. A case study in the wintertime Vaal Triangle Air-Shed Priority Area on the utility of the nitrogen stable isotopic composition of aerosol nitrate to identify NO_x sources. *Clean Air Journal*, 32(1): 1- 8.

Altieri, K. & Keen, L. S. 2019. Public health benefits of reducing exposure to ambient fine particulate matter in South Africa. *Science of The Total Environment*, 684: 610-620.

Andreae, M.O., Atlas, E., Cachier, H., Cofer, W.R., Harris, G.W., Helas, G., Koppman, R., Lacaux, J. & Ward, D.E. 1996. Trace gas and aerosol emissions from savanna fires, J.S. Levine (ed.), Biomass Burning and Global Change, MIT Press, Cambridge, 278-294.

Ballard-Tremeer, G. 1997. Emissions of rural wood-burning cooking devices. Johannesburg. University of the Witwatersrand. (Thesis – PhD).

Baker, K. R. & Foley, K. M. 2011. A nonlinear regression model estimating single source concentrations of primary and secondarily formed $PM_{2.5}$. *Atmospheric Environment,* 45:3758-3767.

Barik, P., Naoghare, P., Sivanesan, S., Kannan, K. & Middey, A. 2021. Increased average annual prevalence of upper respiratory tract infection (UTRI) in the central Indian population residing near the coal-fired thermal power plants. *SN Applied Sciences*, 3(214).

Bauer, S. E., Im, U., Mezuman, K. & Gao, C. Y. 2019. Desert dust, industrialization, and agricultural fires: Health impacts of outdoor air pollution in Africa. *Journal of Geophysical Research: Atmospheres*, 124: 4104–4120.

Bergin, S. M., West, J. J., Keating, J. T. & Russel, G. A. 2005. Regional Atmospheric Pollution and Transboundary air quality management. *Annual Review of Environment and Resources*, 30: 1- 37.

Beukes, J., Vakkari, V., van Zyl, P., Venter, A., Josipovic, M., Jaars, K., Tiitta, P., Kulmala, M., Worsnop, D., Pienaar, J., Virkkula, A., & Laakso, L. 2013. Source region plume characterisation of the interior of South Africa as observed at Welgegund. *Clean Air Journal*, 23(1): 7-10.

Beutner, P. H. 1974. Measurement of opacity and particulate emissions with an on-stack transmissometer. *Journal of the Air Pollution Control Association*, 24:9, 865-871.

Bojanala Platinum District Municipality (BPDM). 2010. 2009/2010 Reviewed Integrated Development Plan.

Boogaard, H., Walker, K. & Cohen, A. J. 2019. Air pollution: the emergence of a major global health risk factor. International Health, 11: 417-421.

Brauer, M., Brook, J. R., Christidis, T., Chu, Y., Crouse, D. L., Erickson, A., Hystad, P., Li, C., Martin, R. V., Meng, J., Pappin, A. J., Pinault, L. L., Tjepkema, M., van Donkelaar, A., Weichenthal, S. & Burnett, R. T. 2019. Mortality-Air Pollution Associations in Low-Exposure Environments (MAPLE): Phase 1. *Research Report (Health Effects Institute)*, 203:1-87

Brewer, E., Li, Y., Finken, B., Quartucy, G., Muzio, L., Baez, A., Garibay, M., Jung, H. S. 2016. $PM_{2.5}$ and ultrafine particulate matter emissions from natural gas-fired turbine for power generation. *Atmospheric Environment*, 131: 141−149.

Britannica, The Editors of Encyclopaedia. 2018 “Photolysis”. *Encyclopedia Britannica*, 10 May. Retrieved from: https://www.britannica.com/science/photolysis.

Brook, R. D., Franklin, B., Cascio, W., Hong, Y., Howard, G., Lipsett, M., Luepker, R., Mittleman, M., Samet, J., Smith, S. C., Jr, & Tager, I. 2004. *Air Pollution and Cardiovascular Disease. Circulation*, 109 (21): 2655-2671.

Brook R. D., Rajagopalan S. & Pope C. A. 2010. 3rd Particulate matter air pollution and cardiovascular disease: an update to the scientific statement from the American Heart Association. *Circulation*, 121: 2331–2378.

Cairncross, E. 2018. Response to: “An economic assessment of SO_2 reduction from industrial sources on the highveld of South Africa” by Steyn and Kornelius. *Clean Air Journal*, 28(2), 5-6.

Cawthorn, R. G. 2010. The Platinum Group Element Deposits of the Bushveld Complex in South Africa. *Platinum Metals Review,* 54(4): 205.

Centre for Environmental Rights (CER). 2022. Major court victory for communities fighting air pollution in Mpumalanga Highveld. Retrieved from: https://cer.org.za/news/major-court-victory-for-communities-fighting-air-pollution-in-mpumalanga-highveld

Chang, J. C. & Hanna, S. R. 2004. Air quality model performance evaluation. *Meteorology and Atmospheric Physics*, 87: 167-196.

Chang, J. C. & Hanna, S. R. 2005. Technical descriptions and user’s guide for the BOOT statistical model evaluation software package, version 2.0. Retrieved from: https://www.harmo.org/Kit/Download/BOOT_UG.pdf

Charlson, R. J., Schwartz, S. E., Hales, J. M., Cess, R. D., Coakley Jr., J. A., Hansen, J. E. & Hoffman, D. J. 1992. Climate forcing by anthropogenic aerosols. *Science*, 255: 423-430.

Chen, H., Burnett, R. T., Copes, R., Kwong, J. C., Villeneuve, P.J., Goldberg, M. S., Brook, R. D., van Donkelaar, A., Jerrett, M., Martin, R. V., Brook, J. R., Kopp, A. & Tu, J. V. 2016. Ambient fine particulate matter and mortality among survivors of myocardial infarction: population-based cohort study. *Environ Health Perspectives* 124: 1421-1428.

Chen, B. & Kan, H. 2008. Air pollution and population health: a global challenge. *Environmental Health and Preventive Medicine*, 13(2): pp. 94-101.

Chidhindi, P., Belelie, M. D., Burger, R. P. Mkhatshwa, G., & Piketh, S. 2019. Assessing the impact of Eskom power plant emissions on ambient air quality over KwaZamokuhle. *Clean Air Journal*, 29(1): 29-37.

Chow, J. C., Watson, J. G. & Kuhns, H. 2004. Source profiles for industrial, mobile, and area sources in the Big Bend Regional Aerosol Visibility and Observational study. *Chemosphere* 54(2):185-208.

Collett, K. S., Piketh, S.J. & Ross, K.E. 2010. An assessment of the atmospheric nitrogen budget on the South African Highveld. *South African Journal of Science*, 106(5/6), Art. #220, 9 pages.

Committee of Transport Officials. 2012. TRH 26: South African Road Classification and Access Management Manual, version 1.0. Roads Coordinating Body of the Committee of Transport Officials, South African National Roads Agency Limited. Retrieved from: http://www.roadclass.co.za/wp-content/uploads/2014/02/TRH26-RCAM.pdf.

Conradie, E. H., Van Zyl, P. G., Pienaar, J. J., Beukes, J. P., Galy-Lacaux, C., Venter, A. and Mkhatshwa, G. V. 2016. The chemical composition and fluxes of atmospheric wet deposition at four sites in South Africa. *Atmospheric Environment*, 146: 113–131.

Corio, L. A. & Sherwell, J. 2000. In-stack condensable particulate matter measurements and issues. Journal of the Air & Waste Management Association, 50(2):207-218.

Cousins, C.A. 1959. The Bushveld Igneous Complex. The Geology of South Africa's Platinum Resources. *Platinum Metals Review*, 3(3) 94.

Council for Scientific and Industrial Research (CSIR), 2018, Human Health Risk Assessment and Human Health Impacts Report. Technical report for DEA funded project Assessing Human Health in the Highveld Air Pollution Priority Area.

Crowson, P. 2001. "Minerals Handbook 2000–01: Statistics and Analyses of the World's Minerals Industry", Mining Journal Books Ltd, Edenbridge, Kent, UK.

Crouse, D. L., Peters, P. A., Hystad, P., Brook, J. R., van Donkelaar, A., Martin, R. V., Villeneuve, P. J., Jerrett, M., Goldberg, M. S., Pope, C. A., Brauer, M., Brook, R. D., Robichaud, A., Menard, R., Burnett, R. T. 2015. Ambient $PM_{2.5}$, O_3, and NO_2 exposures and associations with mortality

over 16 years of follow-up in the Canadian Census Health and Environment Cohort (CanCHEC). *Environ Health Perspective*, 123: 1180-1186.

Demircan, M., & Sensoy, S. 2010. Climatological applications in Turkey. Turkish State Meteorological Service. Ankara.

Department of Environmental Affairs (DEA). 2009. State of the air report 2005. A report on the state of the air in South Africa.

Department of Energy. 2014. Commodity flows and energy balances for 2014. Department of Energy, South Africa.

Department of Energy. 2019. The South African Energy Sector Report 2019. Department of Energy, South Africa.

Diab, R. D. 1975. Stability and mixing layer characteristics over the South Africa. Durban. University of Natal. (Thesis-M.A.).

Dockery, D. W., Pope, A. C. Xu, X., Spengler, J. D., Ware, J. H., Fay, M. E, Ferris, B. G., Jr. & Speizer, F. E. 1993. An association between air pollution and mortality in Six U.S. Cities. *The new* England Journal of Medicine, 329 (24): 1753-1759.

Dodla, V., Satyanarayana, G. & Desamsetti, S. 2017. Atmospheric dispersion of $PM_{2.5}$ precursor gases from two major thermal power plants in Andhra Pradesh, India. *Aerosol and Air Quality Research,* 17(2):

Dominici, F., Wang, Y., Correia, A. W., Ezzati, M., Pope, C. A. III & Dockery, D. W. 2015. Chemical composition of fine particulate matter and life expectancy: In 95 US counties between 2002 and 2007. *Epidemiology*, 26(4): 556-564.

Emmons, L. K., Walters, S., Hess, P. G., Lamarque, J.-F., Pfister, G. G., Fillmore, D., Granier, C., Guenther, A., Kinnison, D., Laepple, T., Orlando, J., Tie, X., Tyndall, G., Wiedinmyer, C., Baughcum, S. L., & Kloster, S. 2010. Description and evaluation of the model for Ozone and related chemical tracers, version 4 (MOZART-4), *Geoscientific Model Development*, 3: 43-67.

Engelbrecht, J.P., Swanepoel, L., Chow, J.C., Watson, J.G. & Egami, R.T. 2002. The comparison of source contributions from residential coal and low-smoke fuels, using CMB modeling, in South Africa. *Environmental Science & Policy*, 5(2): 157-167.

Enstrom, J. E. 2017. Fine particulate matter and total mortality in Cancer Prevention Study Cohort reanalysis. *Dose-Response* 15: 1559325817693345.

Escience Associates (Pty) Ltd. 2017. Atmospheric Impact Report – Matimba and Medupi Power Stations. Eskom Holdings SOC Ltd Sandton, Gauteng. Retrieved from:

https://www.eskom.co.za/wp-content/uploads/2021/07/Matimba-and-Medupi-Annexure-A.1_Atmospheric-Impact-Report-Medupi-and-Matimba-2017.pdf

Ministry for the Environment. 2009. Good Practice Guide for Air Quality Monitoring and Data Management 2009. Wellington: Ministry for the Environment.

Eskom. 2013. A new dawn has arrived 1923-2013: Mpumalanga province. Retrieved from: https://www.eskom.co.za/sites/heritage/Documents/Mpumalanga90th.pdf

Eskom. 2019. Applications for suspension, alternative limits and/or postponement of the minimum emission standard (MES) compliance timeframes for Eskom's coal and liquid fuel fired power stations. Summary document. Report reference: Eskom ENV18-R245 rev 2.1. Retrieved from: https://www.eskom.co.za/wp-content/uploads/2021/07/Annexure-3.pdf

Eskom. (n.d.a). Camden Power station. Retrieved from: https://www.eskom.co.za/heritage/history-in-decades/escom-1963-1972/camden-power-station/

Eskom. (n.d.b). Company Information. Retrieved from: https://www.eskom.co.za/about-eskom/company-information/

Eskom. (n.d.c). Coal fired power stations. Retrieved from: Retrieved from: https://www.eskom.co.za/eskom-divisions/gx/coal-fired-power-stations/

Eskom. 2016. Eskom air quality improvement plan. Retrieved from: https://cer.org.za/wp-content/uploads/2016/07/AQIP.pdf

Eskom. 2020. Medupi power station project. Retrieved from: https://www.eskom.co.za/Whatweredoing/NewBuild/MedupiPowerStation/Pages/Medupi_Power_Station_Project.aspx

Eskom. 2022. Generation Plant Mix. Fact Sheet. Retrieved from: https://www.eskom.co.za/wp-content/uploads/2022/06/GX-0001-Generation-Plant-Mix-Rev-26.pdf

Exchange Rates.org.uk. (n.d.) US Dollar to South African Rand Spot Exchange Rates for 2016. Retrieved from: https://www.exchangerates.org.uk/USD-ZAR-spot-exchange-rates-history-2016.html

Falcon-Rodriguez C. I., Osornio-Vargas A. R., Sada-Ovalle, I. & Segura-Medina, P. 2016. Aeroparticles, composition, and lung diseases. *Frontiers Immunology*, 7: 1-3.

Feig, G., Garland, R. M., Naidoo, S., Maluleke, A. & Van der Merwe, M. 2019. Assessment of changes in concentrations of selected criteria pollutants in the Vaal and Highveld Priority Areas. *Clean Air Journal*, 29(2): 1-13.

Finlayson-Pitts, B. J. & Pitts, J. N. 2000. Chemistry of the upper and lower atmosphere. Theory, experiments and applications. San Diego. Academic Press.

Freiman, M. T. & Piketh, S. J. 2002. Air transport into and out of the Industrial Highveld Region of South Africa. *Journal of Applied Meteorology,* 42(7): 994-1002.

Garcia, C. A., Yap, P. S., Park, H. Y. & Weller, B. L. 2015. Association of long-term $PM_{2.5}$ exposure with mortality using different air pollution exposure models: impacts in rural and urban California. *International Journal of Environmental Health Research* 26: 1-13.

Garland, R., Naidoo, M., Sibiya, B., & Oosthuizen, R. 2017. Air quality indicators from the Environmental Performance Index: potential use and limitations in South Africa. *Clean Air Journal*, 27(1), 33-41.

Garstang, M., Tyson, P.D., Swap, R. &Edwards, M. 1996. Horizontal and vertical transport of air over southern Africa, submitted to Journal of Geophysical Research.

Gatebe, C. K., Tyson, P. D., Annergarn, H., Piketh, S. & Helas, G. 1999. A seasonal air transport climatology for Kenya. *Journal of Geophysical Research*, 104(D12): 14237-14244.

Gauteng City Region Observatory (GCRO). (n.d.) The Gauteng City-Region. Retrieved from: https://www.gcro.ac.za/about/the-gauteng-city-region/

GBD 2019 Demographics Collaborators. 2020. Global age-sex-specific fertility, mortality, healthy life expectancy (HALE), and population estimates in 204 countries and territories, 1950–2019: A comprehensive demographic analysis for the Global Burden of Disease Study 2019. *Lancet* 396:1160-1203.

Global Energy Monitor Wiki (GEM Wiki). 2022. Pretoria west power station. Retrieved from: https://www.gem.wiki/Pretoria_West_power_station#cite_note-1

Govender, K. & Sivakumar, V. 2019. A decadal analysis of particulate matter ($PM_{2.5}$) and surface ozone (O3) over Vaal Priority Area, South Africa. Clean Air Journal, 29(2).

Government Communication and Information System (GCIS). 2012. Pocket Guide to South Africa 2012/13, Mineral Resources. Retrieved from: https://www.gcis.gov.za/sites/default/files/docs/resourcecentre/pocketguide/2012/15%20Mineral%20Resources.pdf

Gray, H. A. 2019. Air quality impacts and health effects due to large stationary source emissions in and around South Africa's Mpumalanga Highveld Priority Area (HPA). Gray Sky Solutions. San Rafael, CA USA. Retrieved from: https://cer.org.za/wp-content/uploads/2019/06/Andy-Gray-Report.pdf

Grobler, M. 2016. Evaluating the costs and benefits associated with the reduction in SO_2 emissions from industrial activities on the Highveld of South Africa. Master of Engineering Thesis. University of Pretoria.

Guarnieri, M. & Balmes, J. R. 2014. Outdoor air pollution and asthma. *Lancet*, 3;383(9928):1581-92.

Guenther, A., Karl, T., Harley, P., Wiedinmyer, C., Palmer. P.I., & Geron, C. 2006. Estimates of global terrestrial isoprene emissions using MEGAN (Model of Emissions of Gases and Aerosols from Nature). *Atmospheric Chemistry and Physics*, 6(11): 3181– 3210.

Harrison, M. S. J. 1993. Elevated inversion over Southern Africa: Climatological properties and relationships with rainfall. *South African Geographical Journal*, 75: 1 - 8.

Hart, J. E., Garshick, E., Dockery, D. W., Smith, T. J., Ryan, L. & Laden, F. 2011. Long-term ambient multi-pollutant exposures and mortality. *American Journal of Respiratory and Critical Care Medicine*, 183: 73-78.

Hart, J. E., Liao, X., Hong, B., Puett, R. C., Yanosky, J. D., Suh, H., Kioumourtzoglou, M. A., Spiegelman, D, & Laden, F. 2015. The association of long-term exposure to $PM_{2.5}$ on all-cause mortality in the Nurses' Health Study and the impact of measurement-error correction. *Environmetal Health* 14: 38.

Health Effects Institute (HEI). 2020. State of Global Air 2020. Special Report. Boston, MA: HEI. Retrieved from: https://www.stateofglobalair.org/resources

Held, G., Gore, B.J., Surridge, A.D., Tosen, G.R. & Walmsley, R.D. (eds) 1996. Air Pollution and its Impacts on the South African Highveld, Environmental Scientific Association, Cleveland.

Hersey, S. P., Garland, R. M., Crosbie, E., Shingler, T., Sorooshian, A., Piketh, S., & Burger, R. 2015. An overview of regional and local characteristics of aerosols in South Africa using satellite, ground, and modeling data. Atmospheric Chemistry and Physics, 15: 4259–4278.

Hoek, G., Krishnan, R. M., Beelen, R., Peters, A., Ostro, B., Brunekreef, B. & Kaufman, J. D. 2013. Long-term air pollution exposure and cardio-respiratory mortality: a review. *Environmental Health*, 12: 43.

Huang, Y., Huang, S., Lin, C., Yang, H., Chen, C. 2020. Evaluation of bias in the measurement of condensable Particulate Matter with Method 202. *Aerosol and Air Quality Research.* 24(1)

Hystad. P., Yusuf, S., & Brauer, M. 2020. Air pollution health impacts: the knowns and unknowns for reliable global burden calculations. *Cardiovascular Research*, 116(11): 1794–1796.

Igbafe, A. I. 2007. Resolving the atmospheric sulphur budget over the Elandsfontein area of the Mpumalanga Highveld. Johannesburg. University of the Witwatersrand. (Thesis – PhD).

Integrated Resource Plan for Electricity (IRP), 2013. Integrated Resource Plan for Electricity 2010-2030, Updated Report.

Jeffrey, L. S. 2005. Characterisation of the coal resources of South Africa. *The Journal of The South African Institute of Mining and Metallurgy*, 105(2): 95-102.

Jiménez, P., Parra, R. & Baldasano, M. J. 2006. Influence of initial and boundary conditions for ozone modelling in very complex terrains: A case study in the northeastern Iberian Peninsula. Environmental Modelling & Software, 22(9): 1294-1306.

Kang, C. M., Gupta, T., Ruiz, P. A., Wolfson, J. M., Ferguson, S. T., Lawrence, J. E., Rohr, A. C., Godleski, J. & Koutrakis, P. 2011. Aged particles derived from emissions of coal-fired power plants: the TERESA field results. *Inhalation Toxicology*, 2011 23(S):11-30.

Karagulian F., Van Dingenen R., Belis C.A., Janssens-Maenhout G., Crippa M., Guizzardi D., & Dentener F. 2016. Attribution of anthropogenic $PM_{2.5}$ to emission sources: a global analysis of source-receptor model results and measured source-apportionment data. EUR 28510 EN. Italy: Publications Office of the European Union.

Katoto, P.D.M.C., Byamungu, L., Brand, A.S., Mokaya, J., Strijdom, H., Goswami, N., De Boever, P., Nawrot, T.S., & Nemery, B. 2019. 'Ambient air pollution and health in sub-Saharan Africa: Current evidence, perspectives and a call to action'. *Environmental Research*, 173: 174–188.

Keir, J. 2014. Reporting of Eskom's emissions: simples, calculations, measurements and challenges. Eskom [PowerPoint presentation]. Retrieved from: http://nla.org.za/webfiles/conferences/2014/TM2014%20proceedings/Presentations/Tuesday,%2030%20Sept/T404%20-%20Reporting%20of%20Eskom%20Emissions.pdf

Kelly, F.J. & Fussell, J.C. 2012. Size, source and chemical composition as determinants of toxicity attributable to ambient particulate matter. *Atmospheric environment*, 60:504–526.

Khumalo N. T. 2020. 2019 State of the air report and national air quality indicator. 2020 NACA Conference [PowerPoint presentation].

Klimont, Z., Smith, S.J. & Cofala, J. 2013. The last decade of global anthropogenic sulfur dioxide: 2000-2011 emissions. *Environmental Research Letters*, 8(1): 1-6.

Kloog, I., Ridgway, B., Koutrakis, P., Coull, B. A. & Schwartz, J. D. 2013. Long- and short-term exposure to $PM_{2.5}$ and mortality: Using novel exposure models. *Epidemiology*, 24: 555-561.

Kniesner, J. T. & Viscusi, W. K. 2019. The value of a Statistical Life. Forthcoming, Oxford Research Encyclopedia of Economics and Finance, Vanderbilt Law Research Paper No. 19-1.

Kok, L., van Zyl P. G., Beukes, J. P., Swartz, J-S., Burger, R. P., Ellis, S., Josipovic, M., Vakkari, V., Laakso, L. & Kulmala, M. 2021. Chemical composition of rain at a regional site on the South African Highveld. *Water SA*, 47(3): 326-337.

Koo, B., Wilson, G., Morris, R., Dunker, A. & Yarwood, G. 2009. Comparison of source apportionment and sensitivity analysis in a particulate matter air quality model. Environmental science & technology. 43(17): 6669-75.

Koplitz, N. S., Jacob, J. D., Sulprizio, P. M., Myllyvirta, L. & Reid, C. 2017. Burden of disease from rising coal-fired power plant emissions in Southeast Asia. Environmental Science & Technology, 51(3):1467-1476.

Kravchenko, J., Akushevich, I., Abernethy, A., Holman, S., Ross, W., Lyerly, K. 2014. Long-term dynamics of death rates of emphysema, asthma, and pneumonia and improving air quality. *International Journal of Chronic Obstructive Pulmonary Disease*, 9: 613–627.

Krewski, D., Burnett, R. T., Goldberg, M. S., Hoover, K., Siemiatycki, J., Jerrett, M., Abrahamowicz, M. & White, W. H. 2000. Reanalysis of the Harvard Six Cities study and the American Cancer Society study of particulate air pollution and mortality. Cambridge, Massachusetts Avenue: Health Effects Institute.

Krewski, D., Jerrett, M., Burnett, R.T., Ma, R., Hughes, E. *et al*. 2009. Extended follow-up and spatial analysis of the American cancer society study linking particulate air pollution and mortality. Research Report. *Health Effects Institute,* 140: 5-114.

Ku, T., Chen, M., Li, B., Yun, Y., Li, G. & Sang, N. 2017. Synergistic effects of particulate matter ($PM_{2.5}$) and sulfur dioxide (SO_2) on neurodegeneration via the microRNA-mediated regulation of tau phosphorylation. *Toxicol Research (Camb)*, 6(1):7-16.

Kylin, H., Bouwman, H. & Evans, S. W. 2011. Evaluating threats to an endangered species by proxy: air pollution as threat to the blue swallow (*Hirundo atrocaerulea*) in South Africa. *Environmental Science and Pollution Research*, 18(2): 282-290.

Laban, T. L., Beukes, J. P. & Van Zyl, P. G. 2015. 'Measurement of surface ozone in South Africa with reference to impacts on human health'. *Clean Air Journal*, 25(1): 9-12.

Lacey, F. G., Marais, E. A., Henze, D. K., Lee, C. J., van Donkelaar, A., Martin, R. V., Hannigan, M. P. & Wiedinmyer, C. 2017. Improving present day and future estimates of anthropogenic sectoral emissions and the resulting air quality impacts in Africa. *Faraday Discuss*. 200: 397−412.

Langerman, K.E. & Pauw, C.J. 2018. A critical review of health risk assessments of exposure to emissions from coal-fired power stations in South Africa. *Clean Air Journal*, 28(2):68-79.

LAND-AMETEK. 2008. Opacity and PM monitoring in emission stacks. Application note. MARCOM0529 Opacity & PM in Stacks Rev 1. LAND Instruments International.

Lelieveld, J., Evans, S. J., Fnais, M., Giannadaki, D. & Pozzer, A. 2015. The contribution of outdoor air pollution sources to premature mortality on a global scale. *Nature*, 367(525):367-371.

Lepeule, J., Laden, F., Dockery, D. & Schwartz, J. 2012. Chronic exposure to fine particles and mortality: an extended follow-up of the Harvard six cities study from 1974 to 2009. *Environmental Health Perspectives*, 120: 965-970.

Li, B., Yang, Y., Dong, H., Li, M., Cai, D., Yang, Z., Zhang, C., Wang, H., Hu, J., Bergmann, S., Lin, G. & Wang, B. 2021. $PM_{2.5}$ constituents and mortality from a spectrum of causes in Guangzhou, China. *Ecotoxicology and Environmental Safety*, 222: 112498.

Li, J. W., Qi, Z. F., Li, M., Wu, D. L., Zhou, C. Y., Lu, S. Y., Yan, J. H. & Li, X. D. 2017. Physical and Chemical Characteristics of Condensable Particulate Matter from an Ultralow-Emission Coal Fired Power Plant. *Energy Fuels*, 31(2): 1778−1785.

Lighty, J.S., Veranth, J.M. & Sarofim, A.F. 2000. Combustion aerosols: factors governing their size and composition and implications to human health. *Journal of the Air and Waste Management Associations*, 50(9), 1565-1618.

Lim, C., Ryu, J., Choi, Y., Jeon, S. W. & Lee, W. 2020. Understanding global $PM_{2.5}$ concentrations and their drivers in recent decades (1998–2016). *Environment International*, 144:106011.

Lin, H., Guo, Y., Di, Q., Zheng, Y., Kowal, P. *et al*. 2017. Ambient $PM_{2.5}$ and stroke effect modifiers and population attributable risk in six low- and middle-income countries. *Stroke*, 48(5):1191–1197.

Lindeque, F. L. 2018. The health and economic benefits of interventions to reduce residential solid fuel burning on the Highveld. (Dissertation – Msc).

Lipfert, F. W., Wyzga, R. E., Baty, J. D. & Miller, J. P. 2006. Traffic density as a surrogate measure of environmental exposures in studies of air pollution health effects: Long-term mortality in a cohort of US veterans. *Atmospheric Environment*, 40: 154-169.

Lippmann, M., Yeates, D. B., & Albert, R. E. 1980. Deposition, retention, and clearance of inhaled particles. *British Journal of Industrial Medicine*, *37*(4), 337–362.

Lippmann, M. 2014. Toxicological and epidemiological studies of cardiovascular effects of ambient air fine particulate matter ($PM_{2.5}$) and its chemical components: Coherence and public health implications. *Critical Reviews in Toxicology*, 44(4): 299–347.

Liu, C., Chen, R., Sera, F., Vicedo-Cabrera, A., Guo, Y., Tong, S., Coelho, M., Saldiva, P., Lavigne, E., Matus, P., Ortega, N., Garcia, S., Pascal, M., Stafoggia, M., Scortichini, M., Hashizume, M., Honda, Y., Hurtado-Díaz, M., Cruz, J., Nunes, B., Teixeira, J.P., Kim, H., Tobias, A., Íñiguez, C., Forsberg, B.,

Åström, C., Ragettli, M.S., Guo, Y.L.L., Chen, B.Y., Bell, M.L., Wright, C.Y., Scovronick, N., Garland, R. M., Milojevic, A., Kyselý,J., Urban, A., Orru, H., Indermitte, E., Jaakkola, J., Ryti, N., Katsouyanni, K., Analitis, A., Zanobetti, A., Schwartz, J., Chen, J., Wu, T., Cohen, A., Gasparrini, A. & Kan, H. 2019. Ambient particulate air pollution and daily mortality in 652 cities. *New England Journal of Medicine*, 381 (8):705-715.

Lourens, A.S.M., Butler, T.M., Beukes, J.P., van Zyl, P. G., Beirle, S., Wagner, T. K., Heue, K., Pienaar, J. J., Fourie, G. D. & Lawrence, M. G. 2012. Re-evaluating the NO_2 hotspot over the South African Highveld. South African Journal of Science 108(9/10), Art. #1146, 6 pages.

Mabahwi, N. A. B., Leh, O. L. H. & Omar, D. 2014. Human health and wellbeing: human health effect of air pollution. *Procedia – Social and Behavioural Sciences,* 153: 221-229.

Makonese, T., Masekameni, D. M., Annegarn, H. J., & Forbes, P. B. 2015. Influence of fire-ignition methods and stove ventilation rates on gaseous and particle emissions from residential coal braziers. Journal of Energy in Southern Africa, 26(4): 16-28.

Malfroy, H., Cope, M. & Nelson, P.F. 2005. An assessment of the contribution of coal-fired power station emissions to atmospheric particle concentrations in NSW. Retrieved from: http://www.cmar.csiro.au/e-print/open/cope_2004b.pdf

Maenhaut W., Salma I., Cafmeyer J., Annegarn H. J., and Andreae M. O., 1996, 'Regional atmospheric aerosol composition and sources in the eastern Transvaal, South Africa, and impact of biomass burning'. *Journal of Geophysical Research. Atmospheres,* 101: 23631–23650.

Mannucci, P. M. & Franchini, M. 2017. 'Health effects of ambient air pollution in developing countries'. *International Journal of Environmental Research and Public Health*, 14(9): 1–8.

Marais, A. E. Silvern, F. R., Vodonos, A., Dupin, E., Bockarie, S. A., Mickley, J. L., & Schwartz J. 2019. Air quality and health impact of future fossil fuel use for electricity generation and transport in Africa. *Environmental, Science & Technology*, 53(22): 13524–13534.

Markandya, A., Ortiz, A. R., & Chiabai A. 2019. Estimating environmental health costs: General introduction to valuation of human health risks. Encyclopedia of Environmental Health (Second Edition), Elsevier, 719-727.

McGranahan, G. & Murray, F., eds. 2003 Air pollution & health in rapidly developing countries. 1st ed. Routledge.

Meth, O. 2018. New satellite data reveals the world's largest air pollution hotspot in Mpumalanga – South Africa. Retrieved from: https://www.greenpeace.org/africa/en/press/4202/new-satellite-data-reveals-the-worlds-largest-air-pollution-hotspot-is-mpumalanga-south-africa/

Department of Mineral Resources (DMR). 2019. South African Mineral Industry 2017/2018. Retrieved from: https://www.dmr.gov.za/LinkClick.aspx?fileticket=PClz-cRGkyg%3D&portalid=0

Morino, Y., Chatani, S., Tanabe, K., Fujitani, Y., Morikawa, T., Takahashi, K., Sato, K & Sugata, S. 2018. Contributions of Condensable Particulate Matter to Atmospheric Organic Aerosol over Japan. *Environmental Science & Technology*, 52(15): 8456-8466.

Morosele, I. P., & Langerman, K. E. 2020. The impacts of commissioning coal-fired power stations on air quality in South Africa: insights from ambient monitoring stations. *Clean Air Journal*, 30(2).

Morrow, E. P. 1973. Alveolar clearance of aerosols. *Archives of Internal Medicine*, 131(1):101-108.

Murat, D. 2017. How air pollution affects subjective well-being: well-being and quality of life - medical perspective. IntechOpen. Retrieved from: https://www.intechopen.com/books/well-being-and-quality-of-life-medical-perspective/how-air-pollution-affects-subjective-well-being

Musina, L. & Rutherford, L. M. (eds) 2010. The vegetation of South Africa, Leostho and Swaziland. Strelitzia 19. South African National Biodiversity Institute, Pretoria.

Muyemeki, L., Burger, R., & Piketh, S. J. 2020. Evaluating the potential of remote sensing imagery in mapping ground-level fine particulate matter ($PM_{2.5}$) for the Vaal Triangle Priority Area. *Clean Air Journal*, 30(1): 1-7.

Muyemeki, L., Burger, R., Piketh, S.J., Language, B., Beukes, J.P. & van Zyl, P.G. 2021. Source apportionment of ambient $PM_{10-2.5}$ and $PM_{2.5}$ for the Vaal Triangle, South Africa. *South African Journal of Science*.117(5/6).

Myllyvirta, L. 2014. Health impacts and social costs of Eskom's proposed non-compliance with South Africa's air emission standards. Retrieved from: https://cer.org.za/wp-content/uploads/2014/02/Annexure-5_Health-impacts-of-Eskom-applications-2014-_final.pdf

Naledzi Environmental Consultants (NEC). 2018. Summary Atmospheric Impact Report (AIR) in support of Eskom's application for postponement of the minimum emission standards for its coal-fired power stations. Retrieved from: https://www.eskom.co.za/wp-content/uploads/2021/07/Annexure-2.pdf

Nel, A., 2005. Air pollution-related illness: Effects of particles. *Science*, 308(5723): 804–806.

Nemmar, A., Holme, J.A., Rosas, I., Schwarze, P.E. & Alfaro-Moreno, E. 2013. Recent advances in particulate matter and nanoparticle toxicology: a review of the in vivo and in vitro studies. *BioMed Research International*, 2013 (279371).

Nenes, A, C. Pilinis, and S.N. Pandis. 1998. ISORROPIA: A New Thermodynamic Model for Multiphase Multicomponent Inorganic Aerosols. Aquatic Geochemistry, 4, 123-152.

Nenes, A., C. Pilinis, and S.N. Pandis. 1999. Continued Development and Testing of a New Thermodynamic Aerosol Module for Urban and Regional Air Quality Models. Atmos. Environ. 33, 1553-1560.

Norman, R., Cairncross, E., Witi, J., Bradshaw, D., and the South African Comparative Risk Assessment Collaborating Group. 2007. Estimating the burden of disease attributable to urban outdoor air pollution in South Africa in 2000. *South Africa Medical Journal*, 97(7): 782-790

Novela, R. J., Gitari, W. M., Chikoore, H., Molnar, P., Mudzielwana, R., & Wichmann, J. 2020. Chemical characterization of fine particulate matter, source apportionment and long-range transport clusters in Thohoyandou, South Africa. *Clean Air Journal*, 30(2).

Organisation for Economic Co-operation and Development (OECD) 2012. Mortality Risk Valuation in Environment, Health and Transport Policies, OECD Publishing. Retrieved from: http://publications.europa.eu/resource/cellar/2efbeb80-138b-40d1-8411-de6241fee009.0002.06/DOC_1

Ostro, B., Hu, J., Goldberg, D., Reynolds, P., Hertz, A. *et al*. 2015. Associations of mortality with long-term exposures to fine and ultrafine particles, species and sources: results from the California teachers study cohort. *Environmental Health Perspectives*, 123:549–556.

Paton-Walsh, C., Emmerson, K. M., Garland, R. M., Keywood, M., Hoelzemann, J. J., Huneeus, N., Buchholz, R. R., Humphries, R. S., Altieri, K., Schmale, J., Wilson, S. R., Labuschagne, C., Kalisa, E., Fisher, J. A., Deutscher, N. M., van Zyl, P. G., Beukes, J. P., Joubert, W., Martin, L., Mkololo, T., Barbosa, C., de Fatima Andrade, M., Schofield, R., Mallet, M. D., Harvey, M. J., Formenti, P., Piketh, S. J., Olivares, G. 2022. Key challenges for tropospheric chemistry in the Southern Hemisphere. *Elementa: Science of the Anthropocene,*10(1).

Pervin. T., Gerdtham, U-G. & Lyttkens C. H. 2008. 'Societal costs of air pollution-related health hazards: A review of methods and results'. *Cost effectiveness and resource allocation*, 6:19.

Petkova, E., Jack, D., Volavka-Close, N. & Kinney, P. 2013. Particulate matter pollution in African cities. Air Quality, Atmosphere & Health, 6(3): 603-614.

Piketh, S. J., Annegarn, H. J. & Tyson, P. D. 1999a: Lower tropospheric aerosol loadings over South Africa: The relative contribution of aerosol dust, industrial emissions, and biomass burning. Journal of Geophysical Research, 104: 1597–1607.

Piketh, S. J., Formenti, P., Annegarn, H. J., & Tyson, P. D. 1999b: Industrial aerosol characterization at a remote site in South Africa. *Nuclear Instruments and Methods in Physics Research Section B*, 150: 350–355.

Piketh, S. J., Annegarn, H. J. & Kneen, M. A. 1996. Regional scale impacts of biomass burning emissions over southern Africa, in J.S. Levine (ed.), Biomass Burning and Global Change, MIT Press, Cambridge, 320-326.

Pinault, L., Tjepkema, M., Crouse, D. L., Weichenthal, S., van Donkelaar, A., Martin, R. V., Brauer, M., Chen, H. & Burnett, R. T. 2016. Risk estimates of mortality attributed to low concentrations of ambient fine particulate matter in the Canadian community health survey cohort. *Environmental Health*, 15: 18.

Planting, S. 2021. Powering up: Eskom completes Medupi – sort of. *Business Maverick*, 2 Aug. Retrieved from: https://www.dailymaverick.co.za/article/2021-08-02-powering-up-eskom-completes-medupi-sort-of/

Pope III, C. A., Burnett, R. T. & Thun, M. J. 2002. Lung cancer, cardiopulmonary mortality and long-term exposure to fine particulate air pollution. *Journal of American Medical Association*, 289(9):1132-1141.

Pope, C. A. & Dockery, D.W. 2006. Critical review: health effects of fine particulate air pollution: lines that connect. Air & waste management association, 709–742.

Pope, C. A., III, Rodermund, D. L., Gee, M. M. 2007. Mortality effects of a copper smelter strike and reduced ambient sulfate particulate matter air pollution. Environ Health Perspect, 115: 679–683.

Power Technology. (n.d.). The Kusile power station project, South Africa. Retrieved from: https://www.power-technology.com/projects/kusilepowerstation/

Preston-Whyte, R. A. & Tyson, P. D. 1993. The Atmosphere and weather of southern Africa. Cape Town. Oxford University Press.

Pretorius, I., Piketh, S. & Burger, R. 2017. Emissions management and health exposure: should all power stations be treated equal? *Air Quality, Atmosphere & Health*, 10(4):509-520.

Pretorius, I. Piketh, S. & Burger, R. 2015a. The impact of the South African energy crisis on emissions. *WIT Transactions on Ecology and the Environment*, 198: 255-264.

Pretorius, I. Piketh, S., Burger, R. & Neomagus, H. 2015b. A perspective on South African coal fired power station emissions. *Journal of Energy in Southern Africa*. 26(3): 27-40.

Prime Africa Consultants (PAC). 2018. The provision of professional, independent consulting services to assist Eskom in compiling applications for renewed postponement of the Minimum Emission Standards: Component 4: Health impact focused cost benefit analyses. Deliverable 2: Final Report (Version 8.0). Retrieved from: https://www.eskom.co.za/wp-content/uploads/2021/07/Annexure-1.pdf

Prueitt, R. L., Li, W., Edwards, L., Zhou J & Goodman J. E. 2021. Systematic review of the association between long-term exposure to fine particulate matter and mortality. *International Journal of Environmental Health Research*.

Puett, R. C., Hart, J. E., Suh, H., Mittleman, M. & Laden, F. 2011. Particulate matter exposures, mortality and cardiovascular disease in the health professionals follow-up study. *Environmental Health Perspectives,* 119: 1130-1135.

Raaschou-Nielsen, O., Andersen, Z. J., Beelen, R., Samoli, E., Stafoggia, M., Weinmayr, G., *et al.* 2013. Air pollution and lung cancer incidence in 17 European cohorts: Prospective analyses from the European Study of Cohorts for Air Pollution Effects (ESCAPE). *The Lancet Oncology*, 14(9): 813–822.

Raes, F., Van Dingenen, R., Vignati, E., Wilson, J., Putaud, J., Seinfeld, H. J. & Adams, P. 2000. Formation and cycling of aerosols in the global troposphere. Atmospheric Environment, 34(25): 4215-4240.

Ramboll Environ. 2016. CAMx User's Guide. Comprehensive Air Quality Model with Extensions. Version 6.4. Retrieved from: https://camx-wp.azurewebsites.net/Files/CAMxUsersGuide_v6.40.pdf

Ramboll. 2020. CAMx Modelling System Overview. Retrieved from: https://camx-wp.azurewebsites.net/Files/CAMx7_Overview_July20.pdf [PowerPoint presentation].

Rao, X., Patel, P., Puett, R. & Rajagopalan, S. 2015. Air Pollution as a Risk Factor for Type 2 Diabetes. *Toxicological Sciences*, 143(2): 231–241.

Reiss, R., Anderson, E. L., Cross, C. E., Hidy, G., Hoel, D., McClellan, R. & Moolgavkar, S. 2007. Evidence of health impacts of sulfate-and nitrate-containing particles in ambient air. *Inhalation toxicology*, 19(5):419–449.

Sacks, J. D., Lloyd, J. M., Zhu, Y., Anderton, J., Jang, C. J., Hubbell, B., & Fann, N. 2018. The Environmental Benefits Mapping and Analysis Program - Community Edition (BenMAP-CE): A tool to estimate the health and economic benefits of reducing air pollution. *Environmental modelling & software: with environment data news*, 104: 118–129.

Samet, J. M., Dominici, F., Curriero, F. C., Coursac, I. & Zeger, S. L. 2000. Fine particulate air pollution and mortality in 20 U.S. Cities, 1987–1994. *The New England Journal of Medicine*, 343 (24): 1742-1749.

Seinfeld, J.H. and Pandis, S.N., 1998: Atmospheric Chemistry and Physics: From Air Pollution to Climate Change, John Wiley and Sons, Inc., New York.

Seinfeld, J.H. and Pandis, S.N., 2006: Atmospheric Chemistry and Physics: From Air Pollution to Climate Change, John Wiley and Sons, Inc., Hoboken, New Jersey.

Scorgie, Y. 2012. Urban air quality management and planning in South Africa. Johannesburg, University of Johannesburg. (Thesis – PhD).

Scorgie, Y., Burger L. W., & Annegarn, H. J. 2004. Socio-economic Impact of Air Pollution Reduction Measures – Task 2: Establishment of Source Inventories, and Task 3: Identification and Prioritisation of Technology Options. Report compiled on behalf of NEDLAC, 25 June 2003. NEDLAC, Rosebank.

Scorgie, Y. & Thomas, R. 2006. Eskom Mpumalanga highveld cumulative planning study: air pollution compliance assessment and health risk analysis of cumulative operations of current, RTS and proposed Eskom power station located within the Mpumalanga and Gauteng provinces, Report No. APP/06/ESKOM-05 Rev 1.0, project done on behalf of Eskom Holdings Limited.

Schraufnagel, D. E., Balmes, J. R., Cowl, C. T., De Matteis, S., Jung, S-H., Mortimer, K., Perez-Padilla, R., Rice, M. B., Riojas-Rodriquez, H., Sood, A., Thurston, G.D., To, T., Vanker, A. &

Schraufnagel DE, Balmes JR, Cowl CT, De Matteis S, Jung S-H, Mortimer K, Perez-Padilla, R., Rice, M. B., Riojas-Rodriquez, H., Sood, A., Thurston, G.D., To, T., Vanker, A. & Wuebbles, D. J. 2018b. Air pollution and noncommunicable diseases: A review by the forum of International Respiratory Societies' Environmental Committee, Part 2: Air pollution and organ systems. *Chest Journal*, 155(2): 417–426

Scheifinger, H. & Held, G. 1997. Aerosol behaviour on the South African Highveld. *Atmospheric environment*, 31(21):3497–3509.

Scorgie Y, Fischer T, Watson R. 2005. Air quality management plan for the Ekurhuleni Metropolitan Municipality. www.ekurhuleni.gov.za/465-air-quality-managementplan-2005/file.

Shah, A. S., Langrish, J. P., Nair, H., McAllister, D. A., Hunter, A. L., Donaldson, K., *et al.* 2013. Global association of air pollution and heart failure: A systematic review and meta-analysis. *The* Lancet, 382(9897): 1039–1048.

Shikwambana, L., Mhangara, P. & Mbatha, N. 2020. Trend analysis and first time observations of sulphur dioxide and nitrogen dioxide in South Africa using TROPOMI/Sentinel-5 P data. *International Journal of Applied Earth Observation and Geoinformation*, 91(102130).

Simon, H., Beck, L., Bhave, P., Divita, F., Hsu, Y., Luecken, D., Mobley, J., Pouliot, G., Reff, A., Sarwar, G. & Strum, M. 2010. The development and uses of EPA's SPECIATE database. *Atmospheric Pollution Research*, 1:196-206.

Sivertsen, B., Matale, C. & Pereira, L. M. 1995. Sulphur emissions and transfrontier air pollution in Southern Africa. Rep. No. 35. Southern African Development Community, Environment and Land Management Sector Coordination Unit, Maseru (Lesotho).

Skamarock, W.C., Klemp, J., Dudhia, J., Gill, D.O., Barker, D., Wang, W. & Powers, J.G. 2008. A Description of the Advanced Research WRF Version 3. Technical Note: NCAR/TN-475+STR. Boulder, Colorado. National Center for Atmospheric Research.

Son, J., Lee, J., Kim, K., Jung, K. & Bell, M. L. 2012. Characterization of fine particulate matter and associations between particulate chemical constituents and mortality in Seoul, Korea. *Environmental Health Perspectives*, 120(6): 872-878.

Song, Y., Tang, X. Y. & Xie, S. D. 2007. Source apportionment of $PM_{2.5}$ in Beijing in 2004. *Journal of Hazardous Materials* 146(1-2):124-130.

South Africa (SA), 1996. Constitution of the Republic of South Africa.

SA. 2007. Declaration of the Highveld as a Priority Area in terms of Section 18(1) of the National Environmental Management: Ait Quality Act 2004 (Act No. 39 of 2004). (Government notice no. 1123). *Government gazette*, 30518, 23 Nov.

SA. 2006. Declaration of the Vaal Triangle Air-Shed Priority Area in terms of Section 18(1) of the National Environmental Management: Ait Quality Act 2004 (Act No. 39 of 2004). (Government notice no. 365) *Government gazette*, 28732, 21 Apr.

SA. 2012. Declaration of the Waterberg National Priority Area in terms of Section 18(1) of the National Environmental Management: Ait Quality Act 2004 (Act No. 39 of 2004). (Government notice no. 495). Government gazette, 35435, 15 Jun.

SA. Department of Environmental Affairs (DEA). 2012a. Highveld priority area air quality management plan. (Government notice no. 144). *Government gazette,* 35072, 2 Mar.

SA. DEA. 2020. 2019 National air quality officer's annual report on air quality management.

SA. DEA. 2009. National ambient air quality standards. (Government notice no. 1210). *Government gazette,* 32816, 24 Dec.

SA. DEA. 2012b. National ambient air quality standard for particulate matter with aerodynamic diameter less than 2.5 micron metres ($PM_{2.5}$). (Government notice no. 486). *Government gazette,* 35463, 29 Jun.

SA. DEA. 2018. The 2017 National framework for air quality management in the republic of South Africa. (Government notice no. 1144). *Government gazette,* 41996, 26 Oct.

SA. DEA. 2015. Waterberg Bojanala priority area air quality management plan. (Government notice no. 1207). *Government gazette,* 39489, 15 Dec.

SA. Department of Environmental Affairs and Tourism (DEAT). 2009. Vaal triangle air-shed priority area air quality management plan. (Government notice no. R. 613). *Government gazette,* 32263, 28 May.

SA. Department of Forestry, Fisheries and the Environment (DFFE). 2021. Second generation air quality management plan for Vaal triangle airshed priority area. (Government notice no. 693). *Government gazette,* 44945, 6 Aug.

SA. Department of Energy. 2019. Integrated Resource Plan 2019. (Government notice no. 1360). *Government gazette,* 42784, 18 Oct.

Southerland, V. A., Brauer, M., Mohegh, A., Hammer, M. S., van Donkelaar, A., Martin, R. V., Apte, J. S. & Anenberg, S. C. 2022. Global urban temporal trends in fine particulate matter (PM2·5) and attributable health burdens: estimates from global datasets. *The Lancet Planetary Health,* 6 (2): e139-e146.

Srivastava, D., Vu, T.V., Tong, S., Shi, Z. & Harrison, M. R. 2022. Formation of secondary organic aerosols from anthropogenic precursors in laboratory studies. *npj Climate and Atmospheric Science*, 5(22).

Stanek, L. W., Sacks, J. D., Dutton, S. J. & Dubois, J. J. B. 2011. Attributing health effects to apportioned components and sources of particulate matter: An evaluation of collective results. *Atmospheric environment*, 45: 5655–5663.

Stats SA. 2014a. National Household Travel Survey, 2013. Statistics South Africa. Pretoria, South Africa, 2014. Data publicly available through the Stats SA Nesstar portal. Retrieved from: http://interactive.statssa.gov.za:8282/webview/

Stats SA. 2022. 60.6 million people in South Africa. Retrieved from: https://www.statssa.gov.za/?p=15601

Stats SA. 2014b. South African Census Community Profiles 2011. Statistics South Africa, Pretoria, South Africa. Dataset accessed through SuperWeb2 tool. Retrieved from: http://superweb.statssa.gov.za/webapi/jsf/login.xhtml

Statistics South Africa (Stats SA), 2018a. Mortality and causes of death in South Africa, 2016: Findings from death notification. Statistical release P0309.3.

Stats SA. 2018b. Provincial profile: Gauteng, Community Survey 2016, Report number 03-01-09.

Stats SA. 2018c. Provincial profile: Limpopo Community Survey 2016 Report 03-01-15, CS 2016.

Stats SA. 2018d. Provincial profile: North West Community Survey 2016 Report 03-01-11.

Stats SA. 2018e. Provincial profile: Mpumalanga Community Survey 2016 Report 03-01-13,

Stats SA. 2018f. Provincial profile: Kwazulu-Natal Community Survey 2016 Report 03-01-10

Stats SA. 2018g. Provincial profile: Free State Community Survey 2016 Report 03-01-12

Steyn M. & Kornelius G. 2018. An economic assessment of SO_2 reduction from industrial sources on the highveld of South Africa, *Clean Air Journal* 28 (1): 23-33.

Strader, R., F. Lurmann, and S.N. Pandis. 1999. Evaluation of secondary organic aerosol formation in winter. Atmos. Environ., 33, 4849-4863.

Streets, D. G., Bond, T. C., Carmichael, G. R., Fernandes, S. D., Fu, Q., He, D., Klimont, Z., Nelson, S. M., Tsai, N. Y., Wang, M. Q., Woo, J. -H. & Yarber, K. F. 2003. An inventory of gaseous and primary aerosol emissions in Asia in the year 2000. 2003. *Journal of Geophysical Research. Atmospheres*, 108.

The World Bank. (n.d.). *GDP per capita, PPP (constant 2017 international $) – South Africa*. Retrieved from: https://data.worldbank.org/indicator/NY.GDP.PCAP.PP.KD?locations=ZA&most_recent_year_desc=false

The World Bank. 2016. The cost of air pollution: Strengthening the economic case for action. Seattle. Retrieved from: https://documents1.worldbank.org/curated/en/781521473177013155/pdf/108141-REVISED-Cost-of-PollutionWebCORRECTEDfile.pdf

Yager, R. T., 2022. The Mineral Industry of South Africa. United States Geological Survey 2017-2018 Minerals Yearbook. South Africa (Advanced Release). Retrieved from: https://pubs.usgs.gov/myb/vol3/2017-18/myb3-2017-18-south-africa.pdf

Thunis, P., Clappier, A., Tarrason, L., Cuvelier, C., Monteiro, A., Pisoni, E., Wesseling, J., Belis, C.A., Pirovano, G., Janssen, S., Guerreiro, C. and Peduzzi, E. 2019. Source apportionment to support air quality planning: Strengths and weaknesses of existing approaches. Environment International, 130: 104825. https://doi.org/10.1016/j.envint.2019.05.019.

Thurston, G. D., Ahn, J., Cromar, K. R., Shao, Y., Reynolds, H. R., Jerrett, M., Lim, C, C., Shanley, R., Park, Y. & Hayes, R. B. 2016. Ambient particulate matter air pollution exposure and mortality in the NIH-AARP Diet and Health Cohort. *Environmental Health Perspective*, 124: 484-490.

Tiitta, P., Vakkari, V., Croteau, P., Beukes, J. P., van Zyl, P. G., Josipovic, M., Venter, A. D., Jaars, K., Pienaar, J. J., Ng, N. L., Canagaratna, M. R., Jayne, J. T., Kerminen, V.-M., Kokkola, H., Kulmala, M., Laaksonen, A., Worsnop, D. R., & Laakso, L. 2014. Chemical composition, main

sources and temporal variability of PM1 aerosols in southern African grassland, *Atmospheric Chemistry and Physics*, 14(4): 1909–1927.

Tomasi, C. & Lupi, A. 2017. Primary and secondary sources of atmospheric aerosol. Atmospheric aerosols: life cycles and effects on air quality and climate. First edition. Wiley-VCH Verlag GmbH & Co. KGaA.

Trozzi, C., Villa, S. & Piscitello, E. 2009. Use of CALPUFF and CAMx Models in Regional Air Quality Planning: Italy case studies. 10.2495/AIR090021.

Trustees for the time being of Groundwork Trust and Another v Mister of Environmental Affairs and Others (Judgement with Case number 39724/2019 delivered on 18 March 2022 in the Pretoria High Court).

Tshehla, C. & Wright, C. Y. 2019. '15 Years after the National Environmental Management Air Quality Act: Is legislation failing to reduce air pollution in South Africa?' *South African Journal of Science*, 115(9/10):27-29

Turner, M. C., Jerrett, M., Pope, A. III, Krewski, D., Gapstur, S. M., Diver, W. R., Beckerman, B. S., Marshall, J. D., Su, J., Crouse, D. L. & Burnett, R. T. 2016. Long-term ozone exposure and mortality in a large prospective study. *American Journal of Respiratory and Critical Care Medicine*, 193: 1134-1142.

Tyson, D. P. & Garstang, M. & Swap, R. 1996. Large-scale recirculation of air over southern Africa. *Journal of Applied Meteorology*, 35 (12): 2218-2236.

Tyson, D. P., Kruger, J. F., Louw, W. C. 1988. Atmospheric pollution and its implications in the Eastern Transvaal Highveld. Council for Scientific and Industrial Research. South African National Scientific Programmes Report No. 150.

Tyson, D. P., Preston-Whyte, R. A. & Diab, R. D. 1976. Towards an inversion climatology of Southern Africa: Part 1, Surface inversions. *South African Geographical Journal*, 58: 151 - 163.

United States Environmental Protection Agency (US EPA). (n.d.a). Air Emissions Factors and Quantification: AP-42: Compilation of Air Emissions Factors. Available at: https://www.epa.gov/air-emissions-factors-and-quantification/ap-42-compilation-air-emissions-factors

US EPA. 2000. Current Knowledge of Particulate Matter (PM) Continuous Emission Monitoring. EPA-454/R-00-039

US EPA. 2019. Integrated Science Assessment for Particulate Matter. EPA/600/R-19/188.

US EPA. (n.d.b). Particulate pollution exposure. Retrieved from: https://www.epa.gov/pmcourse/particle-pollution-exposure

Vakkari, V., O'connor, E. J., Nisantzi, A., Mamouri, R. E., Hadjimitsis, D. G. 2015. Low-level mixing height detection in coastal locations with a scanning Doppler lidar. *Atmospheric Measurement Techniques*. 8(4), 1875-1885.

Vakkari, V., Tiitta, P., Jaars, K., Croteau, P., Beukes, J. P., Josipovic, M., Kerminen, V., Kulmala, M., Venter, A. D., vanZyl, G. P., Worsnop, R. D. & Laakso, L. 2015. Reevaluating the contribution of sulfuric acidand the origin of organic compoundsin atmospheric nanoparticle growth. *Geophysical Research Letter*, 42: 10486–10493.

Valavanidis, A., Fiotakis, K. & Vlachogianni, T. 2008. Airborne particulate matter and human health: toxicological assessment and importance of size and composition of particles for oxidative damage and carcinogenic mechanisms. *Journal of Environmental Science and Health*, Part C, 26(4):339-362.

Van Horen, C.R. 1996. The cost of power: externalities in South Africa's energy sector. Cape Town: University of Cape Town. (Thesis – PhD).

Venter, D. A., Vakkari, V., Beukes, P. J., van Zyl, G. P., Laakso, H., Mabaso, D., Tiitta, P., Josipovic, M., Kulmala, M., Pienaar, J.J., Laakso, L. 2012. An air quality assessment in the industrialised western Bushveld Igneous Complex, South Africa. *South African Journal of Science*, 108(9/10): 1-10.

Venter, D. A., van Zyl, G. P., Beukes, P. J., Swartz, J., Josipovic, M., Vakkari, V., Laakso, L. & Kulmala, M. 2018. Size-resolved characteristics of inorganic ionic species in atmospheric aerosols at a regional background site on the South African Highveld. *Journal of Atmospheric Chemistry*. 75(3): 285-304.

Viscusi, W. & Masterman, C. 2017. Income elasticities and global values of a statistical life. Journal of Benefit-Cost Analysis, 8(2): 226-250.

Walton, M. N., Piketh, S. J., van Zyl, P., Maenhaut, W., Burger, R., Language, B. & Formenti, P. 2021. Source apportionment of ambient fine and coarse aerosols in Embalenhle and Kinross, South Africa. Clean Air Journal. 31(2): 1-13.

Wang, Y., Kloog, I., Coull, B. A., Kosheleva, A., Zanobetti, A. & Schwartz, J. D. 2016. Estimating causal effects of long-term $PM_{2.5}$ exposure on mortality in New Jersey. *Environmental Health Perspective*, 124: 1182-1188.

Wang, Y., Shi, L., Lee, M., Liu, P., Di, Q., Zanobetti, A. & Schwartz, J. D. 2017. Long-term exposure to $PM_{2.5}$ and mortality among older adults in the Southeastern US. *Epidemiology*, 28: 207-214.

Wang-Li, L. 2015. Insights to the formation of secondary inorganic $PM_{2.5}$: Current knowledge and future needs. *International Journal of Agricultural and Biological Engineering*, 8: 1-13.

Warneck, P. 1988: Chemistry of the natural atmosphere., London. Academic press.

Waterberg District Municipality (WDM). 2010. Environmental Management Framework for the Waterberg District.

Watson, J. G., Chow, J. C. & Houck, J. E. 2001. $PM_{2.5}$ chemical source profiles for vehicle exhaust vegetative burning, geological material, and coal burning in Northwestern Colorado during 1995. *Chemosphere* 43(8):1141-1151.

Watson, J. G., Chow, J. C., Lowenthal, D. H., Robinson, N. F., Cahill, C. F. & Blumenthal, D. L. 2002. Simulating changes in source profiles from coal-fired power plants: Use in chemical mass balance of $PM_{2.5}$ in the Mount Zirkel Wilderness. *Energy Fuels,* 16:311–324.

Welgegund.org. (n.d.). *Welgegund measurement station.* Retrieved from: https://www.welgegund.org/history

Weichenthal, S., Villeneuve, P. J., Burnett, R. T., van Donkelaar, A., Martin, R. V., Jones, R. R., Dellavalle, C. T., Sandler, D. P., Ward, M. H. & Hoppin, J. A. 2014. Long-term exposure to fine particulate matter: association with nonaccidental and cardiovascular mortality in the agricultural health study cohort. *Environmental Health Perspective*, 122: 609-615.

Wellenius G.A., Burger, M. R. & Coull, B. A. 2012. Ambient air pollution and the risk of acute ischemic stroke. Archives of Internal Medicine, 172(3): 229-34.

Wells, R. B., S. M. Lloyd, and C. R. Turner, 1996: National air pollution source inventory. Air Pollution and Its Impacts on the South African Highveld, G. Held *et al*., Eds., Environmental Scientific Association, 3–9.

Wiedinmyer, C., Akagi, S.K., Yokelson, R.J., Emmons, L.K., Al-Saadi, J.A., Orlando, J.J. & Soja, A.J. 2011. The Fire INventory from NCAR (FINN): a high resolution global model to estimate the emissions from open burning. *Geoscientific Model Development*, 4(3): 625-641.

World Health Organisation (WHO). 2006. Air quality guidelines. Global update 2005. Particulate matter, ozone, nitrogen dioxide and sulfur dioxide. Retrieved from https://apps.who.int/iris/bitstream/handle/10665/107823/9789289021920-eng.pdf?sequence=1&isAllowed=y

WHO. 2016. Ambient air pollution: a global assessment of exposure and burden of disease. Retrieved from: http://apps.who.int/iris/bitstream/handle/10665/250141/9789241511353-eng.pdf?sequence=1

WHO. (n.d.). Ambient air pollution: health impacts. Retrieved from: https://www.who.int/airpollution/ambient/health-impacts/en/

WHO. 2013. Health risks of air pollution in Europe – HRAPIE project. Recommendations for concentration-response functions for cost-benefit analysis of particulate matter, ozone and nitrogen dioxide.

WHO. 2021a. WHO global air quality guidelines. Particulate matter ($PM_{2.5}$ and PM_{10}), ozone, nitrogen dioxide, sulfur dioxide and carbon monoxide. Retrieved from: https://apps.who.int/iris/bitstream/handle/10665/345329/9789240034228-eng.pdf

WHO. 2021b. New WHO global air qality guidelines aim to save millions of lives from air pollution. Retrieved from: https://www.who.int/news/item/22-09-2021-new-who-global-air-quality-guidelines-aim-to-save-millions-of-lives-from-air-pollution

World Bank Group & Institute for Health Metrics and Evaluation (IHME). 2016. The cost of air pollution: strengthening the economic case for action. Retrieved from: https://openknowledge.worldbank.org/handle/10986/25013

Wuebbles, D. J. 2018a. Air pollution and noncommunicable diseases: A review by the forum of International Respiratory Societies' Environmental Committee, Part 1: The damaging effects of air pollution. *Chest Journal,* 155(2): 409–416.

Xing, Y. F., Xu, Y. H., Shi, M. H., Lian, Y. X. 2016. The impact of $PM_{2.5}$ on the human respiratory system. *Journal of Thoracic Disease*, 8(1): E69-74.

Yang, H. H., Arafath, S. M., Wang, Y. F., Wu, J. Y., Lee, K. T., Hsieh, Y. S. 2018. Comparison of coaland oil-fired boilers through the investigation of filterable and condensable $PM_{2.5}$ sample analysis. *Energy Fuels 32*: 2993–3002.

Yang, H. H., Lee, K. T., Hsieh, Y. S., Luo, S. W., Li, M. S. 2014. Filterable and condensable fine particulate emissions from stationary sources. *Aerosol and Air Quality Research*, 14: 2010–2016.

Yang, Y., Zengliang, R., Xiaojie, W., Yin, Y., Mason, T.G., Lin, H. & Tian, L. 2019. Short-term and long-term exposures to fine particulate matter constituents and health: A systematic review and meta-analysis. *Environmental Pollution*, 247:874-882.

Yarwood. G., Rao, S., Yocke, M. & Whitten, G.Z. 2005. Updates to the Carbon Bond chemical mechanism: CB05. Final Report prepared for United States Environmental Protection Agency. Available at: http://www.camx.com/publ/pdfs/CB05_Final_Report_120805.pdf.

Ye, B., Ji, X., Yang, H., Yao, X., Chan, C. K., Cadle, S. H., Chan, T. & Mulawa, P. A. 2003. Concentration and chemical composition of $PM_{2.5}$ in Shanghai for a 1-year period. *Atmospheric Environment*, 37(4): 499-510.

Zeger, S., Dominici, F., McDermott, A. & Samet, J. 2008. Mortality in the Medicare population and chronic exposure to fine particulate air pollution in urban centers (2000-2005). *Environmental Health Perspectives*, 116(12): 1614-1619.

Zhang, C., Yao, Q. & Junming, S. 2004. Characteristics of particulate matter from emissions of four typical coal-fired power plants in China. *Fuel Processing Technology*, 86(2005): 757-768.

Zhang, X. 2016. Emission standards and control of $PM_{2.5}$ from coal-fired power plant, London: IEA Clean Coal Centre.

Zhao, X., Liu, Y., Han, F., Touseef, B., Yue, Y. & Guo, J. 2021. Source profile and health risk assessment of $PM_{2.5}$ from coal-fired power plants in Fuxin, China. Environmental Science and Pollution Research, 28:40151–40159.

Zhao, X., Yu, X., Wang, Y., & Fan, C. 2016. 'Economic evaluation of health losses from air pollution in Beijing, China'. *Environmental Science and Pollution Research*, 23(12):11716–11728.

Zhou, Y., Levy, J. & Evans, J. & Hammitt, J. 2006. The influence of geographic location on population exposure to emissions from power plants throughout China. Environment International 32 (3) 365–373.

ANNEXURE A – TIME SERIES FOR $PM_{2.5}$

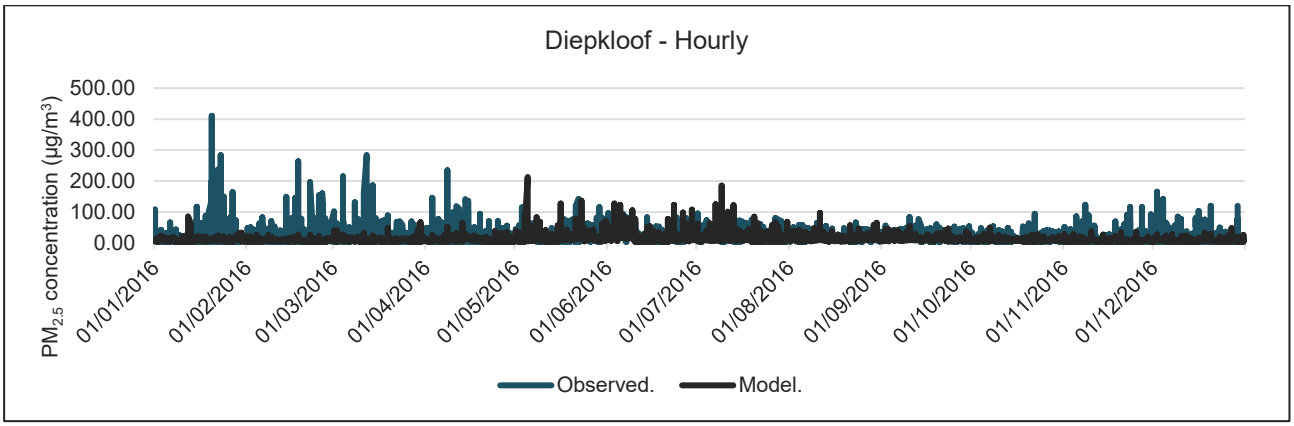

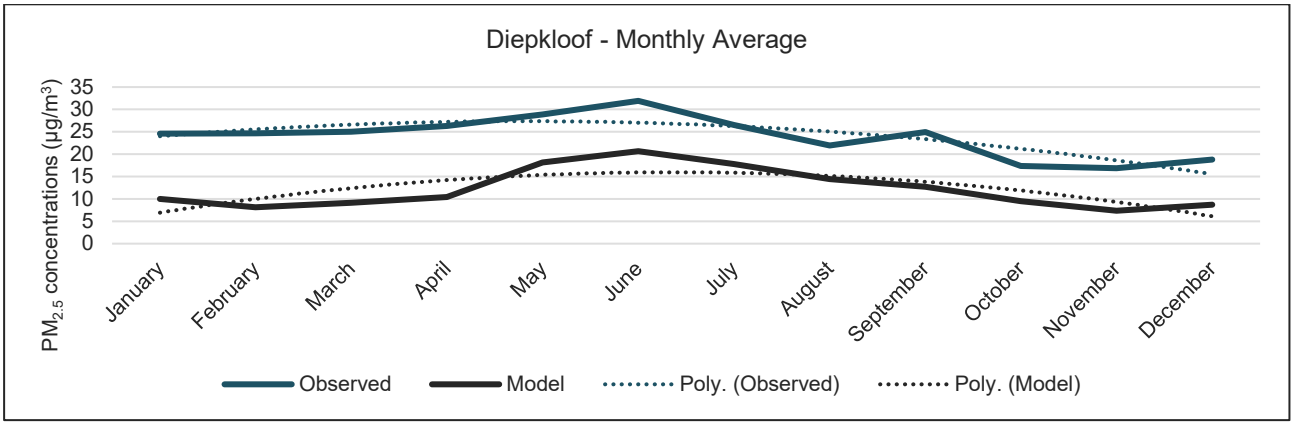

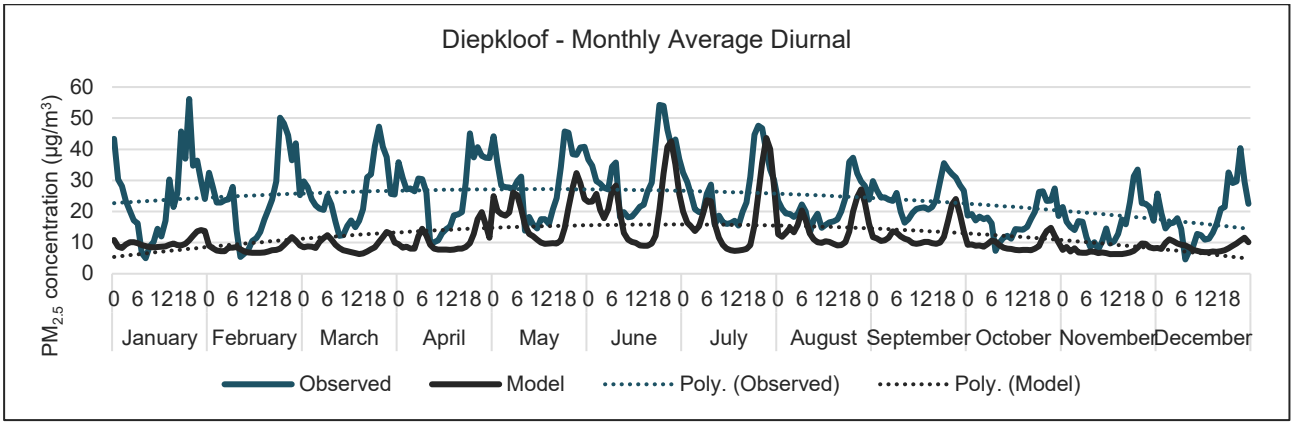

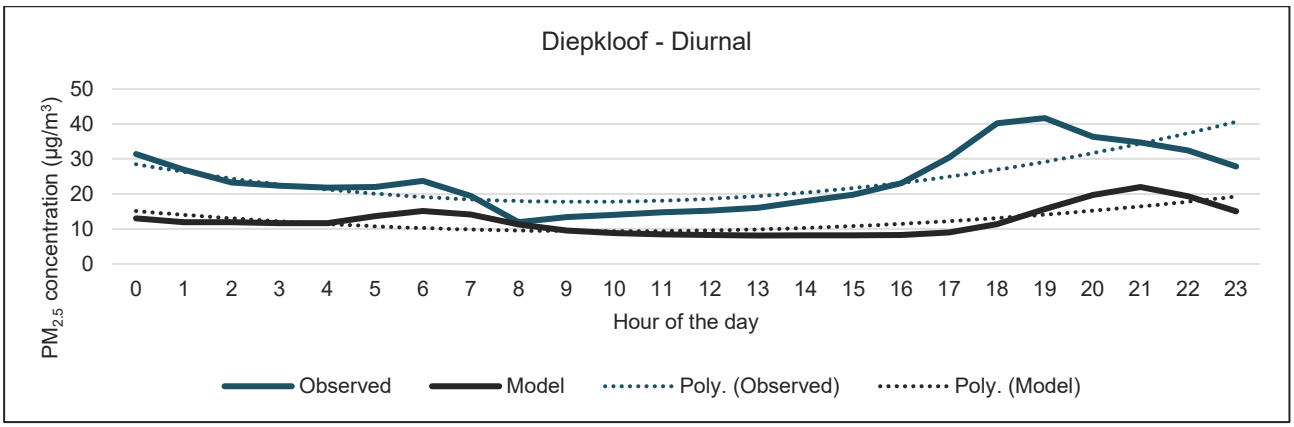

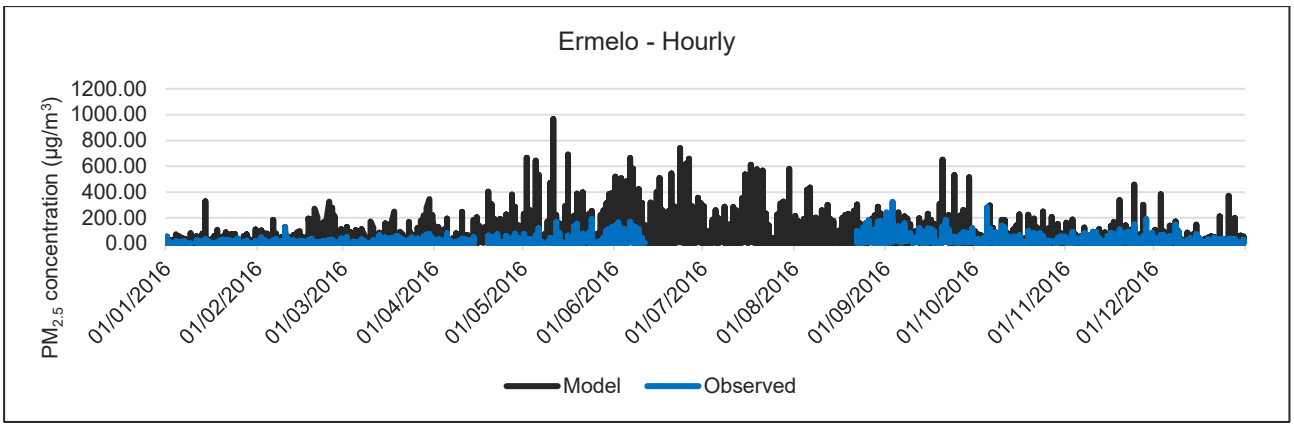
Ermelo - Hourly
PM2.5 concentration (µg/m³)
1200.00
1000.00
800.00
600.00
400.00
200.00
0.00
01/01/2016
01/02/2016
01/03/2016
01/04/2016
01/05/2016
01/06/2016
01/07/2016
01/08/2016
01/09/2016
01/10/2016
01/11/2016
01/12/2016
Model
Observed

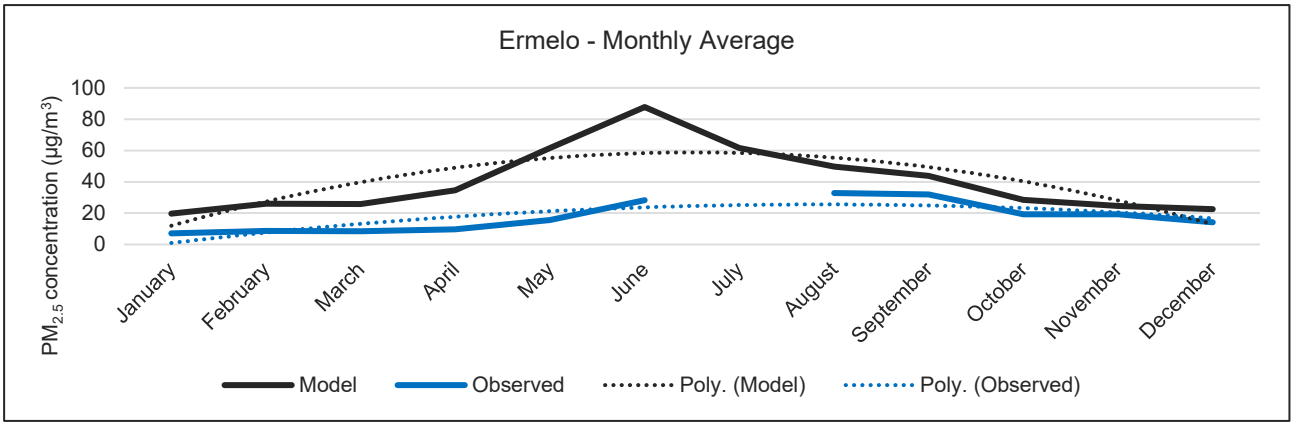
Ermelo - Monthly Average
PM2.5 concentration (µg/m³)
100
80
60
40
20
0
January
February
March
April
May
June
July
August
September
October
November
December
Model
Observed
Poly. (Model)
Poly. (Observed)

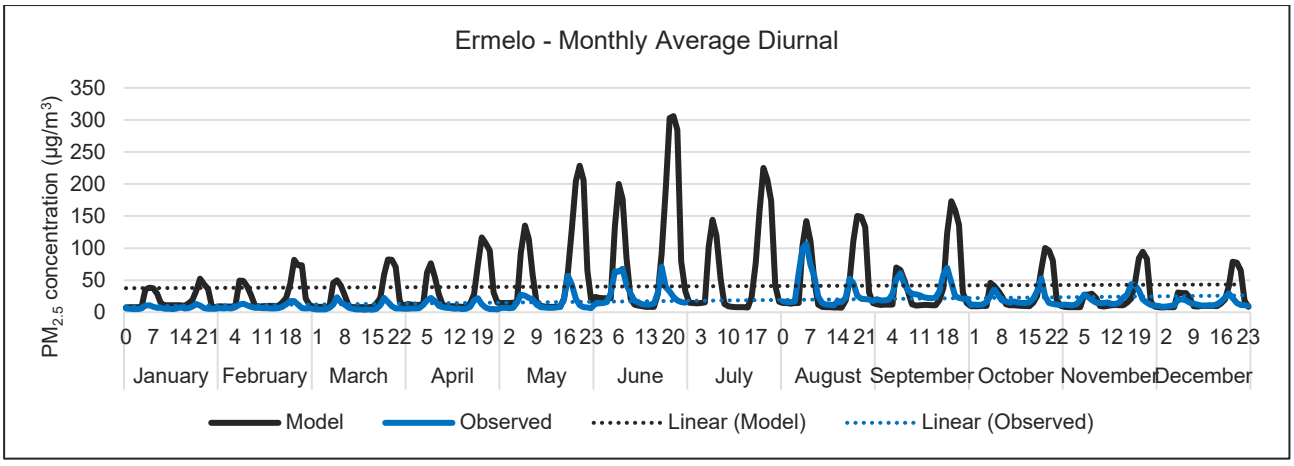
Ermelo - Monthly Average Diurnal
PM2.5 concentration (µg/m³)
350
300
250
200
150
100
50
0
0 7 14 21 4 11 18 1 8 15 22 5 12 19 2 9 16 23 6 13 20 3 10 17 0 7 14 21 4 11 18 1 8 15 22 5 12 19 2 9 16 23
January
February
March
April
May
June
July
August
September
October
November
December
Model
Observed
Linear (Model)
Linear (Observed)

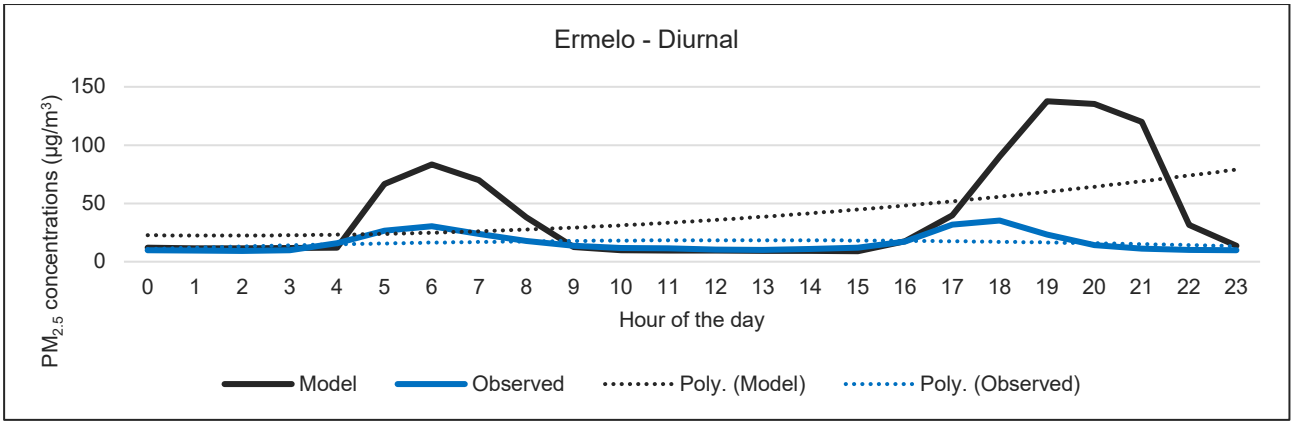
Ermelo - Diurnal
PM2.5 concentrations (µg/m³)
150
100
50
0
0 1 2 3 4 5 6 7 8 9 10 11 12 13 14 15 16 17 18 19 20 21 22 23
Hour of the day
Model
Observed
Poly. (Model)
Poly. (Observed)

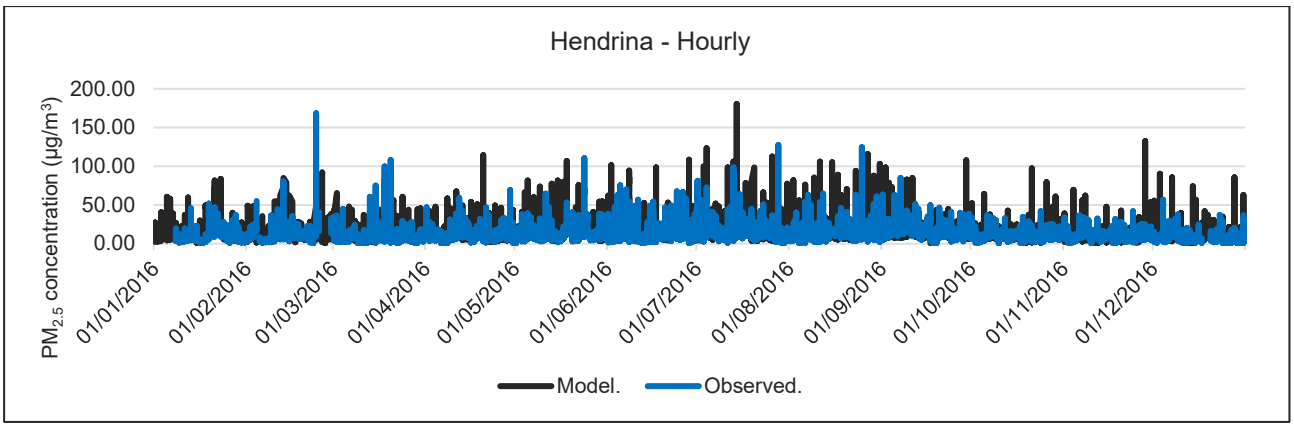
Hendrina - Hourly
PM2.5 concentration (µg/m3)
200.00
150.00
100.00
50.00
0.00
01/01/2016
01/02/2016
01/03/2016
01/04/2016
01/05/2016
01/06/2016
01/07/2016
01/08/2016
01/09/2016
01/10/2016
01/11/2016
01/12/2016
Model.
Observed.

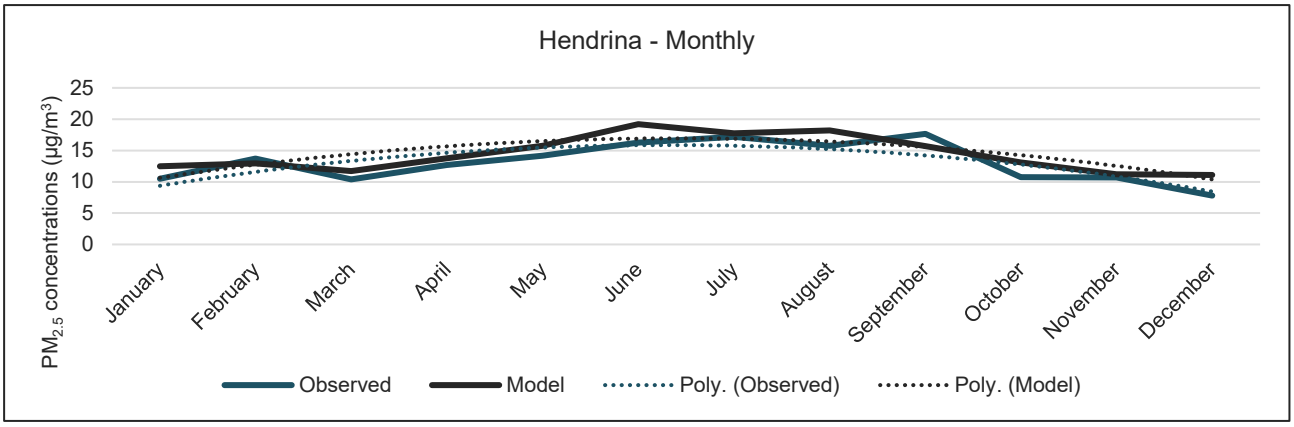
Hendrina - Monthly
PM2.5 concentrations (µg/m3)
25
20
15
10
5
0
January
February
March
April
May
June
July
August
September
October
November
December
Observed
Model
Poly. (Observed)
Poly. (Model)

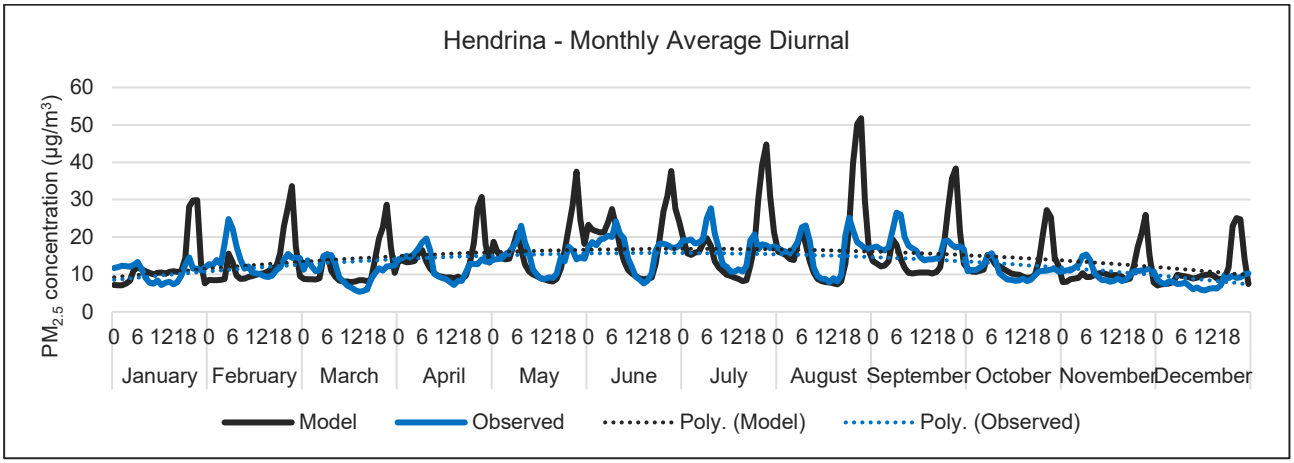
Hendrina - Monthly Average Diurnal
PM2.5 concentration (µg/m3)
60
50
40
30
20
10
0
0 6 1218
January
February
March
April
May
June
July
August
September
October
November
December
Model
Observed
Poly. (Model)
Poly. (Observed)

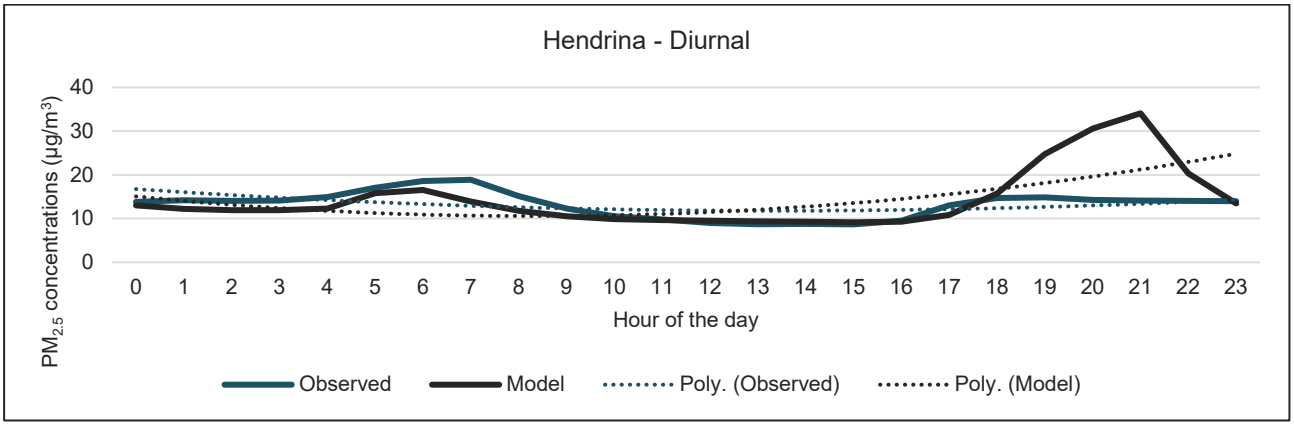
Hendrina - Diurnal
PM2.5 concentrations (µg/m3)
40
30
20
10
0
0 1 2 3 4 5 6 7 8 9 10 11 12 13 14 15 16 17 18 19 20 21 22 23
Hour of the day
Observed
Model
Poly. (Observed)
Poly. (Model)

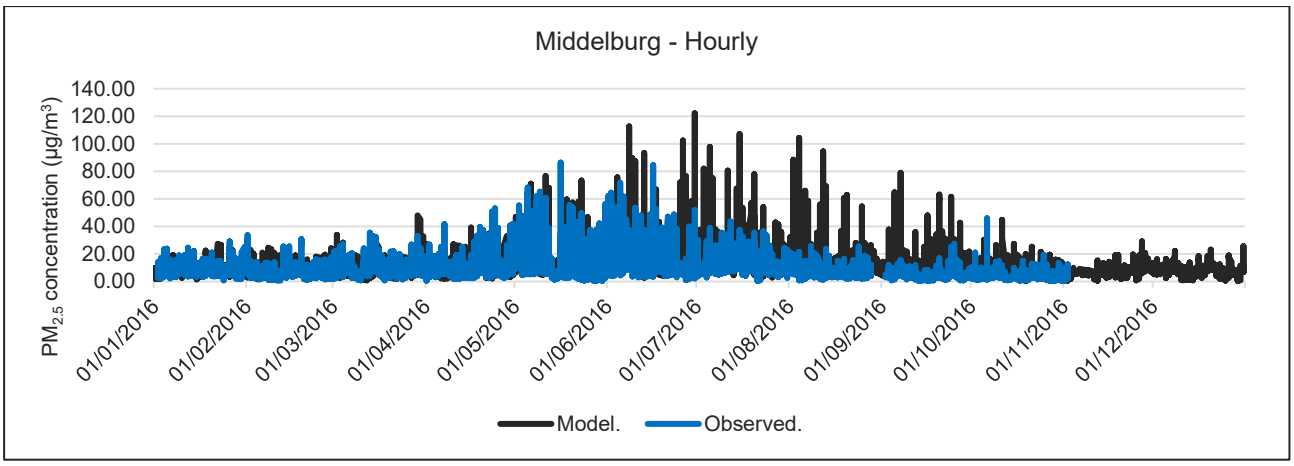
Middelburg - Hourly
PM2.5 concentration (µg/m3)
140.00
120.00
100.00
80.00
60.00
40.00
20.00
0.00
01/01/2016
01/02/2016
01/03/2016
01/04/2016
01/05/2016
01/06/2016
01/07/2016
01/08/2016
01/09/2016
01/10/2016
01/11/2016
01/12/2016
Model.
Observed.

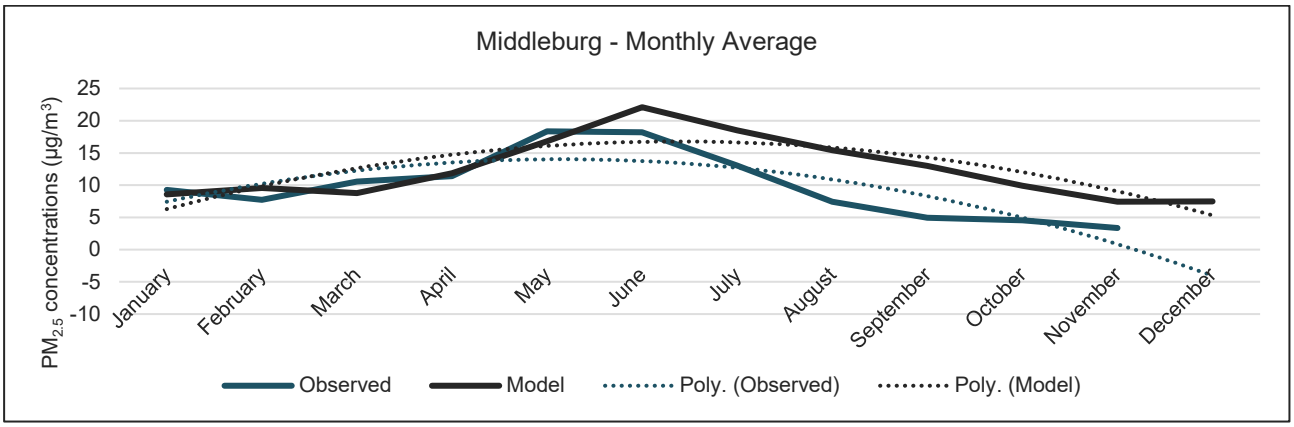
Middleburg - Monthly Average
PM2.5 concentrations (µg/m3)
25
20
15
10
5
0
-5
-10
January
February
March
April
May
June
July
August
September
October
November
December
Observed
Model
Poly. (Observed)
Poly. (Model)

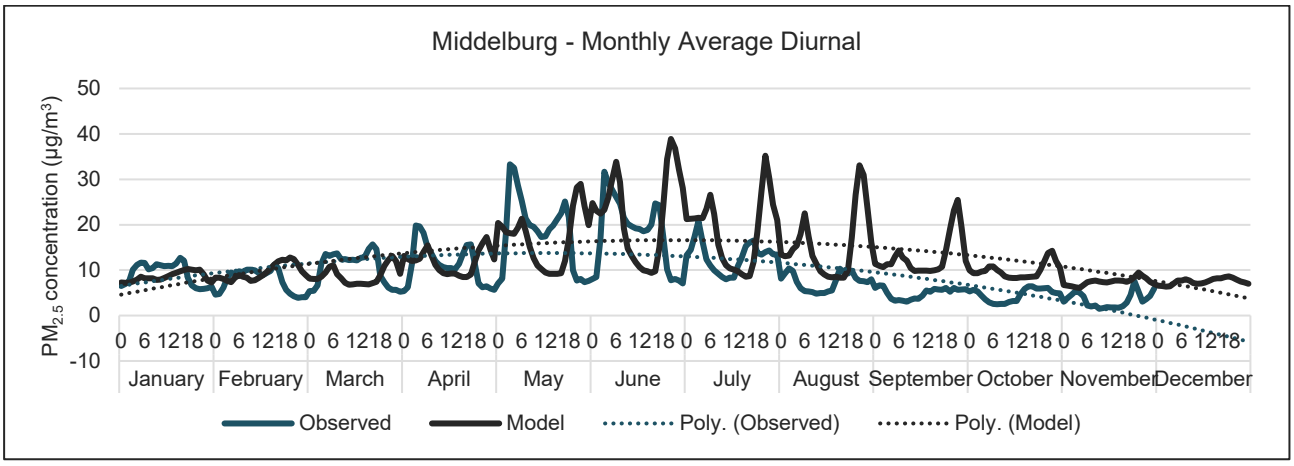
Middelburg - Monthly Average Diurnal
PM2.5 concentration (µg/m3)
50
40
30
20
10
0
-10
0 6 1218
January
February
March
April
May
June
July
August
September
October
November
December
Observed
Model
Poly. (Observed)
Poly. (Model)

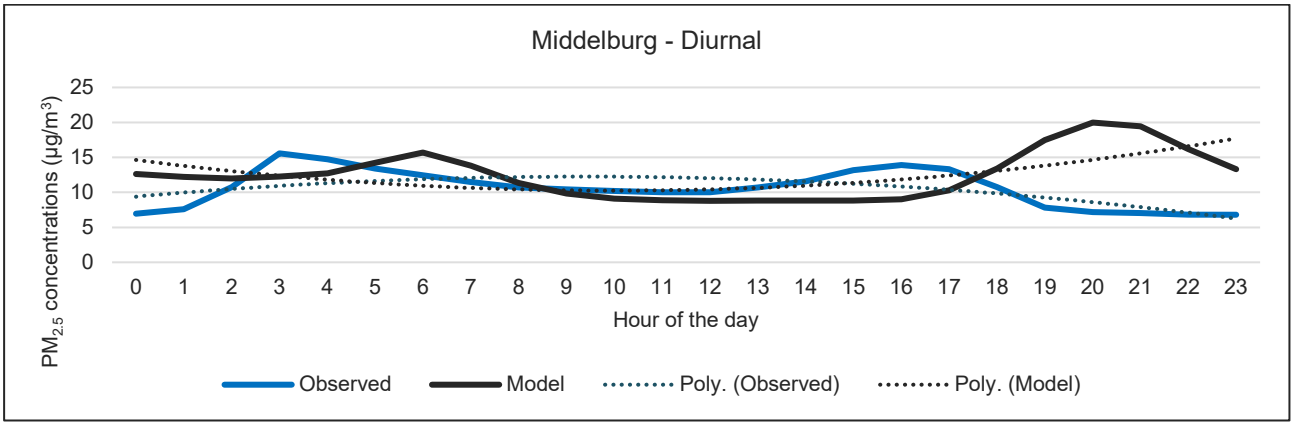
Middelburg - Diurnal
PM2.5 concentrations (µg/m3)
25
20
15
10
5
0
0 1 2 3 4 5 6 7 8 9 10 11 12 13 14 15 16 17 18 19 20 21 22 23
Hour of the day
Observed
Model
Poly. (Observed)
Poly. (Model)

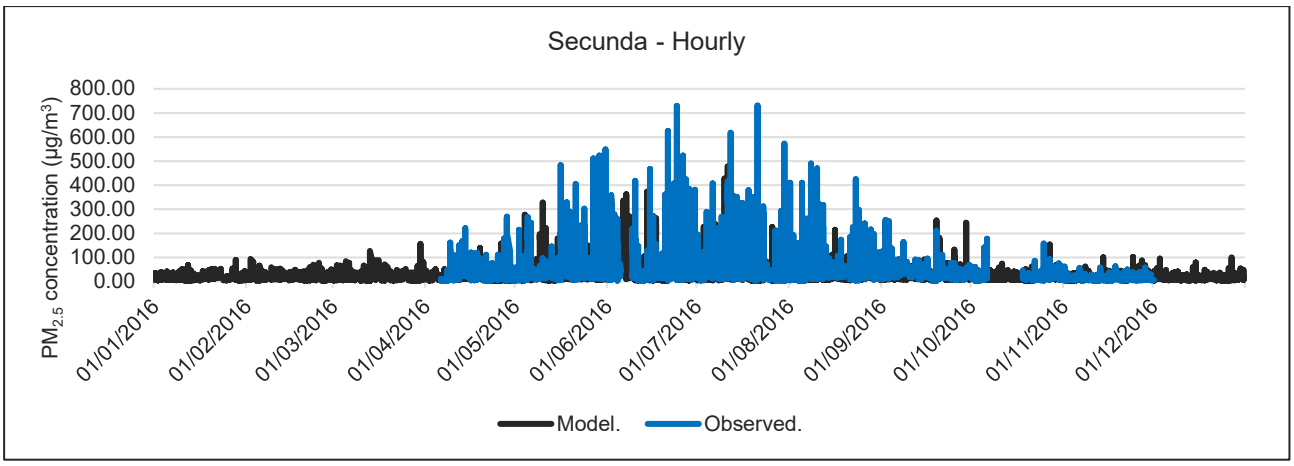
Secunda - Hourly
PM2.5 concentration (µg/m³)
800.00
700.00
600.00
500.00
400.00
300.00
200.00
100.00
0.00
01/01/2016
01/02/2016
01/03/2016
01/04/2016
01/05/2016
01/06/2016
01/07/2016
01/08/2016
01/09/2016
01/10/2016
01/11/2016
01/12/2016
Model.
Observed.

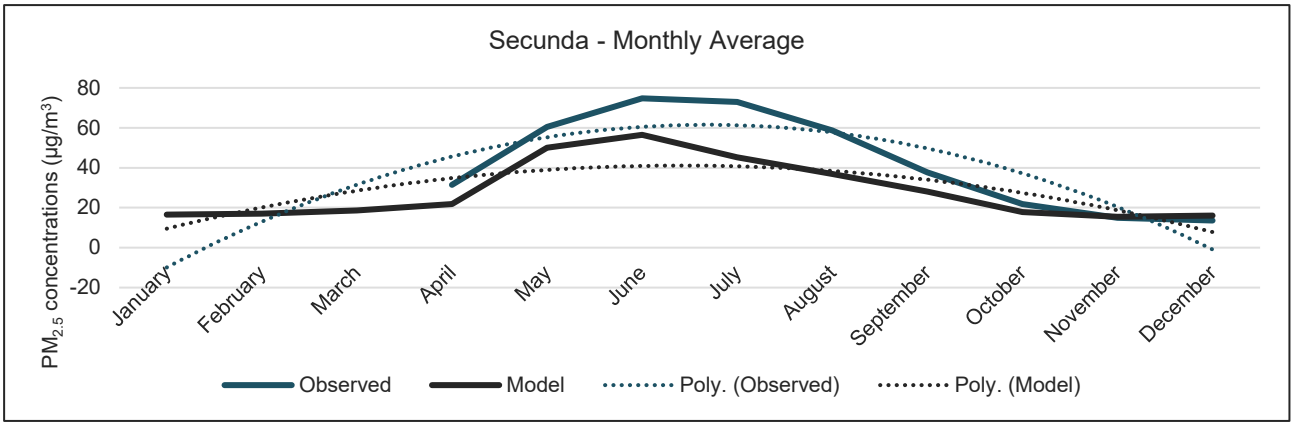
Secunda - Monthly Average
PM2.5 concentrations (µg/m³)
80
60
40
20
0
-20
January
February
March
April
May
June
July
August
September
October
November
December
Observed
Model
Poly. (Observed)
Poly. (Model)

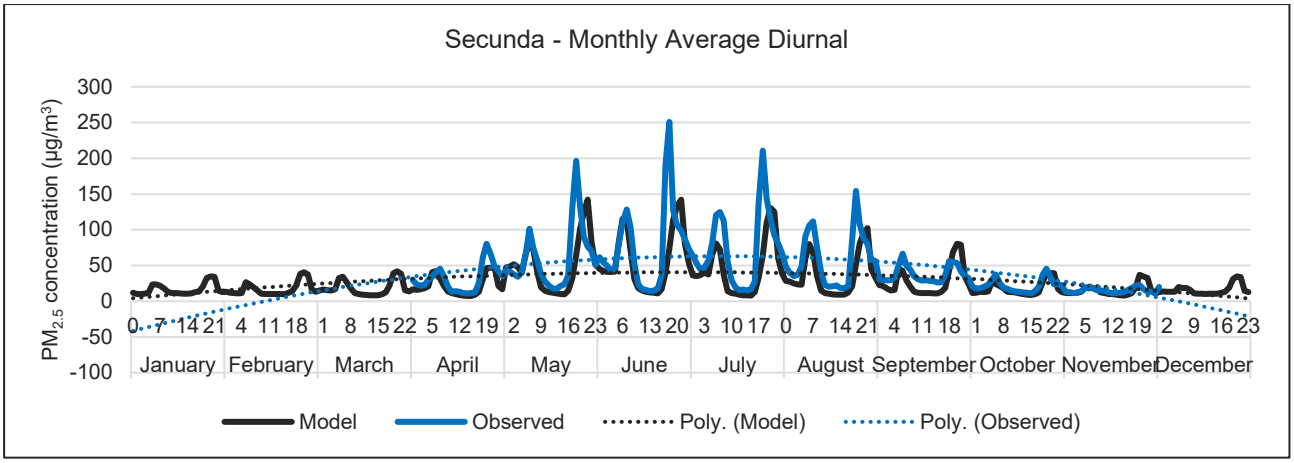
Secunda - Monthly Average Diurnal
PM2.5 concentration (µg/m³)
300
250
200
150
100
50
0
-50
-100
0 7 14 21 4 11 18 1 8 15 22 5 12 19 2 9 16 23 6 13 20 3 10 17 0 7 14 21 4 11 18 1 8 15 22 5 12 19 2 9 16 23
January
February
March
April
May
June
July
August
September
October
November
December
Model
Observed
Poly. (Model)
Poly. (Observed)

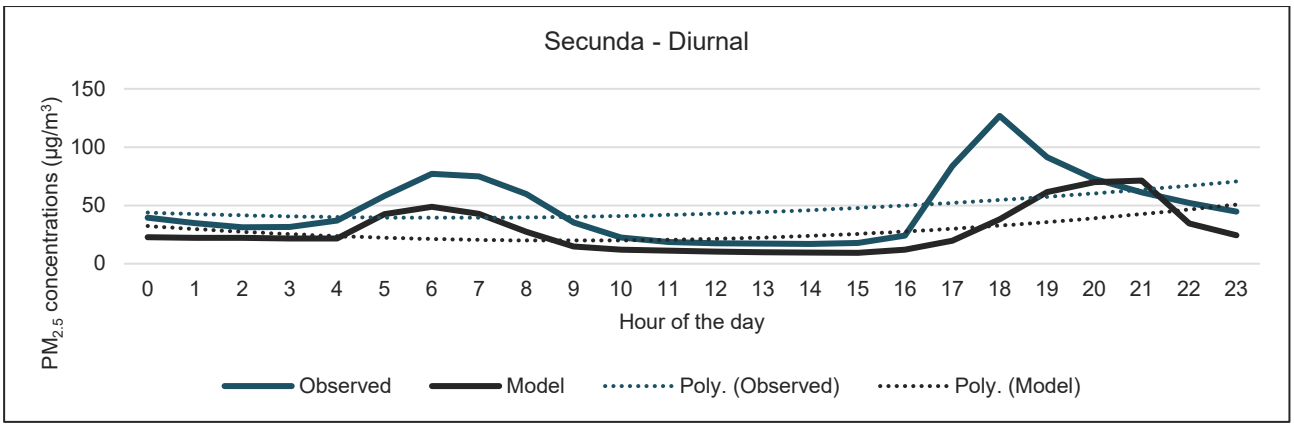
Secunda - Diurnal
PM2.5 concentrations (µg/m³)
150
100
50
0
0 1 2 3 4 5 6 7 8 9 10 11 12 13 14 15 16 17 18 19 20 21 22 23
Hour of the day
Observed
Model
Poly. (Observed)
Poly. (Model)

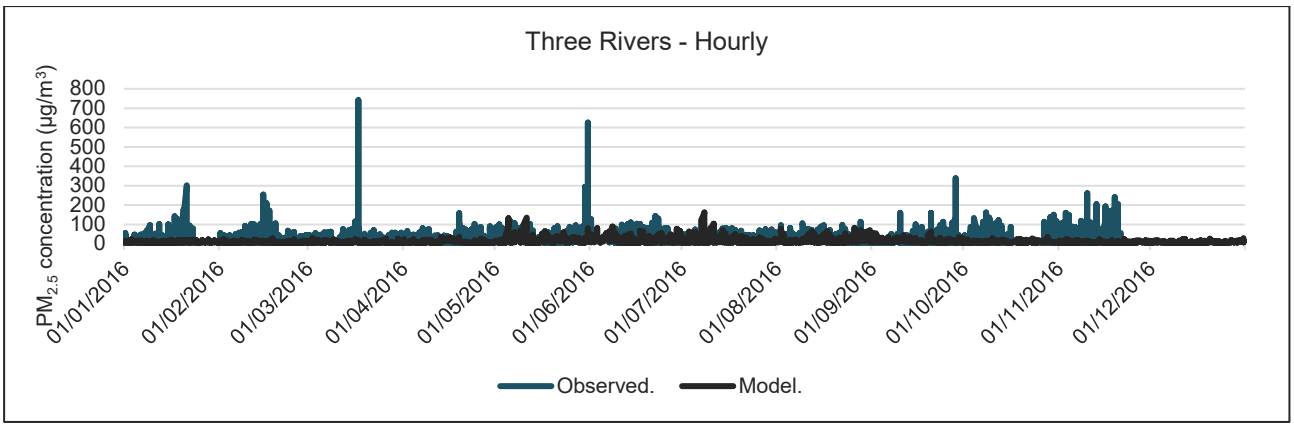
Three Rivers - Hourly
PM2.5 concentration (µg/m3)
800
700
600
500
400
300
200
100
0
01/01/2016
01/02/2016
01/03/2016
01/04/2016
01/05/2016
01/06/2016
01/07/2016
01/08/2016
01/09/2016
01/10/2016
01/11/2016
01/12/2016
Observed.
Model.

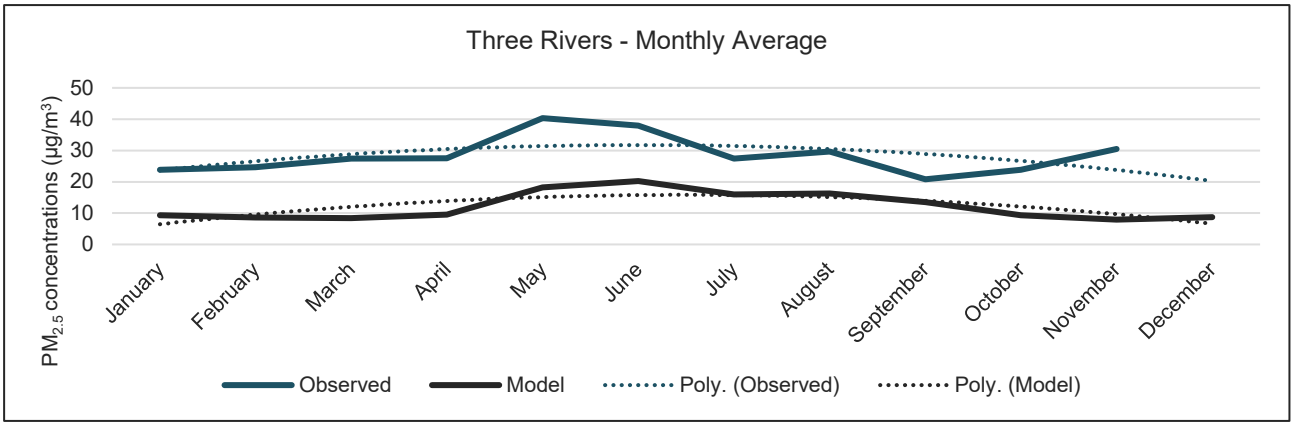
Three Rivers - Monthly Average
PM2.5 concentrations (µg/m3)
50
40
30
20
10
0
January
February
March
April
May
June
July
August
September
October
November
December
Observed
Model
Poly. (Observed)
Poly. (Model)

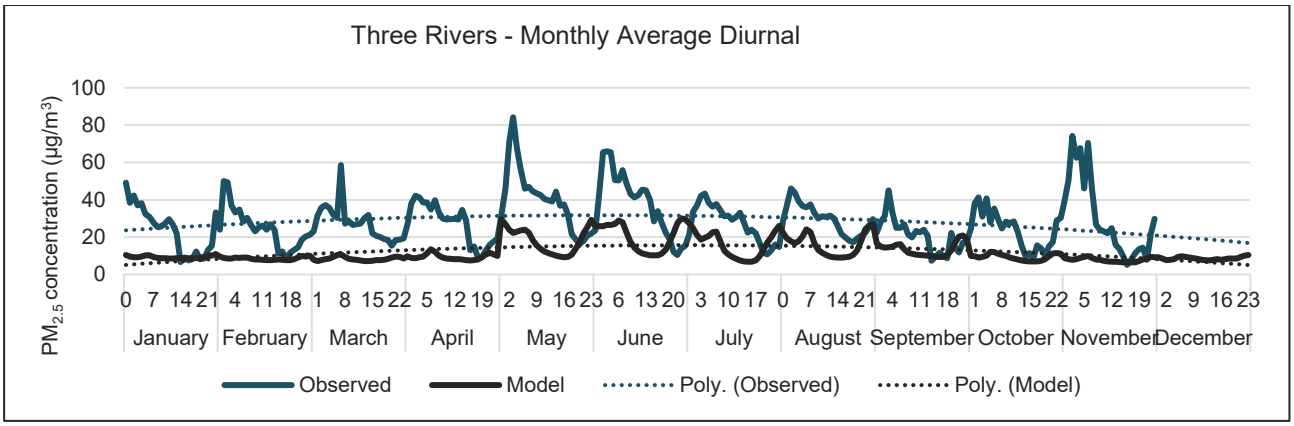
Three Rivers - Monthly Average Diurnal
PM2.5 concentration (µg/m3)
100
80
60
40
20
0
0 7 14 21 4 11 18 1 8 15 22 5 12 19 2 9 16 23 6 13 20 3 10 17 0 7 14 21 4 11 18 1 8 15 22 5 12 19 2 9 16 23
January
February
March
April
May
June
July
August
September
October
November
December
Observed
Model
Poly. (Observed)
Poly. (Model)

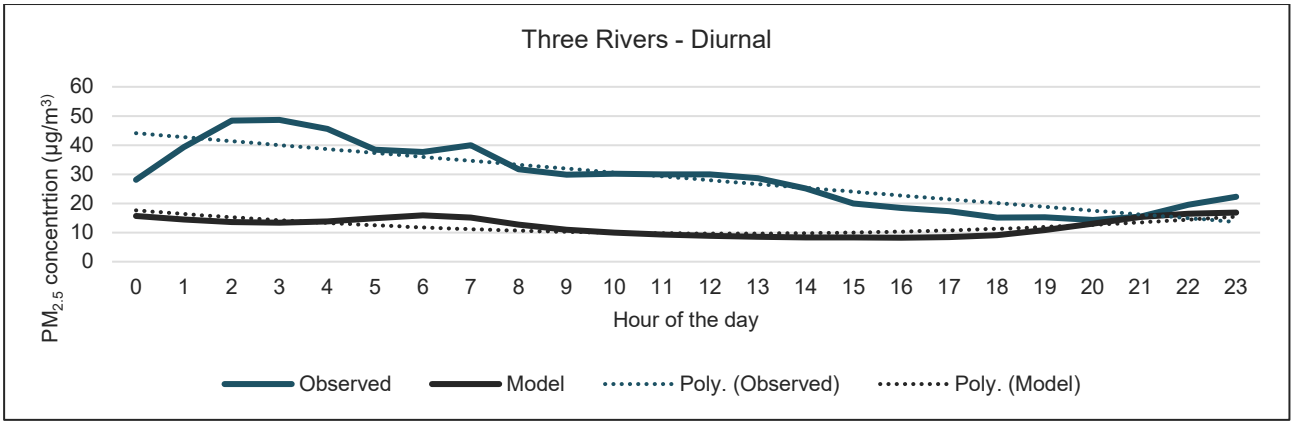
Three Rivers - Diurnal
PM2.5 concentrtion (µg/m3)
60
50
40
30
20
10
0
0 1 2 3 4 5 6 7 8 9 10 11 12 13 14 15 16 17 18 19 20 21 22 23
Hour of the day
Observed
Model
Poly. (Observed)
Poly. (Model)

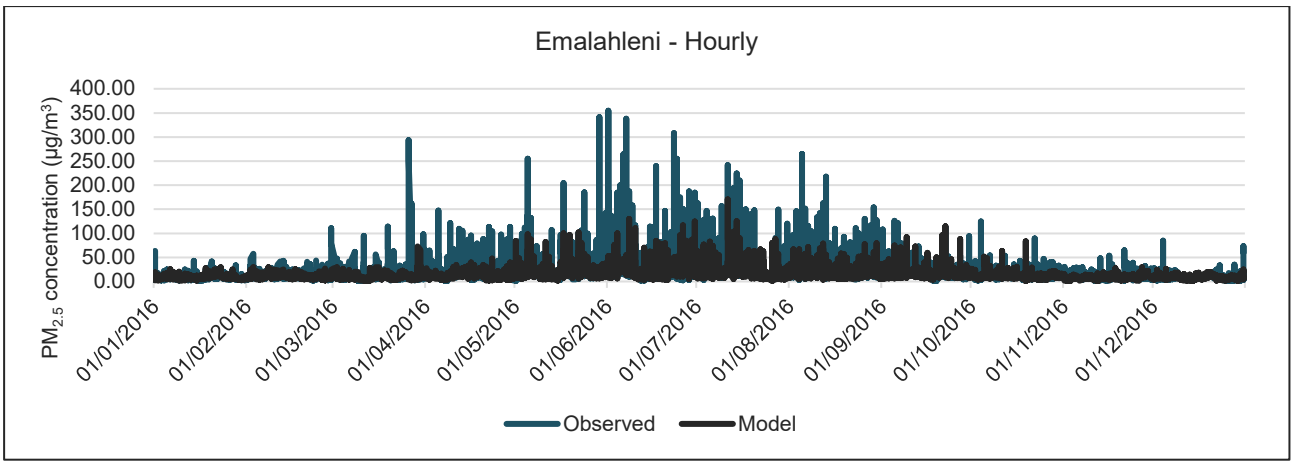
Emalahleni - Hourly
PM2.5 concentration (µg/m3)
400.00
350.00
300.00
250.00
200.00
150.00
100.00
50.00
0.00
01/01/2016
01/02/2016
01/03/2016
01/04/2016
01/05/2016
01/06/2016
01/07/2016
01/08/2016
01/09/2016
01/10/2016
01/11/2016
01/12/2016
Observed
Model

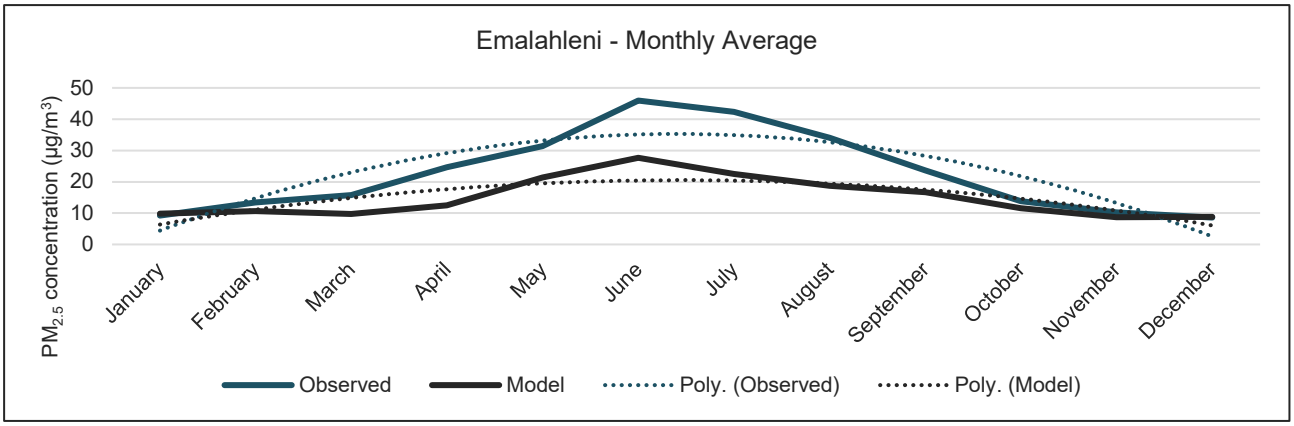
Emalahleni - Monthly Average
PM2.5 concentration (µg/m3)
50
40
30
20
10
0
January
February
March
April
May
June
July
August
September
October
November
December
Observed
Model
Poly. (Observed)
Poly. (Model)

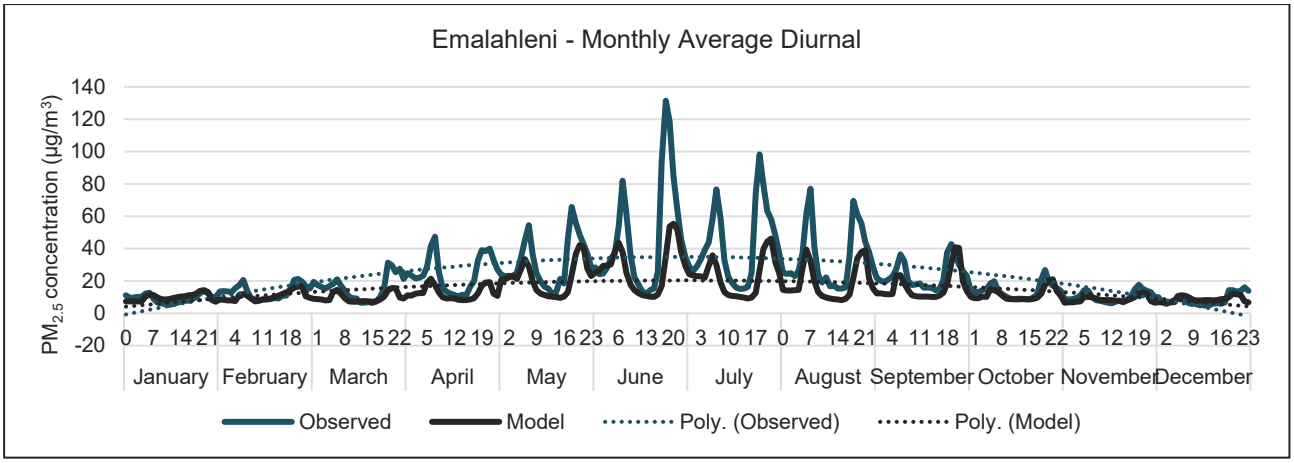
Emalahleni - Monthly Average Diurnal
PM2.5 concentration (µg/m3)
140
120
100
80
60
40
20
0
-20
0 7 14 21 4 11 18 1 8 15 22 5 12 19 2 9 16 23 6 13 20 3 10 17 0 7 14 21 4 11 18 1 8 15 22 5 12 19 2 9 16 23
January
February
March
April
May
June
July
August
September
October
November
December
Observed
Model
Poly. (Observed)
Poly. (Model)

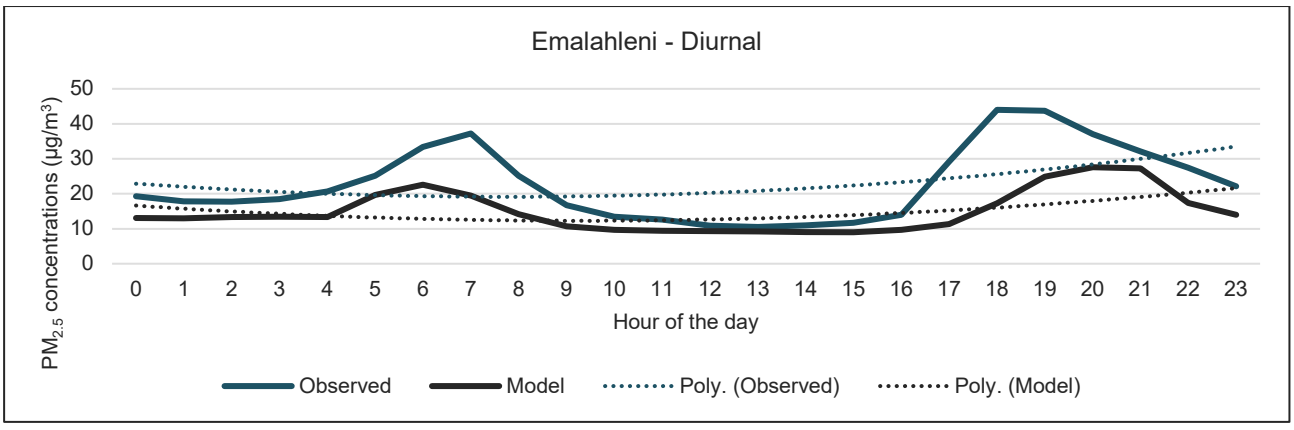
Emalahleni - Diurnal
PM2.5 concentrations (µg/m3)
50
40
30
20
10
0
0 1 2 3 4 5 6 7 8 9 10 11 12 13 14 15 16 17 18 19 20 21 22 23
Hour of the day
Observed
Model
Poly. (Observed)
Poly. (Model)